

University of Colorado  
Department of Aerospace Engineering Sciences  
ASEN 4018-4028: Project Final Report (PFR)

**SpaceNet**  
May 3, 2021

**Project Customers**

Name: Martin Wilson Email: martin.wilson@raytheon.com	Name: Sheldon Clark Email: sheldon.c.clark@raytheon.com
Name: Mark Werremeyer Email: mark.r.werremeyer@raytheon.com	Name: Email:

**Advisors**

Name: Francisco Lopez Jimenez Email: Francisco.LopezJimenez@colorado.edu
---

**Team Members**

Name: Ryan Burdick Email: rybu3974@colorado.edu Phone: (720)299-7830	Name: Samuel Firth Email: safi0652@colorado.edu Phone: (970)227-4062
Name: Noah Fancis Email: nofr6730@colorado.edu Phone: (720)233-3831	Name: Jordan Gage Email: joga0413@colorado.edu Phone: (970)381-6320
Name: E Forest Owen Email: efow4675@colorado.edu Phone: (907)687-9744	Name: Tyler Priner Email: typi6819@colorado.com Phone: (303)437-9106
Name: Keith Poletti Email: kepo6935@colorado.com Phone: (720)375-0117	Name: Ryan Prince Email: rypr9042@colorado.com Phone: (310)968-0386
Name: Israel Quezada-Cordova Email: isqu6841@colorado.edu Phone: (720)545-5237	Name: Colin Ruark Email: coru0688@colorado.edu Phone: (530)613-9230
Name: Benji Smith Email: besm9389@colorado.edu Phone: (303)552-7321	Name: Email: Phone:

# Contents

<b>1</b>	<b>Project Purpose</b>	<b>7</b>
<b>2</b>	<b>Project Objectives and Functional Requirements</b>	<b>8</b>
2.1	Concept of Operations . . . . .	8
2.2	Success Criteria . . . . .	9
2.3	Conceptual System Design . . . . .	10
2.3.1	RF Front End . . . . .	11
2.3.2	Structures . . . . .	11
2.3.3	Electronics and Data Handling . . . . .	12
2.3.4	On-board OS . . . . .	12
2.3.5	TDoA algorithm . . . . .	12
2.3.6	Gibbs Method . . . . .	12
2.3.7	Particle Filter . . . . .	12
2.3.8	Orbit Estimate . . . . .	13
2.4	Functional Block Diagram . . . . .	13
2.5	Functional Requirements . . . . .	13
<b>3</b>	<b>Final Design</b>	<b>15</b>
3.1	Requirements Flow down . . . . .	15
3.2	Final Design . . . . .	21
<b>4</b>	<b>Manufacturing</b>	<b>25</b>
4.1	Hardware . . . . .	25
4.1.1	Packaging . . . . .	26
4.1.2	Antenna Mount . . . . .	26
4.1.3	Mounting . . . . .	27
4.2	Electronics . . . . .	30
4.2.1	RF Front End - Lband . . . . .	31
4.2.2	PPS Timing Scheme . . . . .	31
4.2.3	Circuit Board . . . . .	34
4.3	Software . . . . .	35
4.3.1	Onboard OS . . . . .	35
4.3.2	Time Delay of Arrival . . . . .	35
4.3.3	Orbital Prediction Particle Filter . . . . .	36
4.3.4	TLE Generation and Comparison . . . . .	39
4.4	Summary of Integration . . . . .	39
<b>5</b>	<b>Verification and Validation</b>	<b>41</b>
5.1	Environmental Readiness . . . . .	41
5.2	RF Front End . . . . .	45
5.3	Timing Synchronization . . . . .	47
5.4	Position Vector Estimate using TDoA . . . . .	50
5.5	Orbital Element Determination . . . . .	52
5.6	Summary of Verification and Validation Tests . . . . .	54

<b>6</b>	<b>Risk Assessment and Mitigation</b>	<b>56</b>
6.1	Project Risks . . . . .	56
6.1.1	Technical Risks . . . . .	56
6.1.2	Logistical Risks . . . . .	58
6.1.3	Safety Risks . . . . .	59
6.1.4	Financial Risks . . . . .	59
6.2	Risk Matrix . . . . .	59
6.3	Risk Mitigation . . . . .	60
6.4	Risk Realization . . . . .	60
<b>7</b>	<b>Project Planning</b>	<b>62</b>
7.1	Organizational Chart . . . . .	62
7.2	Work Breakdown Structure . . . . .	62
7.3	Work Plan . . . . .	63
7.4	Cost Plan . . . . .	65
7.5	Test Plan . . . . .	65
<b>8</b>	<b>Lessons Learned</b>	<b>66</b>
<b>9</b>	<b>Individual Report Contributions</b>	<b>67</b>
<b>A</b>	<b>Baseline Design and Trade Studies</b>	<b>69</b>
<b>B</b>	<b>Electronics System Schematics</b>	<b>70</b>
<b>C</b>	<b>Bill of Materials</b>	<b>70</b>

## List of Figures

1	Plot from the ESA that categorizes the location of man made space objects. . . . .	7
2	Plot from the ESA that shows the recent spike in planned mission for LEO space domain. . . . .	8
3	SpaceNet Concept of operations(CONOPS) . . . . .	9
4	Conceptual Block Diagram . . . . .	11
5	Functional Block Diagram . . . . .	13
6	Electronics Functional Block Diagram . . . . .	14
7	External Model . . . . .	21
8	Internal Model . . . . .	22
9	Hardware Block Diagram . . . . .	22
10	Software Block Diagram . . . . .	23
11	State Diagram . . . . .	24
12	Completed Hardware Setup . . . . .	24
13	Housing Cable Pass Through Mounting . . . . .	26
14	PVC Antenna Mount . . . . .	27
15	Lower Aluminum Mounting Bracket . . . . .	28
16	Upper Aluminum Mounting Bracket . . . . .	28
17	Aluminum Antenna Support Bracket . . . . .	29

18	Internal Acrylic Hardware Mount . . . . .	29
19	PPS+HackRF interface . . . . .	31
20	Simulated PPS output . . . . .	32
21	PPS injection header . . . . .	32
22	Example of PPS in HackRF recorded data . . . . .	33
23	Example of one of the circuit boards. . . . .	34
24	Functional Block Diagram detailing a Particle Filter. Source: MathWorks . . . . .	37
25	Two Dimensional Particle Filter after Initialization . . . . .	38
26	SpaceNet Orbital Propagation Tool . . . . .	40
27	Standoff stack up . . . . .	40
28	HackRF housing modification . . . . .	41
29	Completed sensor unit . . . . .	42
30	Water Resistance Test . . . . .	43
31	Water Resistance Tests Progression . . . . .	43
32	Weather Resistant Verification Results . . . . .	43
33	Timeline of the Single Unit Test . . . . .	45
34	Test setup for DR 5.1 . . . . .	47
35	Test setup for DR 5.2 . . . . .	48
36	reported SDR samples . . . . .	48
37	Proposed Test locations for DR 5.3 . . . . .	49
38	TDoA Positioning Problem Setup . . . . .	50
39	Orbital State Error over a Single Flyby . . . . .	53
40	Propagated Truth and Calculated TLE's from State Vector . . . . .	53
41	Propagated Truth and Calculated TLE's from Simulated TDoA values . . . . .	55
42	3D Orbital Propagation . . . . .	56
43	Levels of Success Breakdown . . . . .	57
44	SpaceNet Orbital Propagation Ground Track . . . . .	58
45	Risk Matrix . . . . .	59
46	Risk matrix after considering the mitigation's shown above in table 2 . . . . .	60
47	Organizational chart showing the team members their sub-teams and roles. . . . .	62
48	Deliverable based work break down structure for the fall semester. . . . .	63
49	Gantt chart that outlines the workflow for the Spring semester. . . . .	64
50	Cost budget. . . . .	65
51	Cost budget. . . . .	66
52	Full Schematic of the circuit board . . . . .	70

## List of Tables

1	Levels of Success as defined in CDD . . . . .	10
2	Risks and their associated mitigation's . . . . .	61
3	Test Plan summarizing Rough Time line for critical Test Paths . . . . .	66

## Acronyms

**BOM** Bill of Materials.  
**CBD** Conceptual Block Diagram.  
**CONOPS** Concept of Operations.  
**DR** Design Requirement.  
**EPDS** Electrical Power Distribution Systems.  
**ESA** European Space Agency.  
**FBD** Functional Block Diagram.  
**FOV** Field of View.  
**FR** Functional Requirement.  
**GDOP** Geometric Dilution of Precision.  
**GPIO** General Purpose Input Output.  
**GPS** Global Positioning System.  
**LASP** Laboratory for Atmospheric and Space Physics.  
**LEO** Low Earth Orbit.  
**LNA** Low Noise Amplifier.  
**MATLAB** Matrix Laboratory.  
**NEMA** National Electrical Manufacturers Association.  
**OOF** Out of Family.  
**PC** Personal Computer.  
**PPS** Pulse Per Second.  
**PVC** Polymerizing Vinyl Chloride.  
**RF** Radio Frequency.  
**SD** Secure Digital.  
**SDA** Space Domain Awareness.  
**SDR** Software Defined Radio.  
**SGP4** Simplified General Perturbations Model 4.  
**SN** Sensor Number.  
**SNR** Signal to Noise Ratio.  
**SSA** Space Situation Awareness.  
**STK** Systems Tool Kit.  
**TDoA** Time Delay of Arrival.  
**TLE** Two Line Element.  
**UHF** Ultra High Frequency.  
**US** United States.  
**UTC** Universal Time Coordinated.  
**WFM** Wide Frequency Modulation.

## Definition of Symbols

$\Delta t_{1,i}$  Difference in Time of Arrival  
**H** Jacobian Matrix  
**R** Satellite Position Vector  
 $\mathbf{r}_i$  Sensor Unit Position Vector

$\Omega$	Right Ascension of Ascending Node
$\omega$	Argument of Perigee
$\tau$	Signal Time of Flight
$\theta$	True Anomaly
$a$	Semimajor Axis
$c$	Speed of light in vacuum
$e$	Eccentricity
$G/T$	Antenna Gain to Noise Ratio
$h$	Planck constant
$i$	Inclination
$p_i$	Pseudorange

# 1 Project Purpose

Authors: Ryan Prince

In recent years and the near future there has been, and is expected, to be a massive influx of satellites in Low Earth Orbit (LEO). This is mostly due to privately owned space exploration companies developing and launching huge satellite constellations to provide a variety of services. The Space Debris Environment Report, published by the European Space Agency (ESA), tracks man-made objects that are or were once in orbit. Figure 1 shows the spread of objects in LEO orbits. From this plot it is apparent that a majority of man-made space objects exist in LEO domain. Figure 2 shows the number of planned missions into LEO space. From the plot, it is clear there is a huge spike in commercial launches, and the number continues to grow. Additionally, there has been a rise in the number of amateur missions launched since 2010. As space becomes easier to access, the number of objects in space will continue to grow starting with LEO due to its accessibility.

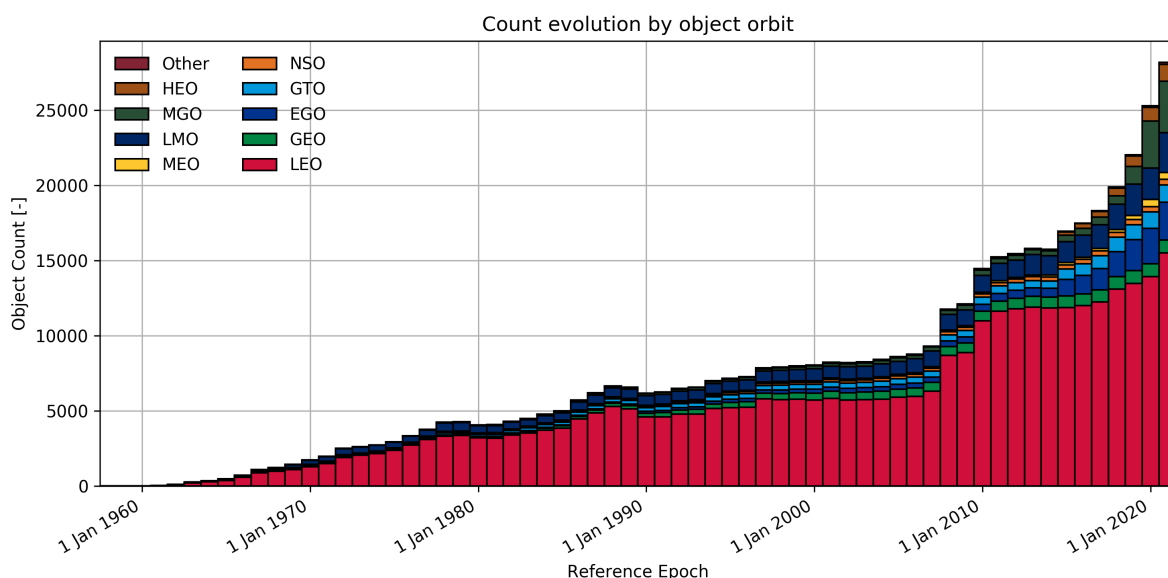


Figure 1: Plot from the ESA that categorizes the location of man-made space objects. It is clear that LEO is a contested domain containing  $\approx 60\%$  of objects to date. <https://sdup.esoc.esa.int/discosweb/statistics/>

Due to this influx in space traffic in the LEO domain, the Defense Intelligence Agency claims we will need "better capabilities to track and identify objects and prevent a collision in space." [1] This has led to a push for what is called Full Space Domain Awareness. Currently, the tracking of space debris is done using large high-fidelity phase array sensors. These sensors are a single large unit that are fixed in a geographical location on Earth. These sensors can be expensive to manufacture and operate; they also have a limited field of view and can potentially become over-saturated depending on how many objects are in their field of view at a given point in time. [2] One proposed solution to improve Space Domain Awareness is SpaceNet.

SpaceNet would be a network of low-cost, low-fidelity ground stations that would relieve high-fidelity sensors by reducing the number of objects they would have to monitor. The concept is that thousands of low-fidelity sensor units could be deployed across the country and monitor radio frequency (RF) signals pinged down from satellites in LEO orbit. The recorded data would be transmitted from ground

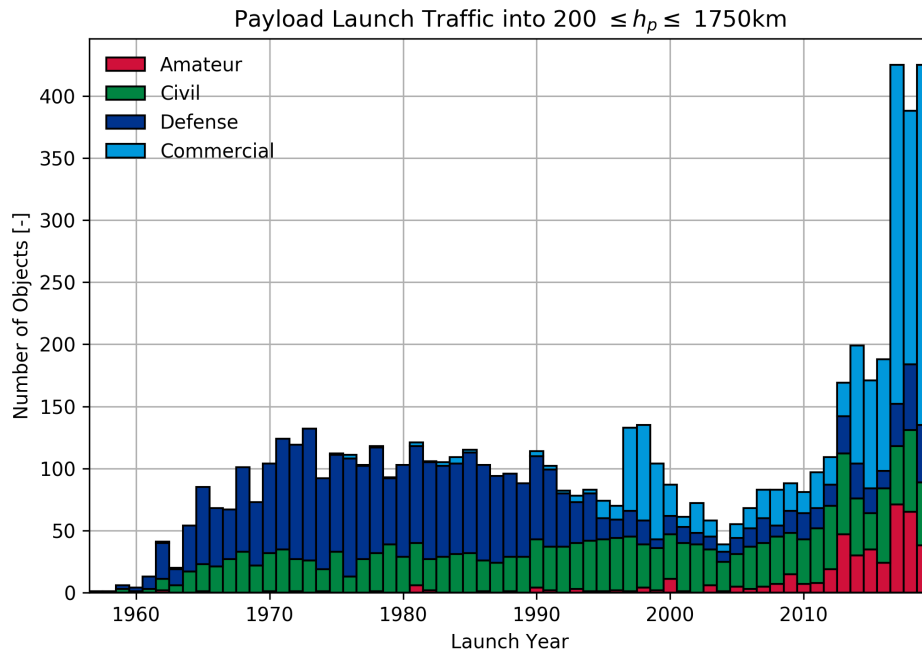


Figure 2: Plot from the ESA that shows the recent spike in planned mission for LEO space domain. A majority of these mission are commercial with a rise in Amateur level missions since 2010. <https://sdup.esoc.esa.int/discosweb/statistics/>

stations back to a central computer. The central computer would perform Time Delay of Arrival (TDoA) algorithms to determine an object's position and orbit. This information could then be parsed and flagged if the object is suspected to be out of place at which the point high fidelity sensors can be utilized to fully assess the situation.

This project serves as a four unit proof of concept for this type of low-cost, low-fidelity ground station network. This project will produce four functional ground units that can record UHF/L-Band satellite Quadrature signal (IQ) data from two target satellites. The recorded data will be used with to produce both a position estimation and orbit estimate.

## 2 Project Objectives and Functional Requirements

Authors: E Forest Owen, Keith Poletti, Ryan Prince, Israel Quezada-Cordova, and Benji Smith

The following section outlines what the SpaceNet prototype must accomplish in order to prove itself as a proof of concept for these low cost ground station networks.

### 2.1 Concept of Operations

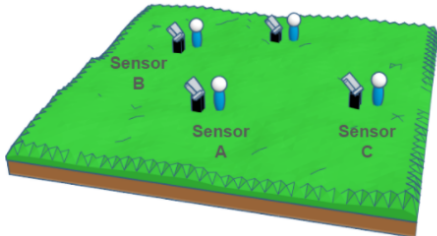
Figure 3 shows the concept of operations and how the SpaceNet prototype will work.

The first step is that the sensor units will be temporarily deployed to predetermined locations. These locations will be areas that we have made arrangements with to leave the units there for extended periods of time while connected to wall power. The units will be pre-programmed with expected passes and frequency ranges. Once all the units have been deployed and powered on they will automatically initiate the SDR and GPS module in preparation for data collection.

1. Sensors are temporarily deployed
2. Sensors synchronize to UTC time



3. Satellite **transmits** during flyby
4. **Transmissions** are received by sensors



5. **Transmissions** are identified post test

6. **Time delay** of signal arrival is calculated from UTC time

Sensor A Data	Sensor B Data
UTC12:00:01	UTC12:00:01
UTC12:00:02	UTC12:00:02 <b>GO CU!</b>
UTC12:00:03	UTC12:00:03
UTC12:00:04	UTC12:00:04
UTC12:00:05	UTC12:00:05
UTC12:00:06	UTC12:00:06
UTC12:00:07	UTC12:00:07
UTC12:00:08	UTC12:00:08
UTC12:00:09 <b>GO CU!</b>	UTC12:00:09
UTC12:00:10	UTC12:00:10

7. **Time delay** is used to estimate satellite position

8. **Position** used to estimate orbit

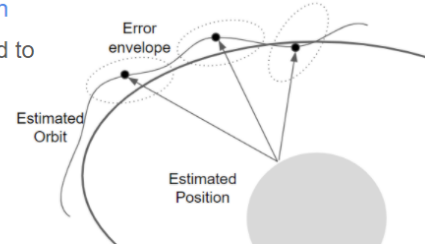


Figure 3: SpaceNet Concept of operations(CONOPS)

As the expected satellite passes over head the units will automatically start data acquisition based on UTC time provided by the GPS. The ground stations will all receive the same transmission that is pinged down from the satellite target. data collection will then be paused and the data saved. This process will happen a minimum of 3 times per satellite pass producing three discrete measurements from each of the four units every pass over. This data will be stored on the sensor units SD card until it is manually off loaded by physically removing the SD card from the sensor unit. The data will then be moved to a central computer for processing.

Each set of RF data from the individual units will have time synchronized RF signatures that can be used to align each of the data sets with on another. Once the data sets have been aligned the data can be parsed to determine at what relative time each of the sensor units received the satellite transmission. Time delay of signal arrival to each of the sensor units can then be calculated by using the earliest instance of signal reception as time zero. Time delay can then be used to produce position vector estimates that can ultimately be converted into a prediction of the satellites orbit.

## 2.2 Success Criteria

Based on the CONOPS shown in Table 1 lists specific objectives for each of the project's core components that must be met to achieve project success. Sections are subdivided into various levels of mission success. Level 1 being marginal performance that meets the project objective of orbital determination. The highest level implies fulfilment of the lower levels and represents completion of the entire project scope.

Table 1: Levels of Success as defined in CDD

<b>Sensor Unit Packaging</b>	
<b>Level 1</b>	<ul style="list-style-type: none"> <li>*Sensor Packaging shall integrate all hardware</li> <li>*Sensor Packaging shall weigh less than 50 lbs and be contained within 5'x5'x5' volume</li> </ul>
<b>Level 2</b>	<ul style="list-style-type: none"> <li>*Sensor packaging shall keep components within operating temperature range in all expected temperatures and conditions (direct sunlight, rain, cold, wind, variable (snow))</li> <li>*Sensor shall be a self-contained with access to an external power source and network interface</li> <li>*Packaging shall use standard USB connectors, Coaxial Radio Frequency(RF) connectors, and National Electrical Manufacturers Association(NEMA) 5-15 socket</li> </ul>
<b>Level 3</b>	<ul style="list-style-type: none"> <li>*Sensor packaging shall withstand 24 hours of autonomous operation with no sign of compromise (no box leaks, or physical damage)</li> <li>*One unit produced (w/ schematics, procedure, and manufacturing analysis)</li> </ul>
<b>Sensor Unit Data Acquisition Subsystem</b>	
<b>Level 1</b>	<ul style="list-style-type: none"> <li>*Sensor shall use an commercial SDR unit</li> <li>*Sensor shall use standard connectors for ease of manufacturability</li> <li>*Sensors shall collect Ultra High Frequency (UHF) radio signals.</li> <li>*Unit shall be autonomous</li> </ul>
<b>Level 2</b>	<ul style="list-style-type: none"> <li>*Onboard software shall be able to store data.</li> <li>*Software shall be able to return to nominal operation after an power outage</li> <li>*Sensors shall be equipped with a Global Positioning System (GPS) receiver for RF signal timing</li> </ul>
<b>Level 3</b>	<ul style="list-style-type: none"> <li>*Sensor shall collect UHF and LBand signals (Dual Band)</li> </ul>
<b>4 Sensor Network</b>	
<b>Level 1</b>	<ul style="list-style-type: none"> <li>*Time Delay of Arrival (TDoA) algorithm produces position vectors with a test data set..</li> </ul>
<b>Level 2</b>	<ul style="list-style-type: none"> <li>*TDoA algorithm produces position vector with recorded data</li> </ul>
<b>Level 3</b>	<ul style="list-style-type: none"> <li>*Four units produced, mounted, and operational.</li> <li>*Manufacturing documentation (schematics, procedure, manufacturing analysis, suggested improvements, and ways to drive down cost )</li> <li>*TDoA result can be used for orbital prediction</li> <li>*Error analysis report comparing SpaceNet to higher fidelity alternatives                             <ul style="list-style-type: none"> <li>- Compare the data gathered with SpaceNet with the data gathered by higher fidelity systems, like LASP ground station.</li> </ul> </li> </ul>

### 2.3 Conceptual System Design

In an attempt to approach satisfying all the success criteria laid out previously, it may be extremely pedagogical to think about the overall flow of the project. Taking into account all the individual components from the physical structures, all the way down to the software making use of the full systems hardware components. Which can be seen at a high level view in the flow diagram, Figure 4. On the very left-hand side of this flow diagram, we can see the entirety of the physical components comprising this system. Namely the RF front end which includes the antennas, LNAs (Linear Noise Amplifier), and the SDR (Software Defined Radio). Followed by the brains and heart of our project, the raspberry

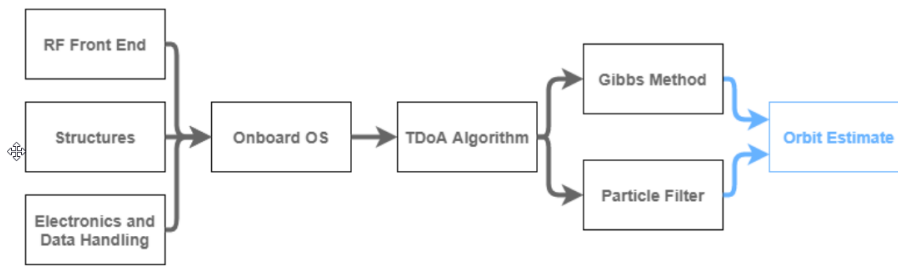


Figure 4: Conceptual Block Diagram

Pi and electrical power delivery system respectively. The last remaining physical component that we had to worry about was the weather proofing and enclosure keeping everything together as a cohesive unit. All of this is directly followed by the data handling system, which is completed by the on-board custom operating system. This reads the raw data received by the SDR with a superimposed PPS (Pulse Per Second) signal and writes to our on-board storage. With the actual usable data now recorded on a removable storage device, our post processing software can now take over beginning with the signal isolation and application of our TDOA algorithms. These 4 pseudo-ranges produced by each of the 4 ground units independently will give us an estimate of the satellites position at the time of transmission. By using these range estimates at multiple different time intervals, our two independent orbital prediction methods can take over the final step in the process. The team handles this portion of the analysis process utilizing Gibbs method and the more experimental and complicated application of a Particle Filter.

### 2.3.1 RF Front End

Beginning first off with a deeper dive into signal acquisition with the RF components. One of the main drives for this part of the project was the dual band requirement specifically being UHF[300MHz-3GHz] and L-Band[1-2GHz]. Though these frequency bands overlap, consistent status and identifier pings from satellites that use these two communications bands require a low data rate and are handled on the lower end of each frequency range[300MHz for UHF, and 1GHz for L-Band]. Each one of these signals requires a different antenna to be captured beginning with a Yagi antenna for the UHF-Band and an active patch antenna for the L-Band. Immediately following these antennas, two separate LNAs will be used to handle the varied frequency ranges. Before our now properly amplified signals can be fed into the SDR, there needs to be way in which we can switch between these signals on the fly, this comes in the form of a computer-controlled RF switch. Finally, the signal data is fed into the SDR for final signal conditioning before being recorded to removable storage by the Raspberry pi.

### 2.3.2 Structures

Holding everything together begins on the inside of our enclosure, starting with a custom designed acrylic plate to act as a mounting surface for the growing list of internal components. It is important to note that not all of these components can just be installed flat on the bottom, due to inherent size constraints placed on our system by the NEMA 4 rated enclosure that we have ended up going with. With all the components like the SDR, GPS chips, and main computer for example, being firmly secured in place inside of the NEMA enclosure, we now need a method in which to mount the antennas on the

exterior of the box. This comes in the form of aluminum L brackets with dedicated holes for screws and zip ties to directly mount it to a pole. T-shaped PVC tubing is being used as mounting points for the antennas.

### **2.3.3 Electronics and Data Handling**

For this project, the electronics in the units will help to determine the orbital position of satellites that are detected. The RF front end will take in RF signals from satellites with signal conditioning applied by the LNA's and SDR. After the signal conditioning of the RF signals, they will be transferred to the on-board computer and then stored locally to be post processed at a later time and location. The GPS module timing and location data will be fed into the on-board computer, this particular data will be useful for the time synchronization of the RF data received by the units. The timing synchronization of the received RF data is helpful for the orbital and positional estimation techniques that will be used in this project.

### **2.3.4 On-board OS**

The on-board OS used with the on-board computer for the units in this project will determine and control all the operations that take place on the units while they are functioning and recording RF data from satellites. The OS will be responsible for initiating the start up routine for the on-board computer for each of the units when they are each powered on or reset. The OS will also interact with the different applications that need to be used in order to control the different electronics used in each unit, such as the SDR and the GPS module. The on-board OS will also help control the flow and storage of collected RF data to memory on the on-board computer.

### **2.3.5 TDoA algorithm**

The TDoA algorithm is the first portion of the primary data post-processing system. Raw radio signal data will be gathered by the four sensor units and transferred manually to a central computer. The TDoA algorithm is responsible for producing satellite positional data for use in the orbital position algorithm from differences in signal time of arrival. To verify the success of the algorithm, the produced positioning estimate will be compared to truth data from public domain sources. The success criterion for this algorithm requires that 99.6% ( $3\sigma$ ) of positioning estimates are precise to 100 km absolute error.

### **2.3.6 Gibbs Method**

The Gibb's Method algorithm is the second portion of the primary data post-processing system. This algorithm will take the positional data produced by the TDoA algorithm to determine velocity data. The velocity and position data make up a state vector, which is passed to the orbital estimate algorithm. The validity of the state vector produced by Gibb's Method will be evaluated by the derived orbital estimate and success criteria will be discussed in the following orbital estimate subsection.

### **2.3.7 Particle Filter**

A particle filter predicts a satellites position and velocity based on raw time delay measurements. A particle filter accounts for noise in its model. This can improve the orbital estimate accuracy. It produces a position and velocity based on iterative measurements. The finer details will be discussed in section four.

### 2.3.8 Orbit Estimate

The orbital estimate algorithm receives a state vector from an orbital determination algorithm and is responsible for producing a set of Keplerian orbital parameters (e.g. inclination, eccentricity, RAAN, etc.) The calculated orbit will be propagated and compared to truth data.

Success criteria for this estimate require that the produced orbit can estimate the time and position in the sky of a future pass. It will be required for success that recorded data can be used to produce a TLE prediction of a known satellite candidate that is able to predict a future passover within one day of data collection to  $\pm 45$  min start time accuracy,  $\pm 30$  deg azimuth accuracy at the start of the passover and  $\pm 15$  deg elevation at the midpoint.

## 2.4 Functional Block Diagram

Figure 5 fleshes out the conceptual block diagram shown in Figure 4 into a functional block diagram that describes the components and their interactions. Note the CBD in Figure 4 and the FBD in Figure 5 only show one of the four units that will be built for the project.

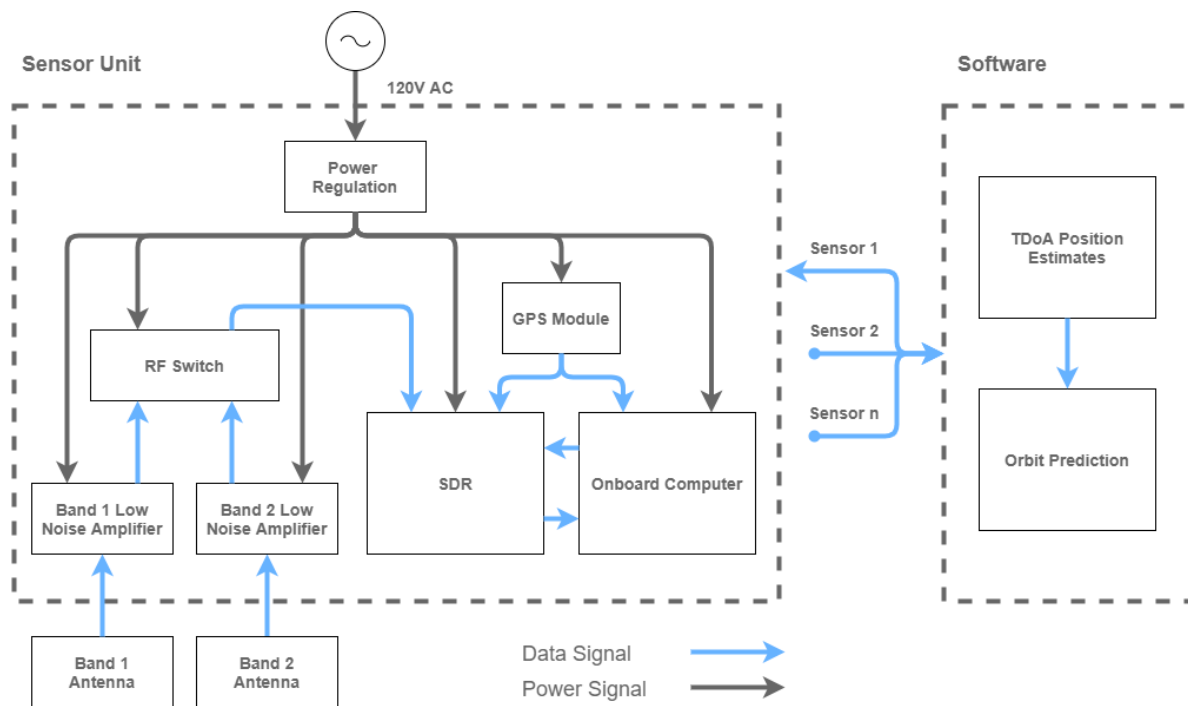


Figure 5: Functional Block Diagram

## 2.5 Functional Requirements

The following is a list of functional requirements based on the explanation of the systems goals and intended operation. Each requirement is accompanied by a justification explaining how it fits into the project scope.

- FR 1. The sensor unit shall be weather resistant and capable of nominal operation outdoors for 24 continuous hours.

**Motivation:** To be able to capture data for this project these sensor units must be placed outside thus must be able to operate nominally outdoors for a period of 24 hours. This allows the sen-

## SpaceNet Electronics and Data handling

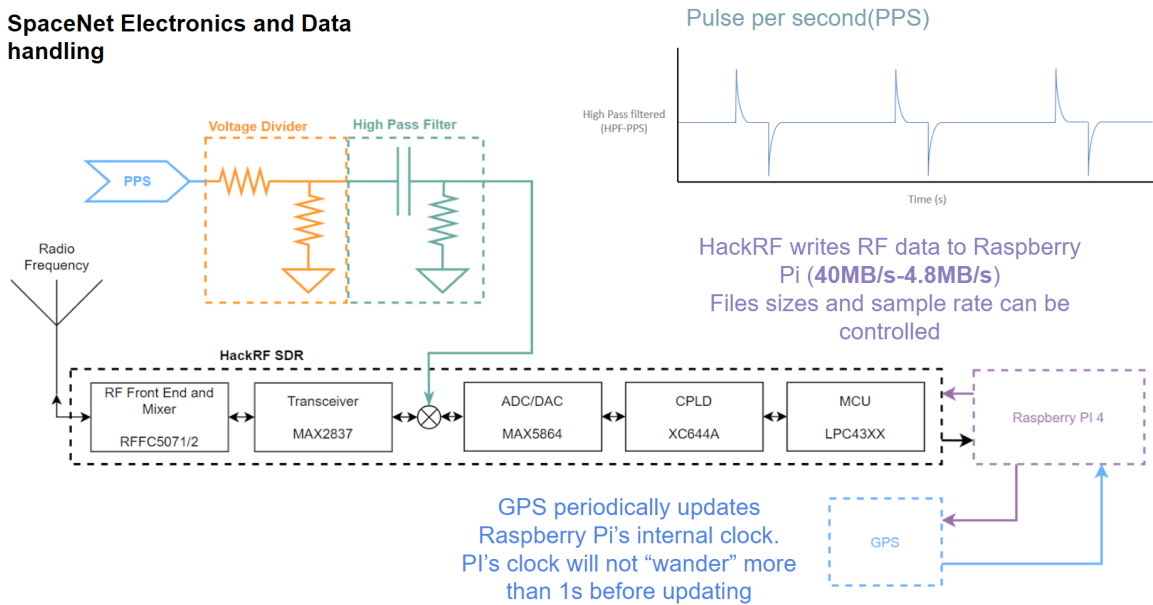


Figure 6: Electronics Functional Block Diagram

sensor unit to remain operation independent when the satellite pass occurs allowing successful data capture and overall successful for our project.

FR 2. The sensor unit shall be transportable and deployable by a single individual

**Motivation:** Since these sensor units will be placed in various geographical locations the the unit must be easily transportable and deployable by a single individual. This ensures that these unit can be placed wherever needed to achieve the required data and can be done so efficiently and effectively.

FR 3. Each sensor unit will be capable of receiving RF signals from both UHF and L-band ranges.

**Motivation:** This requirement is key for the project, showing the feasibility of capturing several different RF signals in a cost effective manner is one of the main goals of this project. The UHF and L-Band signals were selected for capturing in this project due to both the availability of satellites transmitting in these frequency ranges, and the availability of consumer antennas for these selected ranges.

FR 4. The RF system will be capable of obtaining RF lock such that lock is achieved by at least three units at a time.

**Motivation:** This is the minimum number of ground stations needed to perform TDoA ranging. Without this number of units the system will be unable to produce position vectors.

FR 5. Recorded data can be used to produce a orbital position within a  $3\sigma$  confidence of 100 km of a known satellite candidate.

**Motivation:** At a fundamental level, the goal of this project is to be able to say where an overhead satellite is and to predict when it will be overhead again. With 100km  $3\sigma$  allowable error bounds, future positioning estimates will remain within the error bounds and the produced two line element set will accommodate FR 6.

FR 6. Recorded data can be used to produce a TLE prediction of a known satellite candidate that is able to predict a future passover after 1 day within  $\pm 45$  min time accuracy,  $\pm 30$  deg azimuth accuracy at the start of the passover and  $\pm 15$  deg elevation at the midpoint.

**Motivation:** This orbital determination requirement represents the overall culmination of the SpaceNet project. The process of characterizing the usefulness of a TLE is not standardized, and so the specifications detailed in FR 6 show how the quality of our calculated orbital elements will be measured. Being able to satisfy the elements detailed by FR 6 will show that we were not only able to generate orbital elements for a satellite pass over, but also that the orbital elements generated are usable and capable of making actionable predictions.

FR 7. The sensor unit shall be easily accessible and easy to manufacture.

**Motivation:** In order to be able to increase the scope of the system, additional sensor units must be fabricated and placed across a large land area. To facilitate this future expansion, the sensor unit was designed to be easily producible using standard, readily available parts.

### 3 Final Design

Authors: E Forest Owen, Israel Quezada-Cordova, Sam Firth, Benji Smith, Ryan Prince

#### 3.1 Requirements Flow down

This section outlines the functional (FR X.) and derived (FR X.X) requirements for the system explaining why they are necessary in the context of the project. The corresponding verification methods and validation results for each requirement are outlined in section 5.

FR 1. The sensor unit shall be weather resistant and capable of nominal operation outdoors for 24 continuous hours it crucial for this project.

**Motivation:** To be able to capture data for this project these sensor units must be placed outside thus must be able to operate nominally outdoors for a period of 24 hours. This allows the sensor unit to remain operationally independent on when the satellite pass occurs allowing successful data capture and an overall successful project.

FR 1.1. The sensor unit packaging shall be able to maintain a dry environment through rain and snow when in operating position.

**Motivation:** To be able to capture data for this project these sensor units must be placed outside thus must be able to operate nominally outdoors for a period of 24 hours. This allows the sensor unit to remain operationally independent on when the satellite pass occurs allowing successful data capture and an overall successful project.

FR 1.2. The sensor unit packaging shall be capable of maintaining an internal operating temperature range of 0-50 degrees Celsius

**Motivation:** As states above the times at which data collection will have to occur are based on orbital passes as such the electronics hardware inside the unit must stay in operating temperature ranges given the outside weather.

FR 2. The sensor unit shall be transportable and deployable by a single individual.

**Motivation:** Since these sensor units will be placed in various geographical locations the the unit must be easily transportable and deployable by a single individual. This ensures that these units can be placed where ever needed to achieve the required data and can be done so efficiently and effectively.

FR 2.1. The deployed sensor unit and antenna shall fit within a 5'x5'x5' space.

**Motivation:** Further more, in order for the sensor unit to be transportable by a single individual the whole unit shall fit within a 5'x5'x5' space. This further ensure that unit can be easily transportable and deployed by a single individual.

FR 2.2. During operation sensor unit electronics shall be enclosed into a single housing. This does not include antenna, antenna mount, or power source.

**Motivation:** The basis for this requirement is to ensure that the sensor unit electronics will remain operational throughout the whole system deployment. Enclosing the components in the housing ensures operation and protection for each device.

FR 2.3. Sensor unit electronics box, antenna, and antenna mount shall have an individual weight less than or equal to 50 pounds.

**Motivation:** This requirement correlates to the sensor unit being deployable by a single individual as unit must provide adequate user interface with respect to handling. By providing a unit less than or equal to 50 pounds as set by our customer the unit will be deployable by a single individual. An optimized scenario here will be on lower end of this weight spectrum.

FR 2.4. The SDR shall be commandable from the on-board computer.

**Motivation:** Having the SDR commandable from the on-board computer will allow the units to function autonomously. This will let the on-board computer control the SDR so that it does not have to be manually controlled. This will eliminate any human error as well as ensure that there is clean and clear communication between the SDR and computer. Overall, having the SDR commanded by the computer will also result in better precision and more

accurate timing.

FR 2.5. The on-board computer will be able to return the system to nominal operation autonomously.

**Motivation:** Being able to return the system to its nominal operation automatically will allow the team to trust the system while it is operating in the field. This ensures that each sensor unit can be placed in a location and left there without having to physically command the unit. This also improves the capability of the system as there will be no human error associated with the timing and running of the unit.

FR 3. Each sensor unit will be capable of receiving RF signals from both UHF and L band ranges.

**Motivation:** This requirement is key for the project, as showing the feasibility of capturing several different RF signals in a cost effective manner is one of the main goals of this project. The UHF and L-Band signals were selected for capturing in this project due to both the availability of satellites transmitting in these frequency ranges, and the availability of consumer antennas for these selected ranges.

FR 3.1. Each sensor unit shall have a minimum UHF G/T of -20 dB/K with a target value of -15 dB/K.

**Motivation:** The design requirements for gain-over-noise are important, as is a figure of merit in the characterization of antenna performance, where G is the antenna gain in decibels at the receiving frequency, and T is the equivalent noise temperature of the receiving system in kelvins. The noise of the system is induced by the components linking the antenna to the processing hardware, and large losses will result in extreme noise making data analysis difficult or unfeasible. The value of UHF G/T of -20 dB/K with a target value of -15 dB/K was selected, as UHF frequency range encounters a higher system temperature due to common frequency noise in the UHF range.

FR 3.2. Each sensor unit shall have a minimum L-band G/T of -17 dB/K with a target value of -13 dB/K.

**Motivation:** Same as with the UHF band antenna, The design requirements for gain-over-noise are important, as is a figure of merit in the characterization of antenna performance. The noise of the system is induced by the components linking the antenna to the processing hardware, and large losses will result in extreme noise making data analysis difficult or unfeasible. For the L-Band antenna, the requirements for G/T are more stringent as the signal strength from L-Band is much higher gain than that of UHF, resulting in overall more positive G/T values.

FR 3.3. Each sensor unit shall have a minimum UHF link margin of 3 dB with a target of 5 dB.

**Motivation:** Our customer stated that our link margins, calculated by subtracting losses due to hardware and the atmosphere from the satellites transmission power, needed to be above 3 dB for the UHF antennas. This margin parameter was originated from standard ground station protocol in order to allow for gain attenuation that is not modeled correctly in the system.

FR 3.4. Each sensor unit shall have a minimum L-Band link margin of 3 dB with a target of 5 dB.

**Motivation:** The link margin requirements of the L-Band antennas were originated on the same basis as the UHF antenna link margin requirements, as both types of antenna will be subject to the same decibel attenuation conditions throughout the overall system, and 3 dB range is an allowable margin for our project's price point and hardware parameters.

FR 3.5. Each sensor unit shall be capable of supporting both signals (not necessarily simultaneously) without the need for hardware modification.

**Motivation:** This requirement, referring to both the L-Band and UHF band signals, allows for the system to intake both RF signals from either antenna for filtering and storage without needing to allocate a team member/operator to physically switch from the two antennas. This requirement is valuable to this project as the main intention of the system is to be placed in possibly remote locations in which operators cannot be present at all times.

FR 3.6. The RF front end must be able to cover  $\pm 10$  MHz of the target UHF frequency.

**Motivation:** In order to have margins of error for the antenna, the  $\pm 10$  MHz allowance for the UHF Band's satellite's transmission frequency was required, as effects such as Doppler shift could cause frequency variation on the range of  $\pm 10$  kHz.

FR 3.7. The RF front end must be able to cover  $\pm 10$  MHz of the target L-band frequency.

**Motivation:** As with the above requirement, In order to have margins of error for the antenna, the  $\pm 10$  MHz allowance for the L-Band satellite's transmission frequency was required, as effects such as Doppler shift could cause frequency variation on the range of  $\pm 10$  kHz.

FR 3.8. The SDR must have tunable frequency that covers 90% of the UHF/L-band range (300 MHz to 3 GHz)

**Motivation:** This requirement increases the scope of the system but is countered by cost; an expensive SDR will have a larger tunable range. Being able to receive 90% of the UHF/L-band frequencies

FR 4. The RF system will be capable of obtaining RF lock such that lock is achieved by at least four

units at a time.

**Motivation:** This is the minimum number of ground stations needed to perform TDoA ranging with out this number of units the system will be unable to produce position vectors.

FR 4.1. Antenna shall have a 360 degree azimuth FOV.

**Motivation:** This requirement is necessary for both the UHF and L-Band antennas, as full horizontal FOV is necessary in having full view of the horizon, and encountering both RF signals while satellite is within line-of-site of the system.

FR 4.2. Antenna shall have a beamwidth no less than 30 degrees.

**Motivation:** This requirement s necessary for both the UHF and L-Band antennas, as a narrower beamwidth will not allow for a sufficient data capture of the RF signals with regard to time, as the satellite will be out of the field of view.

FR 5. Recorded data can be used to produce a orbital position within a  $3\sigma$  confidence of 100 km of a known satellite candidate.

**Motivation:** At a fundamental level, the goal of this project is to be able to say where an overhead satellite is and to predict when it will be overhead again. With  $3\sigma = 100$  km allowable error bounds, future positioning estimates will remain within the error bounds and the produced two line element set will accommodate **FR 6**.

FR 5.1. Individual sensor units shall maintain timing precision no more than 420 ns

**Motivation:** The process of multilateralization, the method used by the system to produce a positional estimate of an overhead satellite, is highly sensitive to timing error due to the fact that RF signals propagate at the speed of light. Therefore, in order to provide a position estimate precise enough to satisfy **FR 5**, each sensor unit will maintain a timing synchronization via GPS within no more than 420 ns.

FR 5.2. The SDR shall be capable of sample at least 2.4 million samples per second.

**Motivation:** This is a threshold generated through computational modeling necessary to produce accurate enough measurements for positional and orbital predictions.

FR 5.3. The sensor units shall be placed at least 100 km apart.

**Motivation:** This is a threshold generated through computational modeling necessary to produce accurate enough measurements for positional and orbital predictions.

FR 5.4. The onboard SDR shall have a tunable bandwidth of at least 5 MHz in either direction, For a total bandwidth of 10 MHz.

**Motivation:** This is the minimum bandwidth needed to record the satellites transmission and not lose data given a worst case modulation scheme assumed to be WFM.

FR 5.5. Each sensor unit shall have onboard storage capacity for 4 passes worth of RF data.

**Motivation:** Allowing for the capability of tracking multiple targets in a 24 hour period.

FR 6. Recorded data can be used to produce a TLE prediction of a known satellite candidate that is able to predict a future pass-over after 1 day within  $\pm 45$  minute time accuracy,  $\pm 30$  deg azimuth accuracy at the start of the pass-over and  $\pm 15$  deg elevation at the midpoint.

**Motivation:** The flow from satisfying **FR 5** to **FR 6** of our project is entirely defined by the software defined post-processing we apply to our data sets. This means that the positional estimates we gather from the application of TDoA comparison, within the tolerances specified by **FR 5**, we will be able to satisfy with additional software model maturity. Due to a reliance on the positional estimate tolerances defined by **FR 5** in satisfying **FR 6**, the same design requirements driven by **FR 5**, namely **FR 5.1**, **FR 5.2**, and **FR 5.3** are also equally driven **FR 6**.

FR 7. The sensor unit shall be easily accessible and easy to manufacture.

**Motivation:** In order to be able to increase the scope of the system, additional sensor units must be fabricated and placed across a large land area. To facilitate this future expansion, the sensor unit was designed to be easily producible using standard, readily available parts.

FR 7.1. A complete sensor unit and antenna ready for deployment shall have a parts cost less than \$1000.

**Motivation:** Here our goal is to make four sensors, so in order to stay under our \$5000 senior projects budget, our approximate goal for each sensor unit is \$1000. This also helps with the ultimate vision of having a large, cheap deployment of sensors to do SSA as current ground sensor station arrays are more expensive by multiple orders of magnitude.

FR 7.2. Sensor unit shall use all standard connectors

**Motivation:** Keeping in theme with ease of manufacturing, each sensor unit will utilize only standard connectors. This will reduce production complexity and help keep the per-unit cost low.

FR 7.3. Sensor unit shall be powered off of a standard NEMA 15 socket

**Motivation:** Similarly, to maintain manufacturing simplicity and costs, each sensor unit will be powered via the US standard power socket, the three-phase, 15 A, 125 VAC NEMA 15 connector.

### 3.2 Final Design

Starting with the external model as can be seen in the Figure 7, the sensor unit stands at height of 3.8 feet, and weighs approximately 24 lbs. When deployed these units will at a maximum height of five feet to six feet, depending on how far the mounting poll can be driven into the ground as this will vary per location. This provides ample room such that the units will not be submerged upon a large snowfall, and ensures the units are protected to some degree from various hazards on the ground.

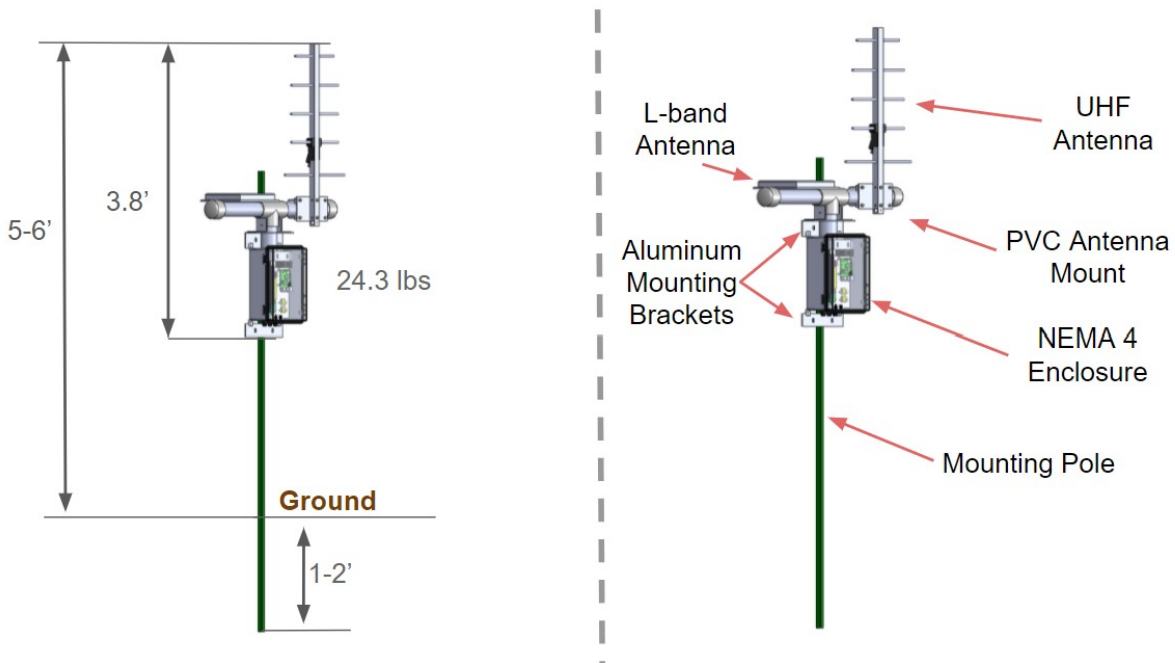


Figure 7: External Model

In terms of hardware, the external aspect of the unit houses the RF-front end which consists of the L-Band and UHF antenna. The chosen housing structure was NEMA 4 enclosure which is secured using aluminum mounting brackets on the top and bottom of the box. These brackets are what are also used to secure the PVC antenna mount for which the antenna are mounted to. This allows the housing unit to be mounted in the configuration above upon deployment.

Stepping into the internal model, this houses the data handling and electronics. A NEMA 4 enclosure was chosen with the following dimensions in order to provide enough maneuverability such that parts may be rearranged if needed, and its inherit waterproofness that provides protection from the outdoor elements.

The structure internally houses the key components such as the antenna switch, each antenna's respective LNA, SDR, GPS, and Raspberry Pi. These components allow the signal acquired by the RF front end to be processed and time stamped, while also providing an on-board operating system for each unit.

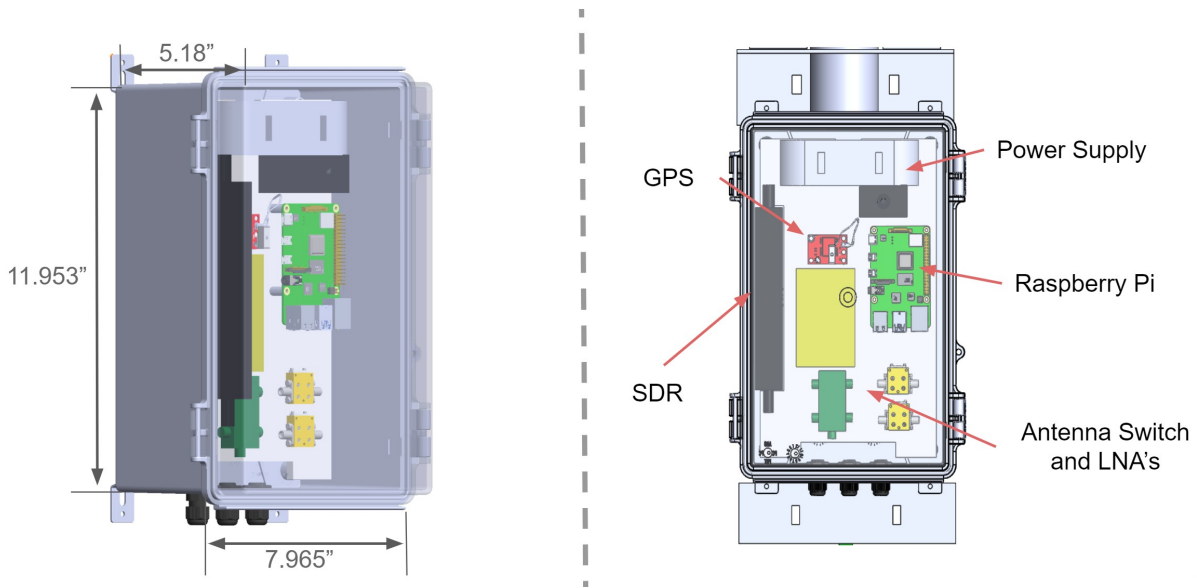


Figure 8: Internal Model

The hardware block diagram can be seen in Figure 9. The main components that were implemented into the on-board operating system consisted of a Raspberry Pi, an SDR, a GPS, a switcher, and finally the USB memory stick. The Raspberry Pi was the backbone of this system as it was used as the computer that was programmed to autonomously run and control all of the external systems and components. As it can be seen in Figure 9, all the components are linked to the Raspberry Pi. The HackRF which was the chosen SDR was connected to the Raspberry Pi via USB. The Neo 7m GPS was linked to the Raspberry Pi via the GPIO pins on one end and linked to the HackRF on the other end. The switcher which switches between the different bands was linked to the Raspberry Pi. Finally, the data storage that stores all the received information was plugged in via USB to the Raspberry Pi. Other electronic components in the unit such as the Low Noise Amplifiers were not attached to the Raspberry Pi, These components were passive components and do not require any software integration or programming.

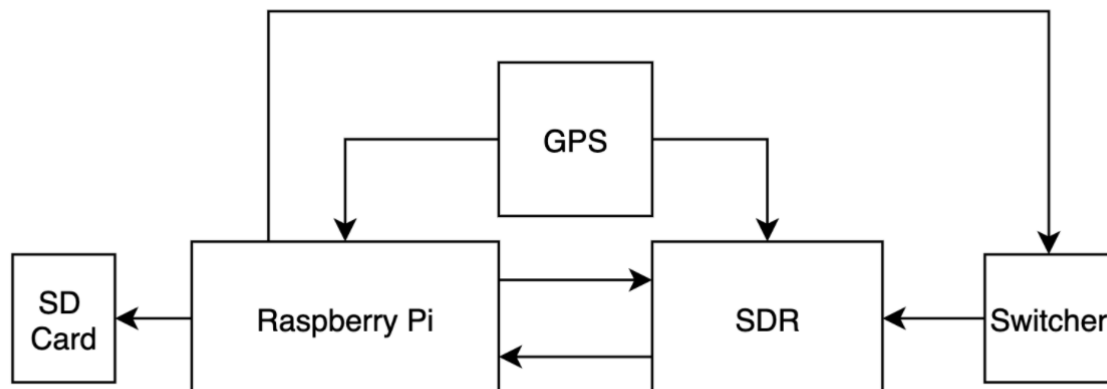


Figure 9: Hardware Block Diagram

The Raspberry Pi was programmed and configured using command line that ran off the Raspbian OS

which is a Linux based system. Here is where all the settings were pre-programmed to ensure that the desired frequency bands, and data sampling was corrected implemented. Through command line the frequency, sample rate, and the amount of time the signal was recorded is programmed on the HackRF. Moreover, the flyby times for the satellites were programmed in the Raspberry Pi. The sequence of events can be referenced in Figure 10: software block diagram. During the system deployment, the Raspberry Pi will be continuously collecting timing data from the GPS. This timing data will be checked with the previously programmed flyby times. When these two times match up, the Raspberry Pi will verify them and thus start the autonomous sequence that will run the required subroutines. Depending on what satellite is passing over, the Raspberry Pi will send a signal to the switcher that is connected to the respective LNA that matches the transmitted signal type. The Raspberry Pi will then instruct the HackRF to start collecting data at the pre-programmed frequency and sample rate. This will then collect data, slim it, and store it onto the USB data storage with the proper naming convention.

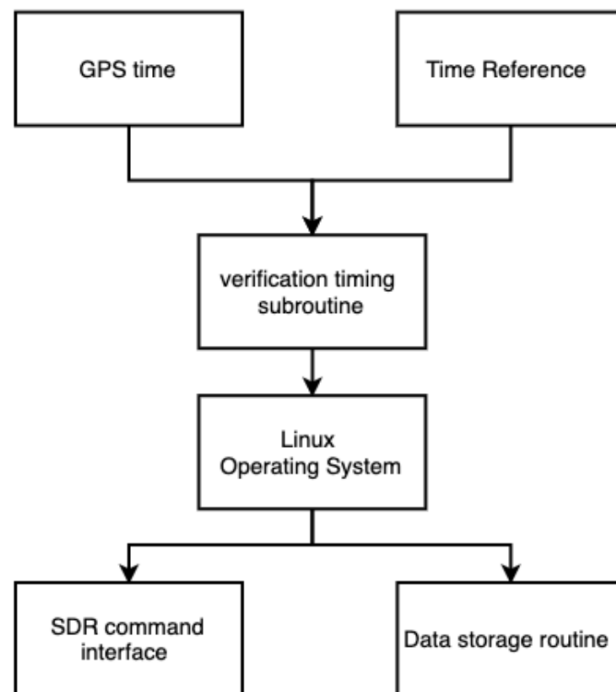


Figure 10: Software Block Diagram

Overall, this process will create a loop. Once the satellite has finished passing over the sensor unit the operating system will verify this using another pre-programmed timestamp and the GPS. This will then command the SDR to stop collecting and storing data. This completes the loop and the sensor unit will go back to its initial steady state waiting for the next time verification and satellite pass over, thus starting the sequence all over again. The loop state diagram can be referenced in Figure 11.

A completed set showing all hardware that utilizes the operating system and its components can be seen in Figure 12:

The on-board GPS is also used to produce a pulse per second (PPS) signal that is doctored and superimposed onto the SDR RF data. The superimposed signal creates a globally synchronized RF signature. This signature is used to align the individual data streams in post processing. As explained later in section 4.2.2, the timing scheme is capable of synchronizing the data with at most 420 ns of error. The

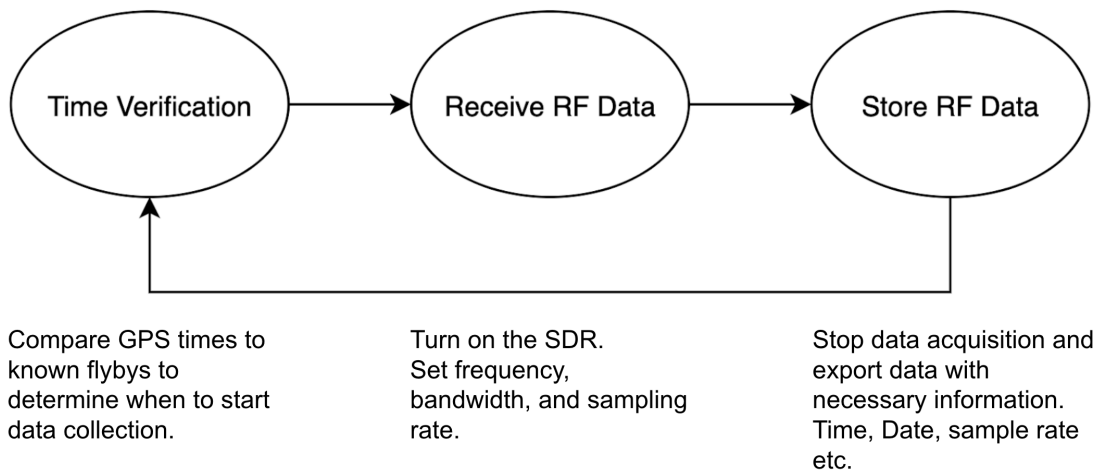


Figure 11: State Diagram

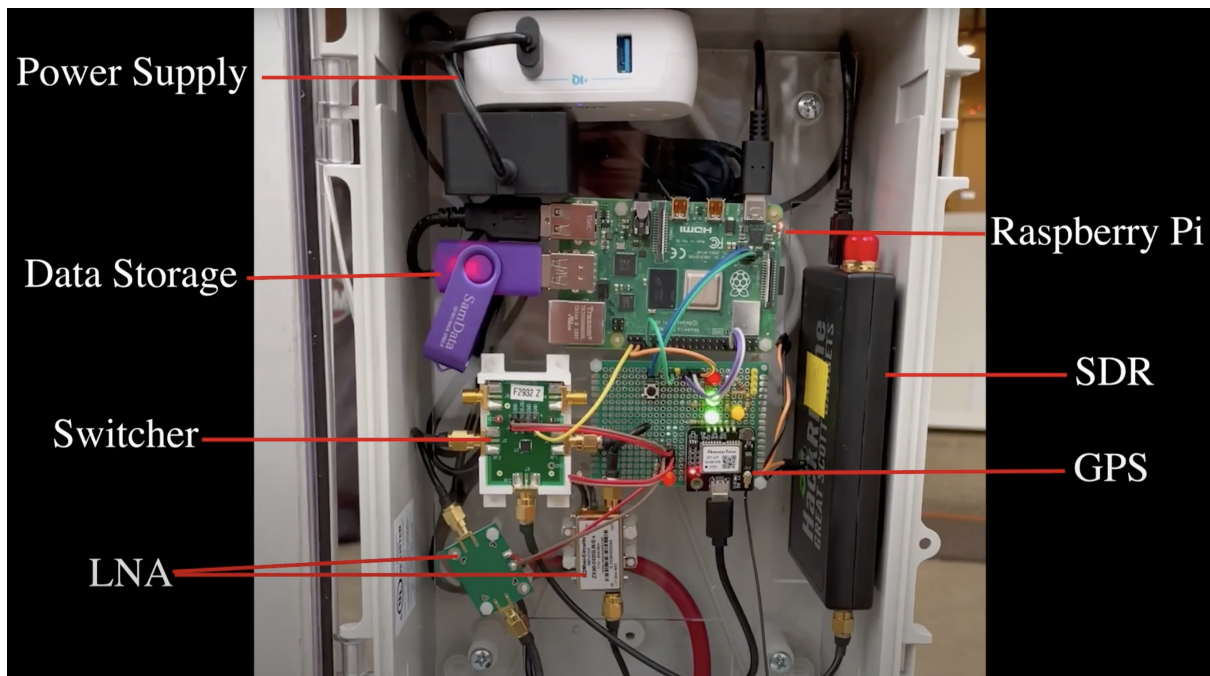


Figure 12: Completed Hardware Setup

requirement of 420 ns is a derived requirement from **FR 5 and FR 6** set forth by the orbital determination algorithm.

Each unit is equipped with two RF front ends that are connected to the the HackRF SDR via an electronically controlled RF switch. Each front end is tuned for separate frequencies. One is in the UHF range and the other is in L-band range. Each target satellite will be transmitting on one of these bands. Each RF front end consists of an antenna and an LNA both tuned for the target frequencies. The antennas are also specified to have adequate gain such that all units will be able to see the satellites as they fly overhead. Depending on the number of units, this requirement could be realized as more units can be used to make orbital guesses. Overall, the RF front ends enable the units to record data on both UHF and L-band frequencies satisfying **FR 3**.

## **4 Manufacturing**

Authors: Ryan Burdick, Noah Francis, E Forest Owen, Tyler Pirner, Keith Poletti, Ryan Prince, Israel Quezada-Cordova, and Colin Ruark

The following section summarizes the scope of the manufacturing tasks in the project. The section explains if the parts were manufactured in house or outsourced, struggles encountered with manufacturing or procurement, the final result and future recommendations. This summarizes mechanical and electrical hardware as well as software.

### **4.1 Hardware**

With respect to the hardware and the overall housing for the project, key factors that played a roll in the selection of materials for these units included the ability to be easily manufactured (required minimum to no specialized tools) in conjunction with ability to withstand outdoor weather conditions. For this reason a NEMA 4 electrical enclosure was chosen as it provides an inert resistance to ingress of dust and water. Furthermore, by selection of a "plastic" enclosure the housing as a whole would be lightweight and easily mountable. Such enclosures were also able to be purchased with a clear cover/lid which provided means for the GPS antenna to easily acquire signal lock and still be enclosed inside the box. The housing also needed to be able to provide the ability to support dual band capability i.e. a mountable location for two antennas as well as a multipurpose mounting bracket for the structure as whole. This lead to the overall mounting solution, for which aluminium angle and flat stock were used as the upper and lower brackets for the box mounting solution.

The aluminum angle was selected for the top of the housing as it would provide a location for the antenna mount as well be able to be equipped with additional brackets to secure the additional antenna mount to the unit. The antenna mount was constructed using 2" PVC pipe and along with respective fittings as this provided a highly customized and easy to manufacture structure for which the two antennas could be fastened too. This along side with the mounting brackets ensured that the units would be able to endure placement outdoors as both PVC and aluminum ensure prolong use in these conditions.

With the respect to the externals of the box, 3/16" aluminum rivets were used to support and permanently secure the aluminum brackets and supports to the housing structure along with the provided housing hardware. This allowed for a snap and fit placement which meant that if desired, these boxes could be easily constructed in the field, and also ensured that the units still could disassembled down to the mounting brackets, box attachments, and independent antenna mount. This allowed for the unit to be broken down into four main pieces providing portability and ease of multiple unit production,

transportation, and storage. The manufacturing process of each respective section is elaborated below.

#### 4.1.1 Packaging

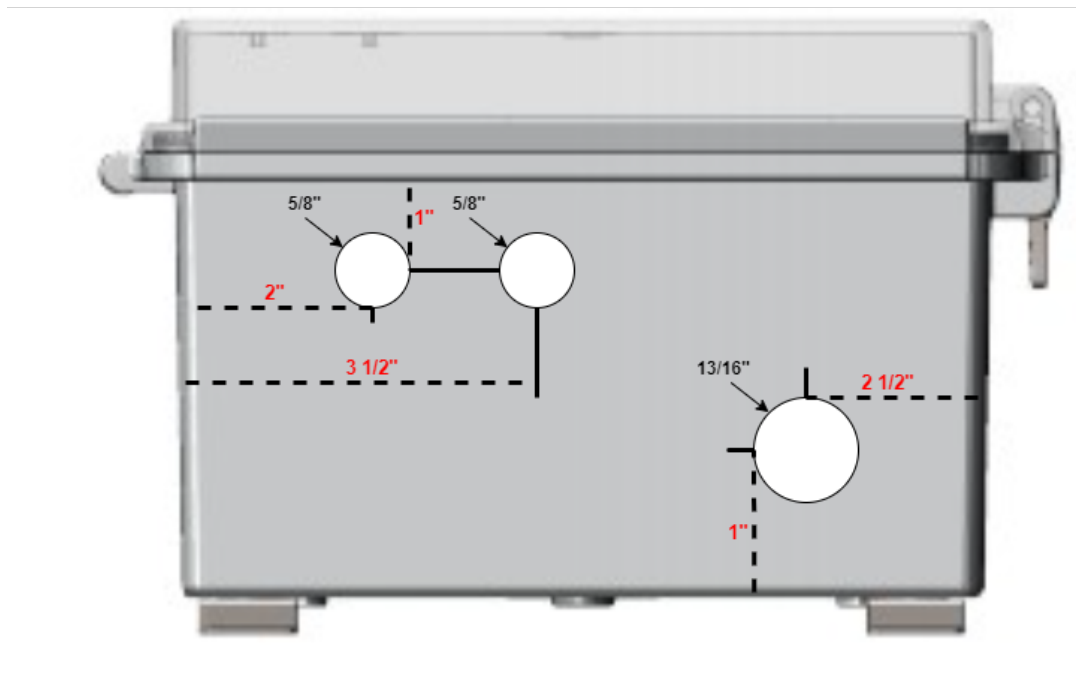


Figure 13: Housing Cable Pass Through Mounting

In correlation to the housing enclosure, NEMA 4 cord grips were drilled into place in order to allow the RF front-end to be connected to the internals of the box while still providing a weather resistant structure capable of maintaining a dry internal environment. For installation, forstner bits were chosen as these would provide clean and precise holes through the enclosure. This in return would ensure a tight seal would be achieved with the cord grips in place and any ingress of water would suggest a fault with the cord grip itself. To precisely determine the proper hole size, the cord grips were measured using a digital caliper and then the closest minimal bit size was chosen. These holes were first drilled into an 1/4" acrylic sheet that roughly matched the thickness of the box wall to ensure a tight fit could be achieved and that the cord grip threads would not interfere upon installment. Once the bit size was finalized from the acrylic sheet test, another simple test was run using a paper towel lined Tupperware container such that the chosen bits were drilled into each of their own respective container then tested by running water over the top and around the edges installed cord grip. Once each box was ran underwater for approximately five minutes, the outside was dried before opening the container to ensure no internal contamination would occur. The container was then opened to determine if there was any noticeable ingress of water. Once assured that the following bit size was deemed suitable, the following holes were drilled into the bottom of the housing structure as indicated in the Figure 13.

#### 4.1.2 Antenna Mount

In regards to creating a fixture for which to mount both desired antenna frequency bands, an external mount was created using PVC pipe and fittings which provided a solid mountable structure that was highly customizable and quick to assemble. This provided modularity in case other antennas were to

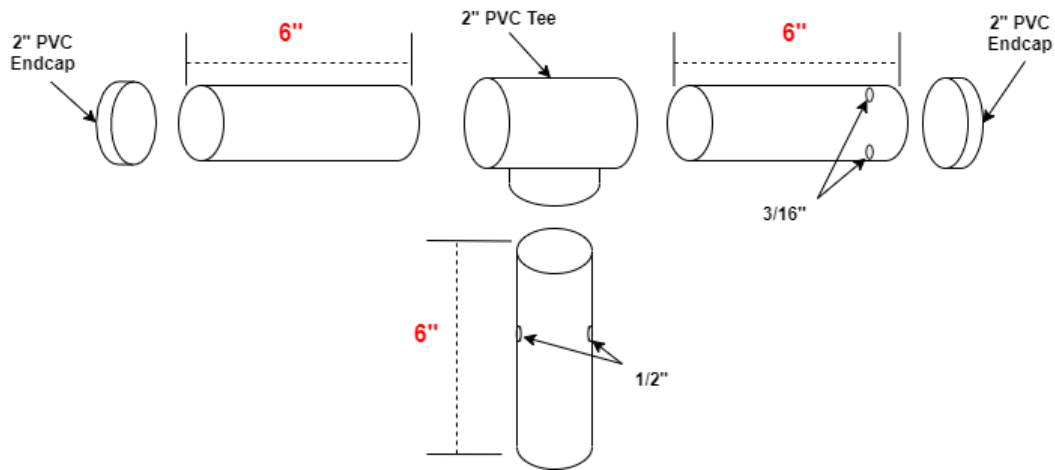
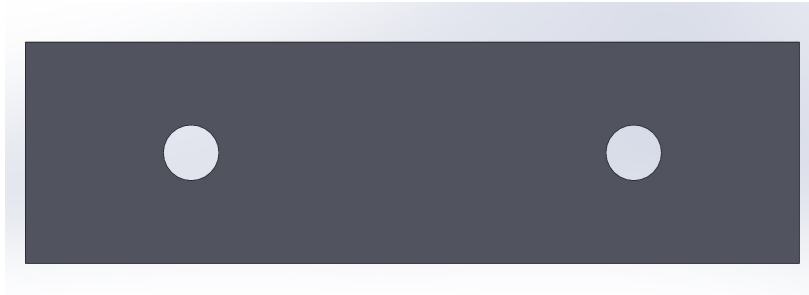


Figure 14: PVC Antenna Mount

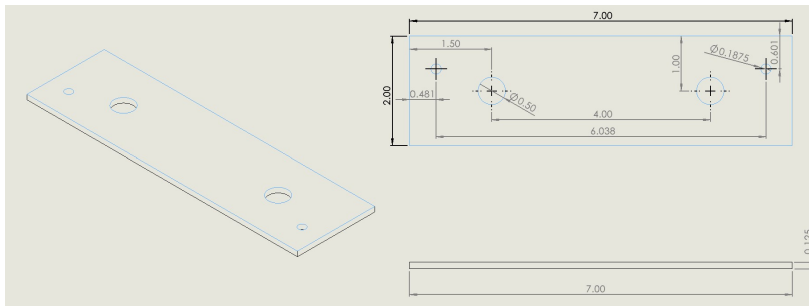
be used, as the length of PVC to the left and right of the tee shown in Figure 14 would only need to be altered. For the chosen UHF and L-Band, the UHF antenna required some adjustments to be readily mounted to PVC structure. This completed using two 3/16" holes that matched the u-bolt fastener provided by the manufacturer. In order to achieve the two narrow 3/16" holes highlighted in Figure 14, the UHF U-bolt back bracket was secured to the desired location of the antenna using a 12" trigger clamp. This bracket acted as the guide for the drill bit to allow the holes to be drilled toward the outer edges of the PVC for which the drill bit could not be held at a 90 angle too. The holes were initially started perpendicular to there location, and once an sufficient indention was made the PVC pipe was then rotated to the correct configuration such that the hole would align as shown Figure 14. For the L-band antenna a custom 3D printed mount was created in order to secure the antenna to the PVC mount. Initially a u-bolt mechanism was going to be placed as the backside of the antenna was equipped with a relatively strong magnet. This was then changed in order to ensure a fixed orientation throughout deployment and transportation.

#### 4.1.3 Mounting

In regards to the manufacturing of the mounts for both the housing and supports, each part was cut from an 4ft section of 2" aluminum flat stock or 2 1/2" aluminum angle. Each mount was individually measured, cut, and checked, then drilled with their respective holes based on mounting location. The lower and upper mounting brackets were mounted to the housing structure first, followed by the antenna support brackets. This was due to the antenna support brackets placement was directly dependent on the upper mounting bracket and PVC antenna mount interface as the brackets needed to sit flush with the antenna mount. Two holes were drilled diagonally in each of the supporting brackets before placement. The following hole placement was used in order to reduce the necessary hardware for stabilization as this would provide the most rigid configuration using two rivets. The two mounting holes for each were then marked and drilled on the upper mounting bracket following a friction fit placement of the two brackets with respect to the PVC antenna mount. To ensure minimal movement of the antenna a half inch hole was also drilled such that a bolt and nut assembly could be placed through both supporting brackets and PVC pipe to completely secure the antenna structure to the main housing. The provided box mounting hardware was then mapped, drilled, and installed to the lower and upper mounting brackets respectively using aluminum rivets. Aluminum rivets were the choice of fasteners as they are cost efficient, strong,

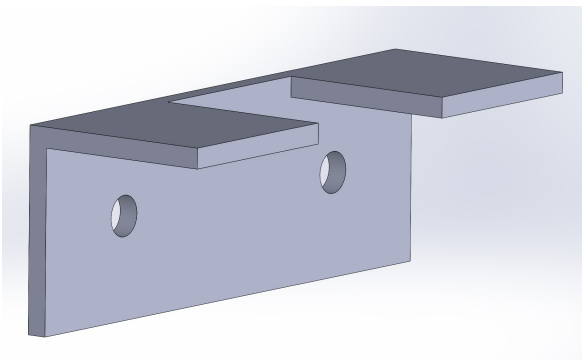


(a) CAD Model

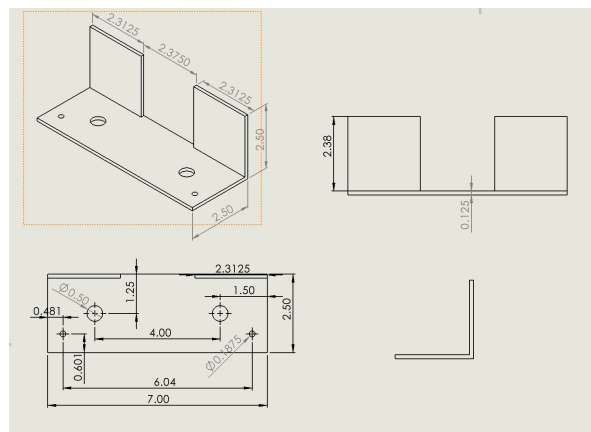


(b) Drawing

Figure 15: Lower Aluminum Mounting Bracket

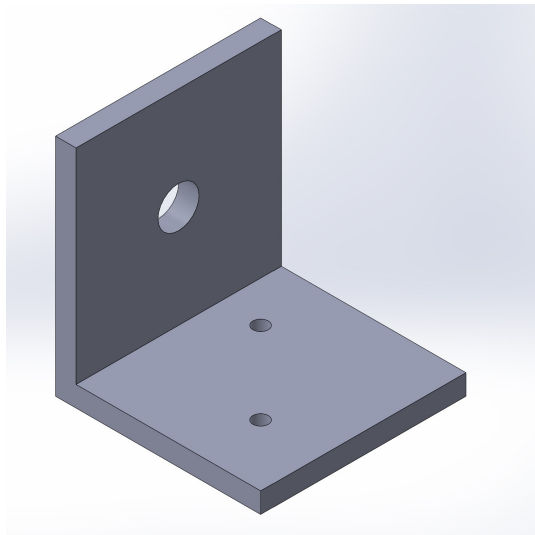


(a) CAD Model

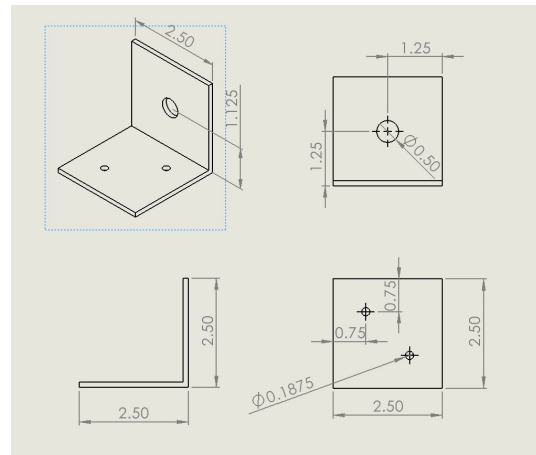


(b) Drawing

Figure 16: Upper Aluminum Mounting Bracket



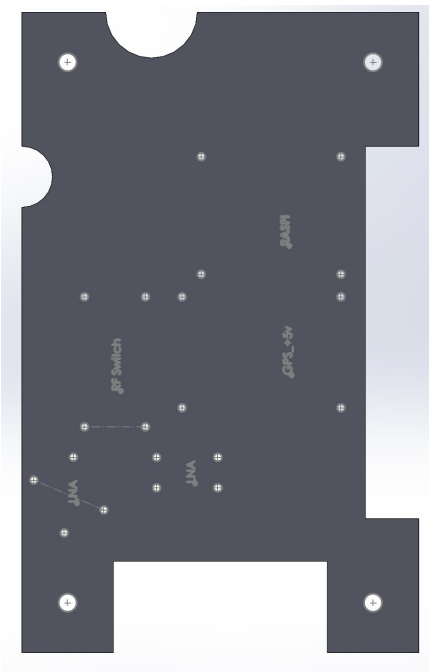
(a) CAD Model



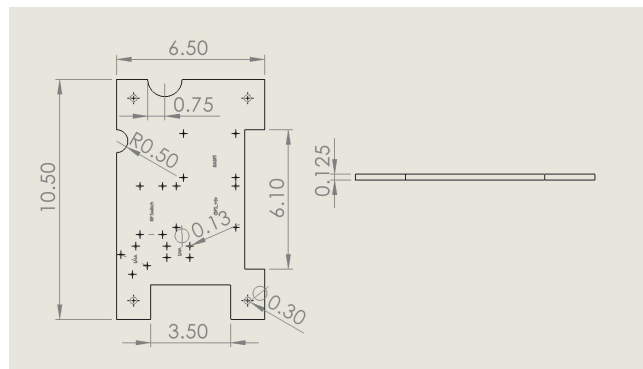
(b) Drawing

Figure 17: Aluminum Antenna Support Bracket

and weather resistant.



(a) CAD Model



(b) Drawing

Figure 18: Internal Acrylic Hardware Mount

Finally, the acrylic mount was designed to provide a platform for all internal hardware mounting along with each components respective mounting holes/location. This was accomplished by determining hardware location on a fabricated test internal mount and copying the placement of components to a replicated full size paper version. Following the paper replication, the layout was then adjusted and subsequent internal mounts were manufactured using a laser cutter. The holes were included in the following models to ensure that these would not need to be drilled post manufacturing thus mitigating the possi-

bility of fracturing the acrylic mount and time spent during installation.

Following the manufacturing for each of the key components in terms of hardware, there are a few places for improvement that would improve time spent manufacturing and hardware accuracy. One of the first recommendations would be to proceed by cutting the smaller pieces such as the supporting mounts first, followed by the larger parts of the mounting scheme. Following the same process it may also be beneficial to pre-drill at least the half inch holes for the antenna mount in those smaller brackets first then proceed by cutting them as it would provide more options to secure the material before drilling. This would allow the manufacturer the option for more material to be clamped and secured, and in return allow the user to use both hands to deal with the torque provided by the bit binding on the aluminum when emerging from the other side upon completion. One might also consider to use a drill press rather than a handheld cordless drill to ensure a more manageable and precise hole placement. Furthermore, for more accurate cuts a horizontal bandsaw or saw of that nature could be used instead of a jigsaw in order to achieve cleaner and more level cuts. This would also decrease manufacturing time as a jig/stop could be produced such that multiple parts of the same dimension could be fabricated subsequently in an assembly line fashion. The final recommendation one might suggest would be to use more aluminum specialized tools such as blades and drill bits will increase the longevity of the tools and provide a more seamless/time efficient manufacturing process.

## **4.2 Electronics**

Given the desired capabilities of our system the electrical components being used were all generally readily available off the shelf components. All arriving prefabricated and constructed minus a few screws or soldered leads for powering various devices. Beginning first with the outer most component the antenna. In the case specifically our team purchased a pre-built five-element yagi antenna that covers 400-470 MHz. The main problem we had with this piece of electronics was finding out weather or not the SMA connections that we were using were waterproof or not. For some reason this information was essentially missing in our research, but by visual inspection there of the collars being used to secure the connections. There was a small gasket that would provide a waterproof seal let alone the length of threads the water would have to travel up to possibly interfere with our signals. Other than that issue this antenna was plug and play in conjunction with our other components. Speaking of which the next in the chain was the LNA we had selected to further boost our signal above the noise floor. All that this component required our team to do post purchase was solder in some leads to the device to supply 5V of accessory power to properly use the device. Much like it's name implies (Low noise amplifier) this device barely altered the noise floor whilst simultaneously boosting our received signals. The last link in the chain is the RF switch which is a shared device in both of the bands that we designed for. This component was a computer controlled RF switch with two possible ports to switch between with the same SMA connectors as the rest of the system. The UHF system worked very well over all just as we had originally designed it. Initial there was some concerns with the data we were receiving due to the CSIM being drowned out a DC off set. But once we electronically filtered out this DC component from the raw IQ data the pings became clear and distinct and easier for us to work with. The only real recommendation that could be made here is given a bigger budget or during the buying process it may have helped us to buy higher quality antennas. This complaint/ recommendation goes for both UHF and L-Band systems.

#### 4.2.1 RF Front End - Lband

Following suit to the previously discussed band a very similar list of components. Beginning first with a specifically tuned patch antenna for the Iridium constellation (approximately 1616-1626 MHz) which came in factory manufactured waterproof housing and cable. This antenna also had a strong magnet on the underside for mounting to metal surfaces like a car. The LNA for this subsystem required the very same special touch of soldering leads onto the manufactured device to provide the same 5V accessory power. Due to the fact that this purchased LNA was more directly turned to the frequencies we were targeting it did a great job boosting the iridium signals out of the noise floor. Before application of this device the signals were for all intensive purposes invisible for our application. After which these same signals were pushed on average 15-20 dB above this same noise floor. The devices worked directly as we designed them to but unfortunately they were not enough for our teams purpose of calculating TDOA values. The IQ data that we received was so chaotic that IQ became essentially unusable in terms of finding a unique enough signal to use for cross correlation. In the future this problem could probably be solved through the application of AIML processing due to L-Band being a very active and noisy environment. Things like wifi, GPS, Bluetooth, and other sources populate this area making it highly contested. In addition to this a reflector could drastically boost received signals at the cost of beam width unfortunately.

#### 4.2.2 PPS Timing Scheme

The PPS timing scheme was built in house and was based off of an idea presented by Jakub Kaderka, and Tomas Urbanec in their paper[3]. The timing scheme utilizes the universally synchronized pulse per a second signal that is produced by most GPS Integrated Circuits. The PPS is a square wave with a frequency of 1 second. The pulse is triggered high based on the UTC second received in the GPS data. These means that all PPS pulses should go high at the same time regardless of global position. The paper uses an additional capacitor between PPS and ADC on the SDR to produce a high pass filter. This removes the DC component of the PPS. The filtered PPS is then superimposed directly into the I or Q stream of the RF data to produce a 1Hz universally synchronized RF signature.

Because this project uses a different SDR than what was used in the original paper a few preprocesssing steps were added to the PPS before it was superimposed on the RF stream. Figure 19 shows a basic schematic of the interaction between the HackRF and PPS. A detailed schematic can be found in Appendix B.

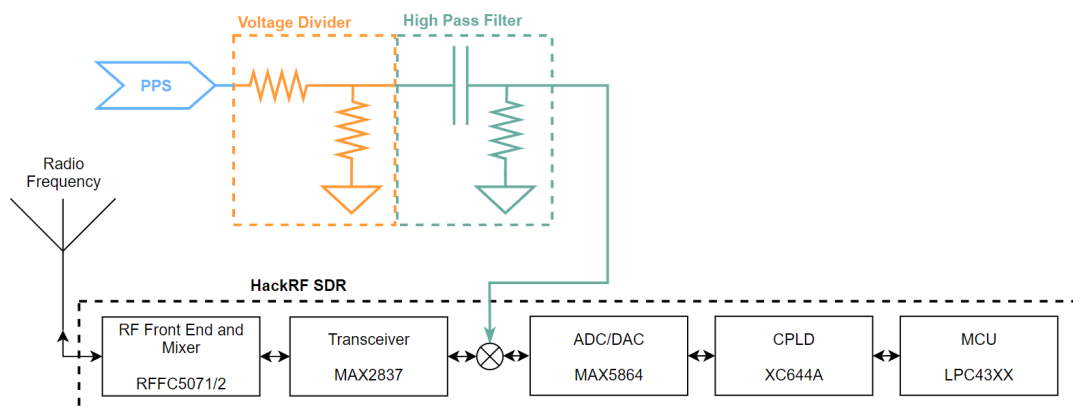


Figure 19: Basic diagram of the PPS + HackRF interface

In the configuration shown in Figure 19 the PPS is first divided down to a lower voltage via voltage divider. This is done to ensure the the PPS is with in the operating limits of the ADC on the HackRF. The PPS is then passed through a high pass filter removing the DC component of the pulse. The circuit was modeled in LTspice and the modeled output is shown in Figure 20.

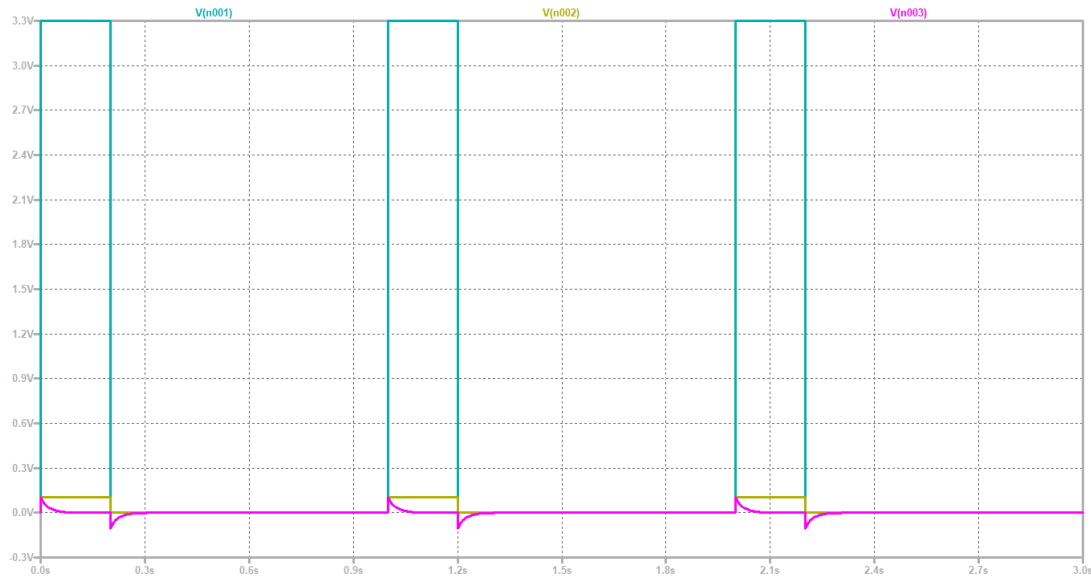


Figure 20: LTspice simulation of the PPS processing circuitry

From the simulation and calculations the PPS has been dropped down to a pk-pk voltage of  $100mV$ . With the doctored PPS ready it can conveniently be superimposed onto either the I or Q streams of the intermediate frequency RF data right before reaching the ADC. Figure 21 shows header P9 used to inject the PPS.

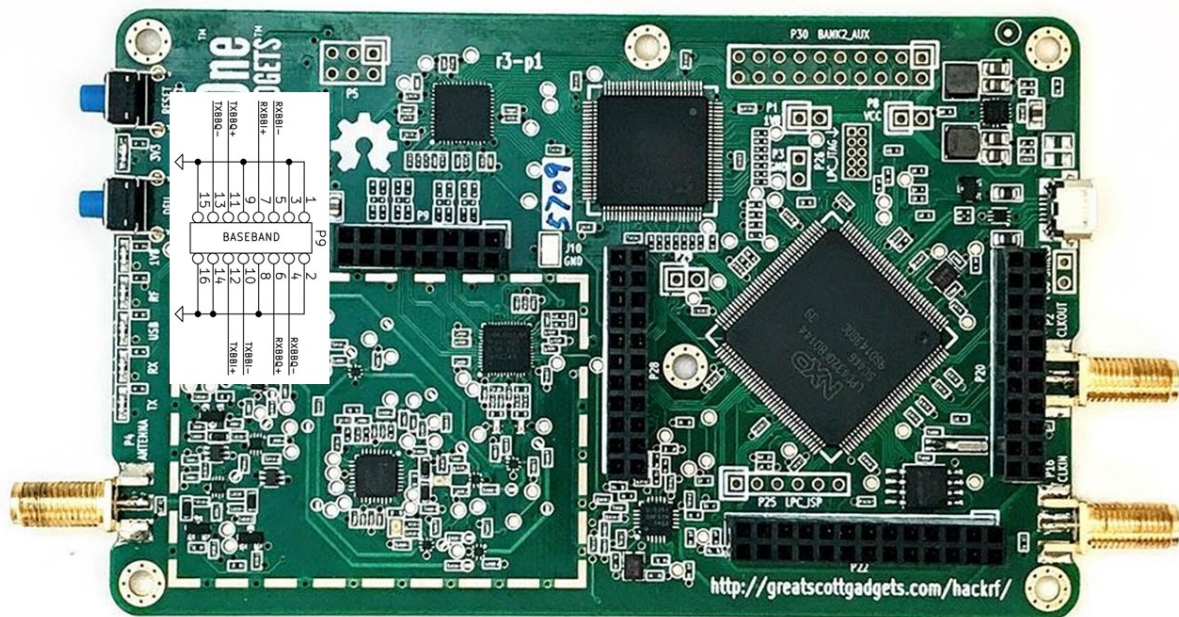


Figure 21: Header on the HackRF SDR used to super impose the PPS onto the RF stream

With the PPS connected at the target frequencies for both Lband and UHF there are no major changes to

the waterfall plots of the RF data. Exporting and plotting the amplitude of the data versus time the PPS is easily identifiable over the noise floor. Figure 22 shows a small sample of the RF data with the PPS.

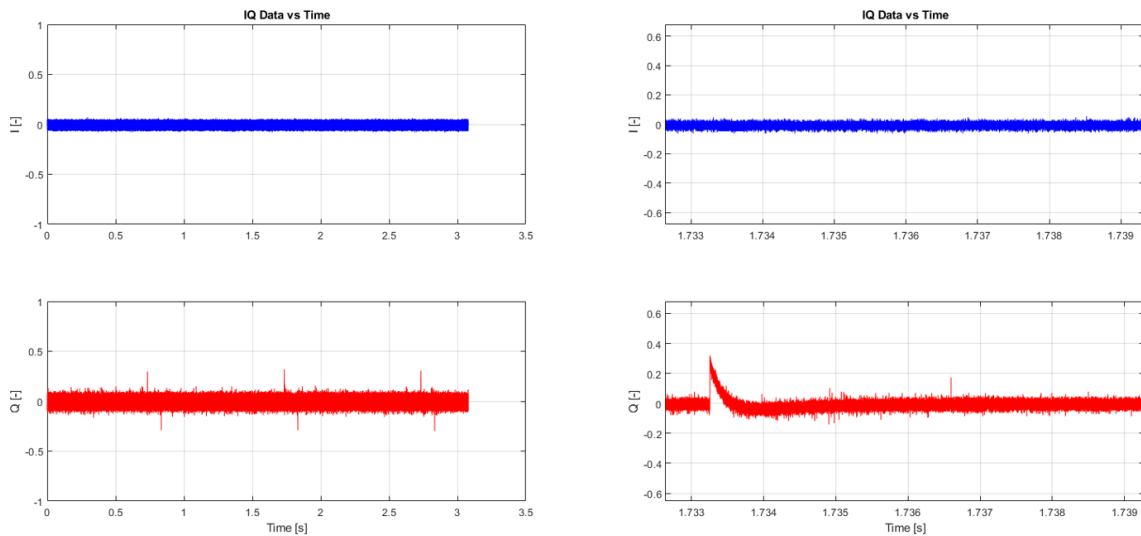


Figure 22: Small example of the RF stream and the PPS in the stream. Data taken at 437.25MHz. The plot on the right shows a close up and how the PPS shape is retained after being superimposed on the RF stream

There are a few variables that could limit the accuracy of this synchronization method. The first is the PPS itself. If the pulses are not perfectly synced or have some inherent offset from one another this error will propagate through to the time delay. From testing, the PPS's from NEO 6M GPS units used are all "perfectly" synced with one another (within 10ns of each other). It's unclear what the precise error is as the Oscilloscope used for this measurement maxed out at 100M samples per second. However, this error may change based on the type of IC used and could increase or decrease. The NEO 6m was chosen out of convenience but higher end more accurate chips do exist that should theoretically have better time resolution.

The second possible bottleneck is the SDR's sample rate. Because the PPS is superimposed before the ADC and the data used in post processing is the digital data, the sample rate limits how precisely the PPS can be aligned. Depending on when the sample is taken the PPS could appear a full sample behind. Based on the previous test the ADC sample rate is the limiting factor in terms of data alignment accuracy. Because the SDR is capable of sampling at a consistent 20M samples per second the minimum alignment error is  $\pm 50ns$ . An error of  $\pm 50ns$  is well within the requirements set by the orbital prediction scheme. While the system meets the orbital prediction scheme requirements and was easy to manufacture with off the shelf parts several improvements could be made. Both the GPS chip and HackRF components can be purchased individually as surface mount components. Ideally the parts should be placed on a all inclusive PCB for better RF performance and less assembly steps. The PPS can also be drowned out at frequencies with high power signals at them such as FM stations. Having an adjustable voltage divider and filter would make the system more reliable as the PPS magnitude could be increased to rise above the noise floor or the time constant shortened to limit its footprint on the RF data.

### 4.2.3 Circuit Board

The circuit board for this project was hand soldered and contains the GPS, PPS doctoring circuits, Power distribution, GPS data lines, Reset button and indicator LEDs. An example of one board is shown in Figure 23 and the full schematic can be found in Appendix B. 5V power is delivered via micro USB and is broken out using the GPS breakout board headers. The board uses break out headers and jumper wires to route signals and power to the SDR, Raspberry pi, RF switch and LNAs. Having these long wire loops is usually far from ideal as the loop inductance can generate excess noise and wire inductance produces even more noise when carrying high frequency switching signals. However none of the jumper wires in this application were carrying high frequency switching signals and wires were used as twisted pairs to reduce loop inductance. Because of the low frequency signals the jumper wires were carrying this approach was deemed okay for this application. Another note is that for safety reasons it is generally bad practice to use exposed contacts on the powered side of a connection. Based on the hardware readily available and the low voltage the exposed rails carried (5V, 2.3A) this was deemed okay for this application.

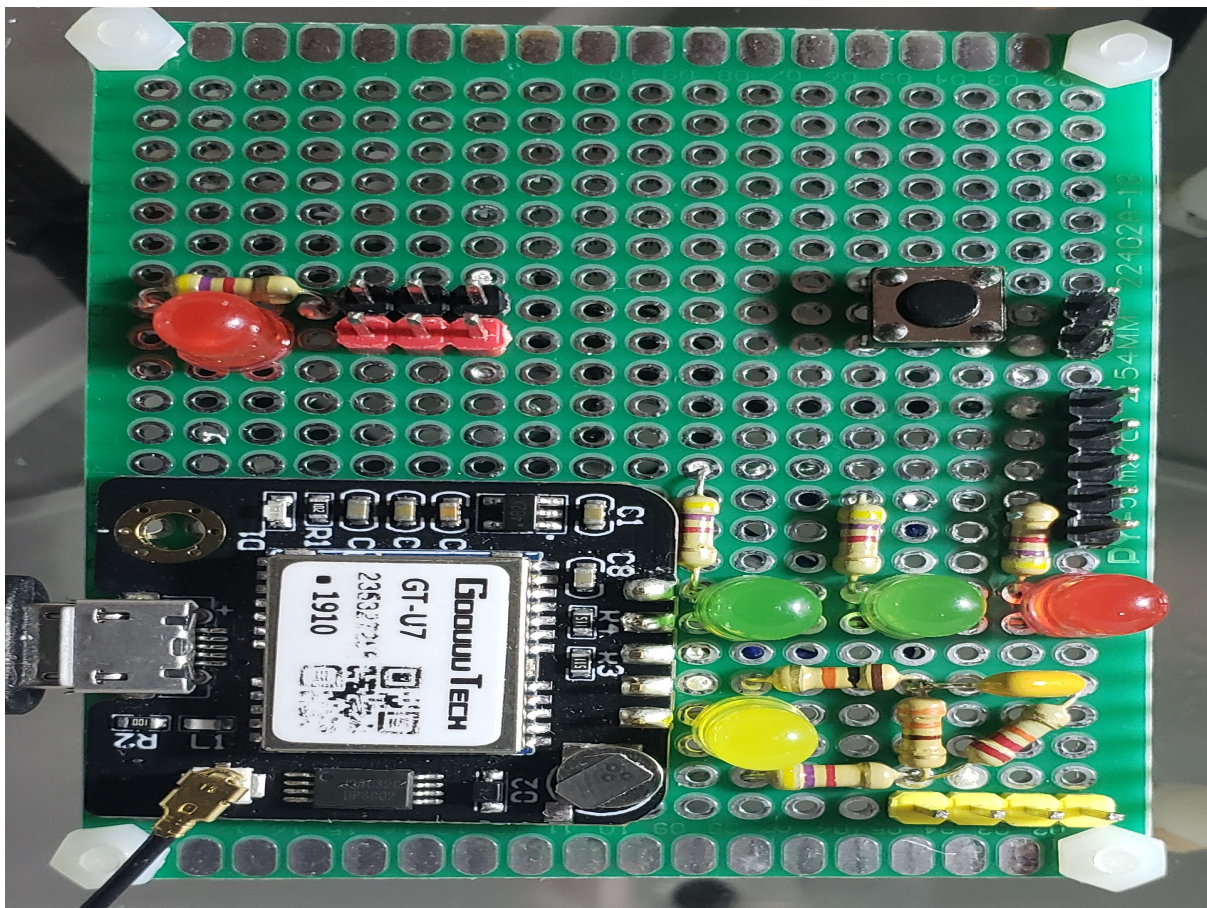


Figure 23: Example of one of the circuit boards.

All boards performed as expected carrying power and data to the appropriate locations. While the 4 boards were not difficult to manufacture it is highly recommended that they be replaced by a purpose built PCB. A PCB will have a smaller footprint, remove unique human induced errors from board manufacturing and be far easier to produce on a large scale. This PCB could potentially also house the computing unit and RF components such as the switch, SDR and LNAs improving RF performance.

## 4.3 Software

### 4.3.1 Onboard OS

For this project, there was a combination of using both manufactured software and a small amount of pre-built software. The software manufactured for this project dealt with using python with the Raspberry Pi on-board computer. The manufactured software in this project was developed to interface with the many different devices and components within each testing unit, this includes but not limited to the: HackRF, RF switch, and GPS Module, etc. There were several times in this project where we found example code from an online source of how to control a certain component within each unit, and we would take this pre-built code and then modify it for our particular project needs. We also needed to download and include several required python packages that were necessary to operate and control the HackRF and GPS Module components within each unit.

There was not many initial difficulties regarding the software development for the sensor units. However, our greatest source of difficulties for the software development arose when we began full unit testing. During the early phases of full unit testing there was multiple errors that were occurring within the software. Because of these early initial troubles with the full unit software testing, this required much more time than we initially intended to solve these full unit software issues. Another software difficulty that we encountered initially was trying to configure the HackRF to be ready to record data and record for a certain amount of time. We initially tried to use the GNU radio companion program to try to configure the HackRF to record satellite data, however learning this software came with a very steep learning curve. Instead we found and began using the libHackRF linux package that allowed us to control and configure the HackRF via command line. Through these initial difficulties and troubleshooting the full unit testing, we were able to achieve the required autonomous functionality of the sensor units we set out to achieve at the beginning of the project. With the autonomous functionality of the units, this displays a crucial part of the projects success.

Moving forward with this project, knowing what we know now in terms of the difficulties that we have encountered with the software, It would be beneficial to have a better system interface for the Raspberry Pi and the SDR. There were many unknown inconsistencies in terms of collecting samples with the HackRF at different samples rates. While using command line to control and configure the HackRF, it quickly became apparent that it was not the most user friendly interface and it was difficult to find where inconsistencies with the HackRF existed. It would be beneficial to have a better system interface that could help with the debugging of the system and thus save alot of man power and time. One possible solution could be a better understanding of GNU radio companion, but as previously stated there is a very steep learning curve to this program. Another possibility is for this program to be added as a package to a known programming language, such as MATLAB or Python.

### 4.3.2 Time Delay of Arrival

The Time Delay of Arrival (TDoA) software package was aimed at taking the received candidate satellite signals from different sensor units to calculate and output the associated TDoA. The order of operations for this process is as follows:

1. Load in four associated sensor unit data sets with GUI.
2. Choose one data set as the reference (TDoA= 0).
3. Use PPS to align each set in time.

4. Perform a cross-correlation and find the value that gives the highest correlation.
5. Output this argmax as the TDoA associated with that data set.
6. Use the three TDoA values to compute a position vector.

Ideally, this is how the package would work if we would have had more time to test with real data. We were ultimately impeded by the large size of the data sets and hardware issues that ate up software debugging time. The software as it stands is quite slow and manual data set loading is required. Without the necessary development time and data, the process ended up as follows:

1. Manually load in two associated sensor unit data sets.
2. First is chosen as reference (TDoA= 0).
3. Use PPS to align each set in time.
4. Perform a cross-correlation and find the value that gives the highest correlation.
5. Output this argmax as the TDoA associated with that data set.

While this process represents a capacity less than what was initially intended, there are many promising points for improvement. These points are mainly comprised of optimizing the data file sizes by saving only a couple seconds instead of ten and data set naming-convention uniformity. Once there is a clear naming-convention the data sets can be potentially loaded in with a MATLAB GUI to lessen the time a user has to take to manually load each one.

### **4.3.3 Orbital Prediction Particle Filter**

The particle filter aimed to solve the noisy data error and improve the accuracy of the orbit. The team chose a particle filter based on a paper [4]. While purely theoretical, the paper matched the project's objective and methodology. With minimal knowledge on the optimal state estimation, the team decided to attempt developing a particle filter. While simultaneously, the team used a simpler method, Gibb's method, as a backup. Figure 24 shows how a particle filter functions. First, the nonlinear system was defined by creating the differential equations and noise in the system. Next, an initial sampling of possible states (i.e. positions and corresponding velocities) was created based on an educated guess of a satellite's orbit. Each sampled state is referred to as a particle. The initial sampling produced a few thousand particles. With the initial particles already sampled, differential equations that govern the system predicted the next state. For the project, we propagated the particles' positions and velocities using simple Newtonian gravity. Next, the filter simulated the measurement for each particle. The measurement for the project was the TDoA values for a particle. The filter compared the simulated measurement to the hardware's measurement. Each particle is assigned a likelihood proportional to how similar its measurement is to the hardware's measurement. Based on this likelihood, new particles were sampled at locations with high likelihood. The weighted mean of the new particles found the best estimate. This process was repeated for each measurement.

Given the complexity, the particle filter development started with a simplified case. The first particle filter estimated the velocity of a 1-D mass-spring system. This filter was built from scratch. The lack of built-in functions helped develop an intuition of how the filter worked. Multiple issues were discovered through the simplified case, most notably, what ODE propagator to use. The team initially used Matlab's

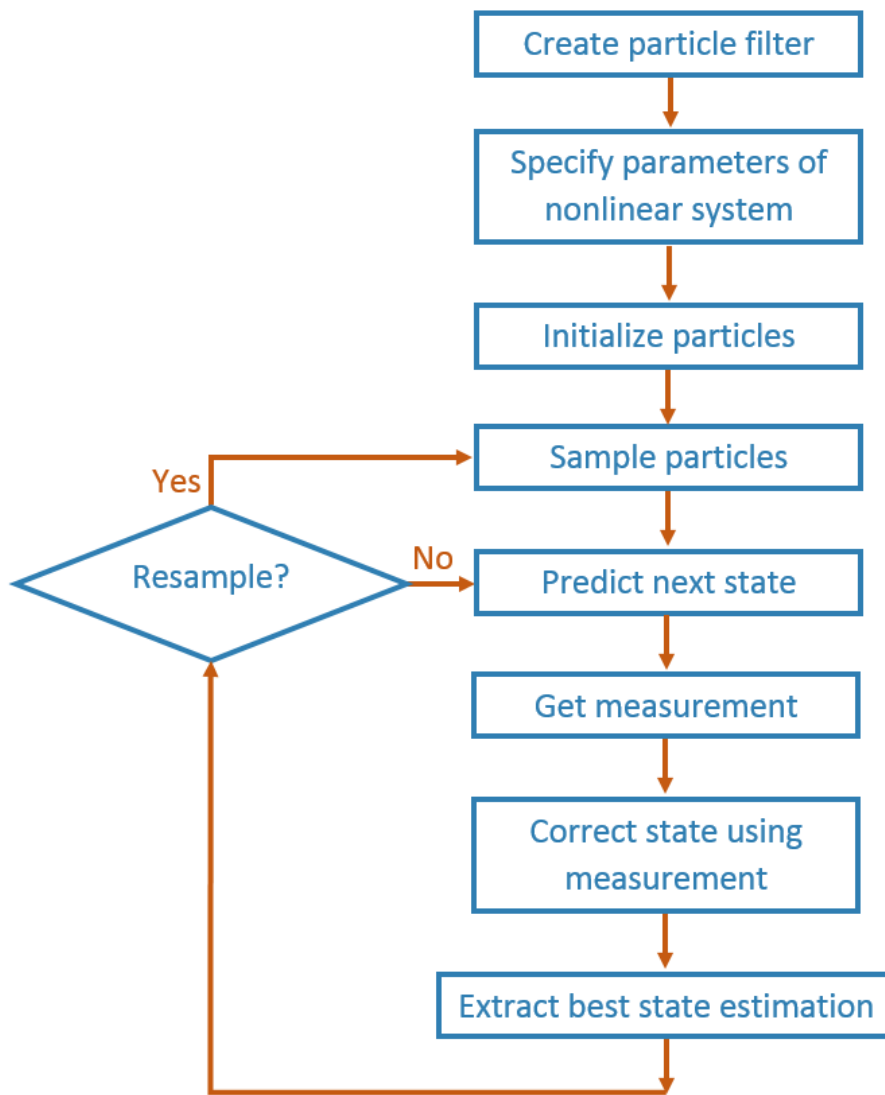


Figure 24: Functional Block Diagram detailing a Particle Filter. Source: MathWorks

*ode45.m* due to familiarity. The problem arose from the function's dynamic time stepping. This caused any noise to be muted in the system, and the filter would obtain an incorrect estimate with minuscule uncertainty. Because of the low covariance, the filter believed it found the 'correct' state estimate and never located the mass' state. The solution required using a 'dumber' ODE propagator. The team wrote a Runge-Kutta propagator as the new ODE propagator that did not have dynamic time stepping. After the simplest case, the team began using Matlab's *ParticleFilter.m*. Using pre-built functions allowed for more complex resampling techniques, decreased the runtime, and reduced possible bugs in the code. The main downside was the limitation to what had been implemented by Matlab; certain techniques could not be used. With the built-in function, the team progressed to more complex systems. The first system was a two-dimensional model of a satellite with three units on the ground. In this case, the measurements were the TDoA values. Figure 25 depicts the particles after the initialization. The left part of Figure 25 is on the scale of the Earth. The particles were randomly sampled by a Gaussian distribution. On the right, a view of particles around the satellite.

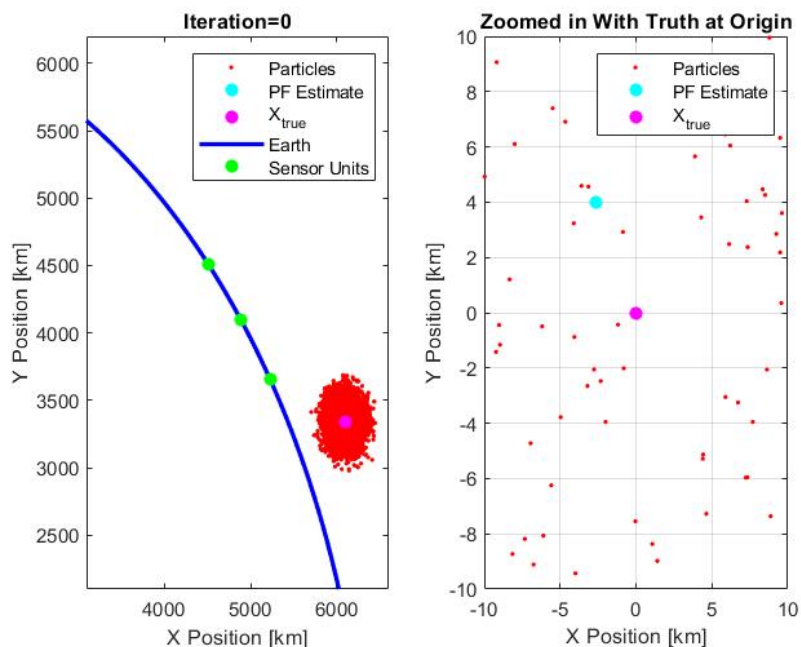


Figure 25: Two Dimensional Particle Filter after Initialization

After the two-dimensional particle filter, the code was scaled into three dimensions. Because of the slow ramp-up, the three-dimensional particle filter had minimal errors. Simulated data tested the accuracy of the filter. STK created the satellite truth data and distance from the satellite to each unit.

For ways to improve, the particle filter is likely not the best state estimator for this problem. An Unscented Kalman Filter would be more efficient, but the estimate will not be as accurate. To evaluate all the methods, a trade study between different estimators would be a strong next step. The main reason why the team did not conduct a trade study was the lack of knowledge about optimal state estimation techniques. Regardless, the particle filter is only as good as the measurements it receives. Toward the end of a flyby, the measurement corresponds to multiple locations causing the estimate to become less accurate. Certain techniques, such as an innovation filter, could improve what quality of data that is fed to the filter. The innovation filter is beyond the scope of the project. Another improvement could be feeding in raw RF data instead of TDoA values, but these would likely increase the runtime by some

margin. Still, the main next goal for the particle filter is testing with real data. This will likely reveal multiple issues overlooked in the software.

#### **4.3.4 TLE Generation and Comparison**

The state vectors of the satellite candidate as produced by statistical analysis from the particle filter are then converted into the respective Keplerian elements. This process of generating the TLE for a satellite candidate passover from our collected data and then comparing our newly calculated TLE to a reference TLE is all accomplished in a Matlab application. This application as seen in Figure 26 was developed by the team specifically for this project but incorporates several prebuilt SGP4 propagation functions published and made available by celestrak.com. The application serves as a wrapper for these functions to be packaged and integrated into a seamless visual interface. Any required debugging or update to these functions can be done so through the traditional Matlab program and avoid the Matlab app designer tool all together. While the application currently accomplishes everything we initially intended it to, there are several points of improvement that should be pursued. The biggest challenge that comes from generating a TLE from a state vector is determining the exact time it was generated. While this may seem like a simple enough task, current formatting standards for our data files mean that it is often difficult to pinpoint which exact time an outputted state vector represents. This uncertainty serves to compound error in our comparison process. Additionally, the application only allows for the input of a single calculated state vector from a satellite pass over. The nature of our particle filter step means that incorporating state vectors of the satellite from multiple points in time would be much more effective at driving down noise discrepancy between our calculated state vector and the actual state vector. Information flow is currently set up such that the particle filter output need be manually inputted. This point additional point of human error can be removed all together by integrating the particle filter into the application. Doing this would allow for better process flow overall and help encapsulate our projects post processing routine into a much more manageable interface.

#### **4.4 Summary of Integration**

The first integration step involved creating standoffs that attach to the acrylic mount. The electronic components were mounted to the acrylic plate via standoff stack ups shown in Figure 27. The stack up was designed such that the mount could be installed in the box before components were attached to it. When the mount was loaded with standoffs, power wires were run under the acrylic to their appropriate cutouts, and the mount was placed in the box.

Components were then mounted to the the standoffs in no particular order. Before the HackRF was mounted a small hole needed to be drilled in its top cover. This hole aligned with the pin headers that are used to superimpose the PPS signal. The HackRF was removed from its casing and a small hole was drilled as shown in Figure 28.

The power strip and HackRF were mounted in place using high strength Velcro. All wiring was done by hand. RF cables were cut to length based on part placement and terminated by hand. Handmade pigtail cables were used to pass antenna cables and power through the waterproofing grommets. With the antennas mounted the completed sensor units look similar to that shown in Figure 29.

The bridge between the hardware and the post processing software was a USB drive that was physical retrieved and moved to over to a computer that could run the post processing software. Once on the post processing machine the steps to producing an orbit are finding and calculating TDOA measurements, running the particle filter and passing the estimate state vector to the TLE generation app.

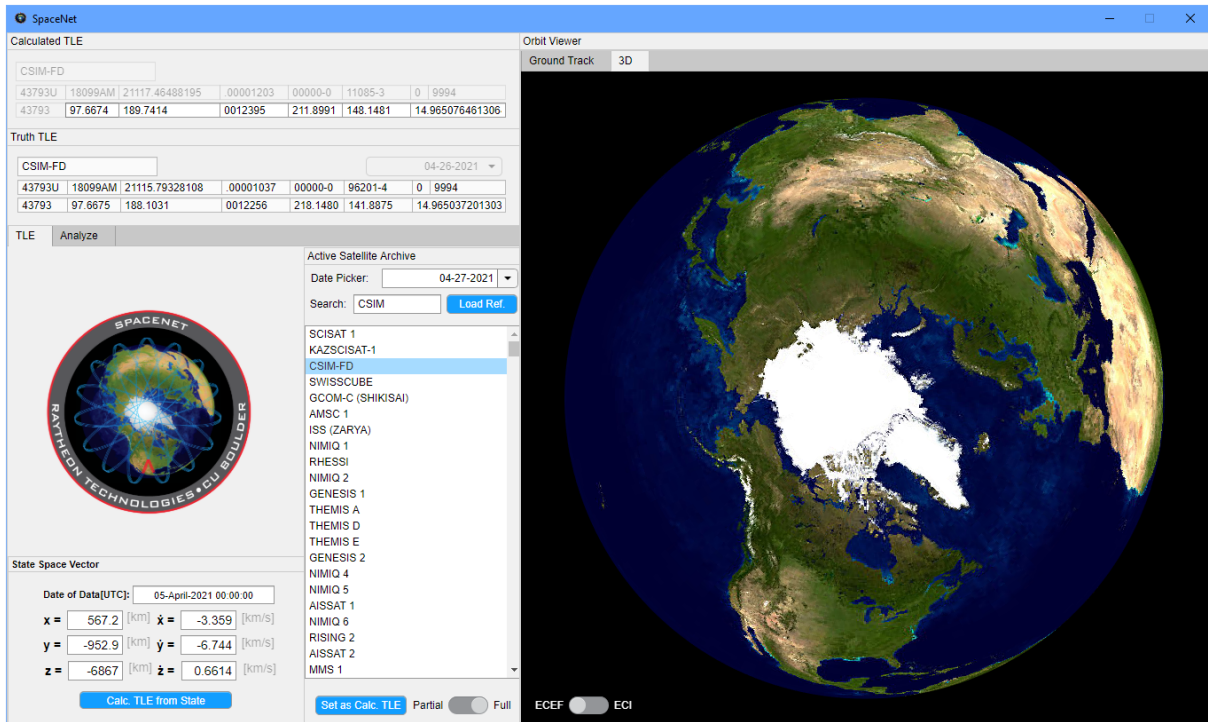


Figure 26: SpaceNet Orbital Propagation Tool

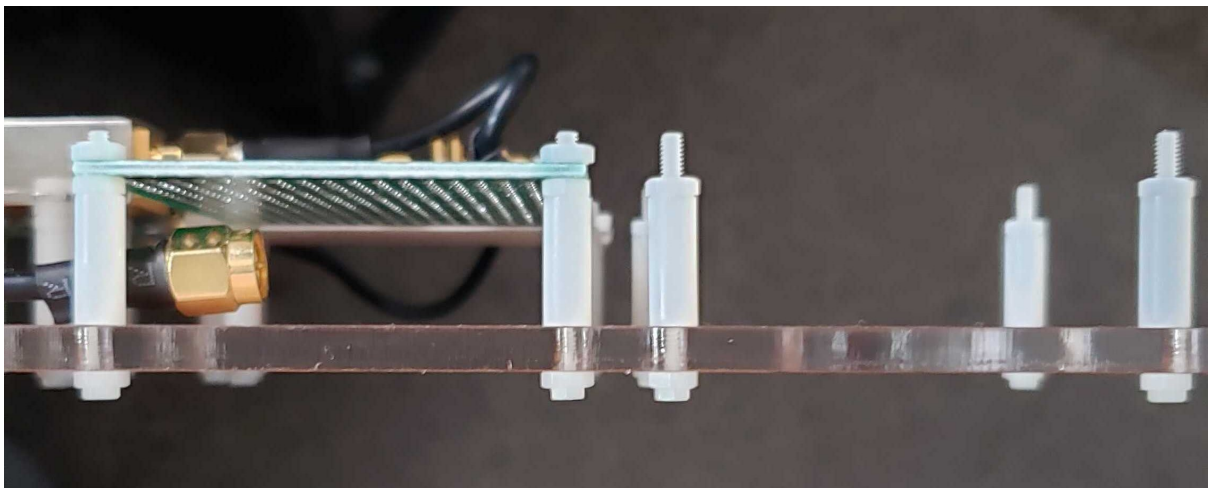


Figure 27: Standoff stack up used to mount components to the acrylic mount



Figure 28: Hole used to access header P9 on the HackRF

## 5 Verification and Validation

Authors: Authors: Ryan Burdick, Noah Francis, E Forest Owen, Tyler Pirner, Keith Poletti, Ryan Prince, Israel Quezada-Cordova, Colin Ruark, and Benji Smith

### 5.1 Environmental Readiness

#### Verification test for FR 1.1

In order to satisfy **FR 1.1**, a NEMA 4 rated enclosure was chosen as the main housing component. This rating gave confidence that the sensor unit would survive outdoor conditions without modification. In order to ensure the housing enclosure and the cable pass through that were used provided a weather resistant environment a series of waterproof test were conducted. The idea behind these tests was to mitigate the risk of non-fully operational hardware, but also to ensure the longevity of the units during satellite pass overs. The original test set up and test progression can be seen in figure 31 from manufacture guarantee to overall unit deployment.

Multiple verification steps were taken through each of the demonstrated tests. These included subjecting the unit to an on flow of water from a faucets, shower head, or pressurized nozzle. This was then proceeded by the external parts of the unit being dried to ensure no contamination from the exterior post testing i.e when opening the enclosure. The units were then opened and inspected for any ingress of water which would have been demonstrated by a damp paper towel for which each of the units were lined with. Once the units as a whole were ensured to be water resistant, the cable pass throughs were then installed and subjected to the same sequence of steps. Each test was carried out multiple times to ensure the same results were achieved, and from these tests the box maintained a dry environment, thus solidifying FR1.1 and ensured the outdoor capability of the unit.

#### Verification test for DR 1.2

In order to verify **FR 1.2** two tests will be conducted. First, the units will be fully integrated and operated indoors at room temperature to ensure proper operations under ideal conditions. This was

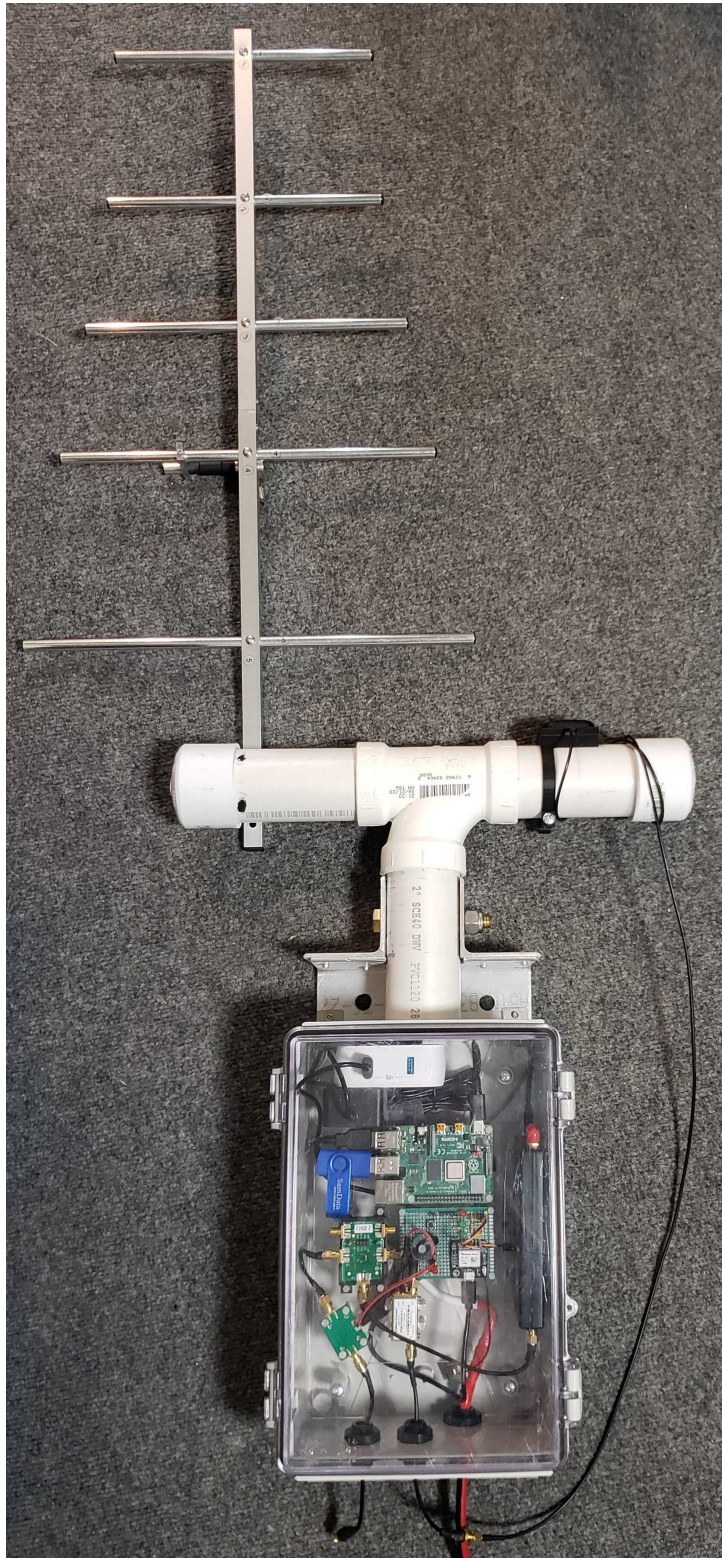


Figure 29: Completed sensor unit. Note the UHF antenna is not connected in this picture.

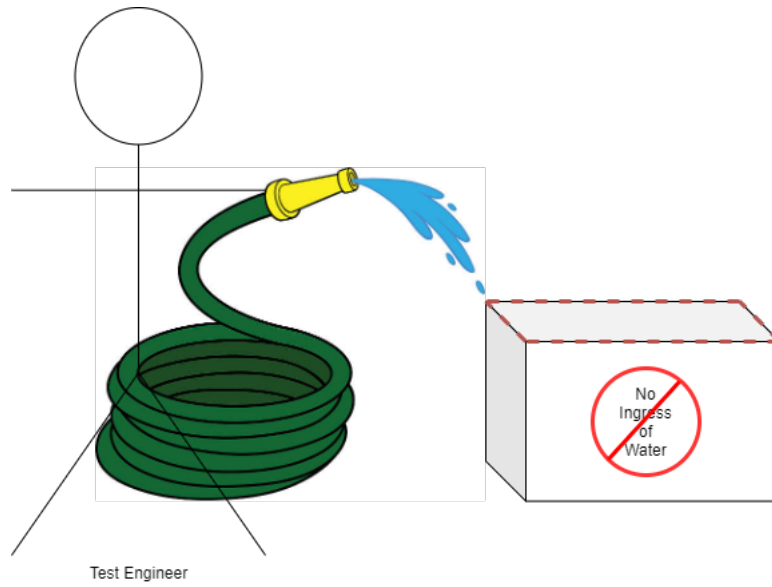


Figure 30: Water Resistance Test



Figure 31: Water Resistance Tests Progression



(a) Water Subjection



(b) Post Inspection

Figure 32: Weather Resistant Verification Results

verified after powering on the system and ensuring the LED indicating the system was powered and operational remained on. Once the system proved operational the sensor unit was then subjected to outdoor conditions for an extended period of time. To ensure the units was operation, the LED indicator was periodically checked, especially during low temperatures and resulted in a fully operational system during these time frames.

#### **Verification test for FR 2.1**

**FR 2.1** will be verified by taking multiple measurements with respect to the x,y, and z coordinates of the full housing assembly. These measurements will then be recorded and verified such that the box is within a 5'x5'x5' space. Upon satisfaction of the functional requirement, the largest unit dimension was 3.8' which is well within the design requirement.

#### **Verification test for FR 2.2**

**FR 2.2**, is satisfied by the design as all electrical components are set to be within the NEMA 4 enclosure. This was accomplished by manufacturing a internal acrylic mount such that all the components could me installed and fixed within the structure, thus ensuring the functional requirement would be met.

#### **Verification test for FR 2.3**

The last verification test to be conducted in regards to the the sensor unit assembly is in relation to **FR 2.3** which states that the senor unit shall weigh less than 50 lbs. This was planned to be verified by taking the weight of each component and assembly and recording them respectively. These weights will then be added together to account for a full integration of the sensor unit hardware and components and if the the total weight is less than or equal to 50 lbs the test will be deemed a success.

The way that this verification test for FR 2.3 was conducted, was by taking a fully assembled unit and placing it on a scale to measure the total weight of each individual unit. Through this method, a direct weight measurement of each component would not being taken, but by measuring a fully assembled unit the FR 2.3 can still be sufficiently satisfied. By conducting this test, we found that a single fully assembled unit weighed 24.2 lbs. This weight is under the maximum 50 lb weight limit set by FR 2.3, thus satisfying the requirement.

#### **Verification test for FR 2.4**

In order to establish communication between the SDR and the on-board computer, software processing and configuration will be performed for both the Raspberry Pi on-board computer, and the SDR. The software 'SoapySDR' will be utilized. This is a python based program that functions as a SDR interface that will be used to program the HackRF One. The on-board computer will be programmed through its linux based operating system: Raspbian. Together the software for both the SDR and the on-board computer will be programmed and verified such that the Raspberry Pi will be commanding the SDR during normal unit operation, thus fulfilling **FR 2.4**.

#### **Verification test for FR 2.5**

As mentioned from the verification of **FR 2.4**, the on-board computer will be programmed through the use of its operating system: Raspbian. This software allows the computer to be programmed in such

a way that it will run autonomously while in the field during nominal operation. The integrated unit tests planned will work for verification of this requirement as well. Ensuring autonomy was one of the toughest requirements to fulfill. Verification required the unit to record all scheduled flybys, to cycle to the next day, and to log any errors in the software. While those three tasks seem trivial, the verification of **FR 2.4** delayed the entire project by a month.

In the test, the team deployed a unit for 24 hours. The test was a simple pass or fail. To pass, the unit must record at least four flybys, cycle to the next day, log any errors, and cycle to the next day. Figure 33 shows a timeline of the test. The unit was deployed at 7:30 am. It recorded seven flybys over the following 24 hours. At 6:00 pm (12:00 am UTC), the unit cycled to the next day list of flybys. The autonomy test was considered a success.

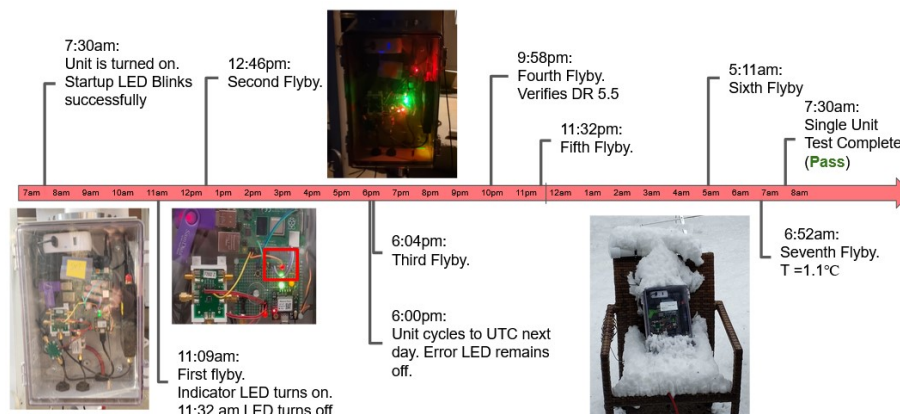


Figure 33: Timeline of the Single Unit Test

## 5.2 RF Front End

### Verification test for FR 3.1 and FR 3.2

The design requirements for gain-over-noise are important, and needed to be both calculated and characterized for our system. The noise of the system is induced by performance losses across the cabling, the LNAs, and the antenna switch. Per the requirements given by our customer, the minimum and target bounds for the gain-over-noise ratio utilizing the UHF band was -20 dB/K to -15 dB/K, while the minimum and target bounds for the gain-over-noise ratio utilizing the L band was -17 dB/K to -13 dB/K. As seen in the above sections, theoretical  $G/T$  has been found for the system though overall loss assumptions, coupled with manufacturer information regarding various system noise temperatures. Once the team had access to the components, testing could be performed by measuring the signal loss the individual components, finally giving us experimental values to calculate  $G/T$  for both sides of the system L-Band and UHF to be exact.

The testing we ended up performing for this functional requirements consisted of primarily doing simulations in Matlab in order to model return losses for each of the antenna systems, then using these results inside of a link margin analysis tool for system gain predictions from both methods namely the  $E_b/N_0$  and SNR methods of link margin analysis. From this modeling along with extensive physical testing of the antennas with real spacecraft down-links all of minimum  $G/T$  values were met. The only obstacle we had to overcome is that we were not able to test for this functional requirement directly was due to the requirement for a transmitting license from FCC to broadcast the down linking signal to the antenna.

In order to get this broadcasting license, the increased costs and time required would have pushed beyond what we could afford as a team.

#### **Verification test for FR 3.3 and FR 3.4**

Ensuring that the link margins predicted are achievable with the procured hardware, it was essential for us to know the complete down link quality for our system. This testing was carried out through similar means as the previously described test **FR 3.1-3.2**, being preformed through matlab simulations calculating return losses of both the L-Band and UHF band antennas. The newly found gain loss values, along with the other inherent losses from the construction of our system as a whole were fed into the same link margin analysis tool. Which our Requirement states explicitly that we must achieve a minimum of 3 dB for each of the respective Link margins. Given all of the simulated/calculated values for loss and other in dependant signal characteristics our calculated link margin values of 12.1 dB for UHF, 4.4 dB L-Band. Both of which fall within the minimum parameters specified by the functional requirements.

#### **Verification test for FR 3.5**

Testing the sensor units ability to receive both desired signal bands without modification will be done during the integrated unit testing. Since the ability for the links to close will be verified during the tests for **FR 3.3** and **FR 3.4**, detailed above, the only thing to check is that the system can switch between the bands on its own. This test is easy achieved during the fully integrated unit tests. While deployed, the units will be programmed to record data for two different target satellites, one in each desired transmission band, and be left to take that data. Afterward, the data will be check to ensure both signals were properly received and stored, which will prove the unit is capable of switching between the bands as commanded. This was tested by full suite analysis testing, and the switcher operated flawlessly, allowing us to see either signal through a single SDR setup.

#### **Verification test for FR 3.6 and FR 3.7**

The first verification method is a subsystem level test used to test the validity of the two selected antennas frequency ranges as described in the specification sheets. This test was conducted via matlab simulation as well, with return loss calculated at the  $\pm 10$  MHz bandwidth of both the desired UHF and L-Band signals. From these results, we found that the bands can be seen within the  $\pm 10$  MHz range of both the UHF and L-Band.

#### **Verification Test for FR 4.1 and 4.2**

In order to verify both **FR 4.1** and **FR 4.2**, the selected antennas were tested to determine both the azimuth field of view, along with the beamwidth to ensure that the antennas have a  $360^\circ$  horizontal field of view, and a beamwidth greater than  $30^\circ$ . The testing procedure for these requirements involves physical unit testing, having an RF emission device output RF signals at the appropriate limits of the antenna to ensure angle requirements are met. For the azimuth FOV test, the emitter will be orbited around the antenna to ensure  $360^\circ$  coverage satisfying **FR 4.1**. The beamwidth test will consist of placing the emitter  $30^\circ$  off of the antenna's pointing axis, checking if the antenna is indeed receiving a signal, confiming the minimum bounds of **FR 4.2**. From these tests, along with matlab simulated results of radiation patterns for both antennas, it was determined that both functional requirements were met.

### 5.3 Timing Synchronization

#### Verification test for FR 5.1

The verification for **FR 5.1** includes showing that the individual sensor units shall maintain a timing precision of at least 420ns. In order to accomplish this, a GPS module will be used to output a PPS signal. Each PPS signal will be 1 second apart on each GPS unit. After the PPS signal has been transmitted, it will pass through a high pass filter to reduce the amount of time that the signal is held high. Reducing the length of time the signal is held high limits the amount of data that is lost. Once the signal reaches the SDR it will be superimposed onto the RAW data. The filtered signal provides a recognizable and universal synchronized RF signature between all 4 sensor units that will then be used to align the recorded data in post-processing.

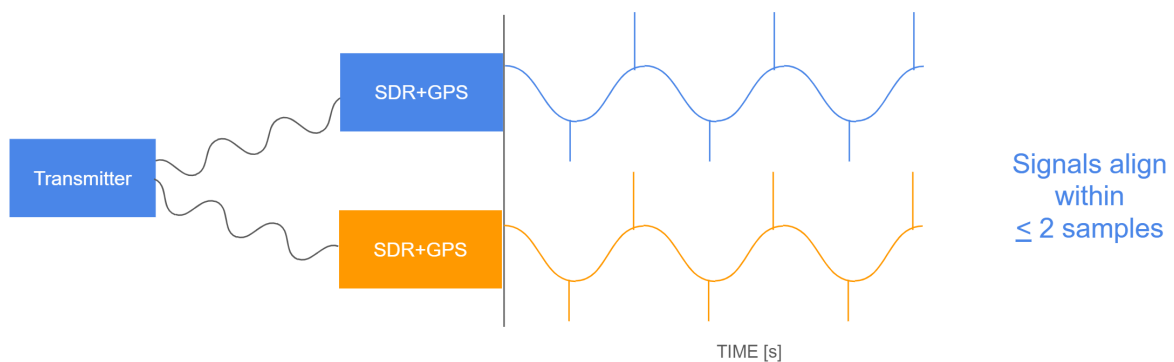


Figure 34: Test setup for DR 5.1

As discussed in manufacturing section 4.2.2 the PPS+HackRF timing scheme has already been tested and it has been determined that the sample rate of the SDR is the current limiting factor in terms of being able to produce a synced timing pulse. Depending on the sample rate the SDR is set to the minimum timing precision which can be anywhere from 420ns at 2.4M samples per second to 50ns at 20M samples per second. Both of these numbers would satisfy requirement **FR 5.1** stating that the timing precision of each unit has to be at most 420ns. However being able to align the pulses with this precision can be tricky and potentially introduce more error into the system. This is talked about more in section 5.4.

#### Verification test for FR 5.2

Validating **FR 5.2** involves setting the SDR's sampling rate to 20 million samples per second, recording the data and comparing the number of samples produced versus the setting. The number of samples should be 20M which exceeds **FR 5.2**, satisfying the requirement. Standard deviation will be used to verify the alignment. The proposed setup for **FR 5.2** is shown in Figure 35.

After recording data as described in 4.2.2 a simple peak finding function was used to place markers where the PPS pulses were identified. The number of samples between markers can then be used to verify sample rate.

From testing, it was found that the data output from the SDR could be bottlenecked by the USB controller on the host computer. Further testing was done on a standard Windows machine and it was found that the SDR was capable of producing a steady 20M samples/s. This was also confirmed by the SDR output which logs the bytes per second being written. Knowing that the HackRF SDR outputs 8 bits per a sample and that there are two streams I and Q, the expected data/second is easy to calculate. However,

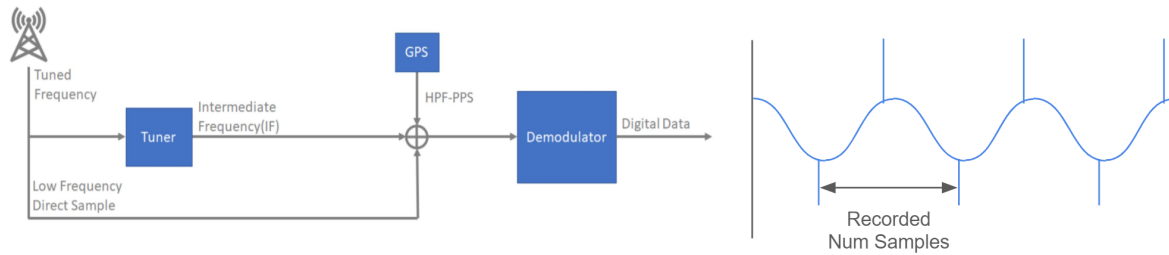


Figure 35: Test setup for DR 5.2

when hosted by the raspberry pi the SDR would drop samples unexpectedly. Figure 36 shows the reported samples rate. From the picture its easy to see that some samples are lost and not being written to the file as expected. This was further confirmed after plotting the data sets.

```

Receive wav file: HackRF_20210416_040909Z_437250kHz_IQ.wav
call hackrf_set_sample_rate(5000000 Hz/5.000 MHz)
call hackrf_set_freq(437250000 Hz/437.250 MHz)
samples_to_xfer 75000000/75Mio
Stop with Ctrl-C
10.0 MiB / 1.000 sec = 10.0 MiB/second
10.2 MiB / 1.000 sec = 10.2 MiB/second
10.0 MiB / 1.000 sec = 10.0 MiB/second
10.2 MiB / 1.000 sec = 10.2 MiB/second
10.0 MiB / 1.001 sec = 10.0 MiB/second
0.3 MiB / 1.000 sec = 0.3 MiB/second

Exiting... hackrf_is_streaming() result: streaming terminated (-1004)
Total time: 16.00335 s
hackrf_stop_rx() done
hackrf_close() done
hackrf_exit() done
fclose(fd) done
exit

```

Figure 36: Screen cap of the reported number of samples written to file.

From some research and testing it's believed that the dropped samples are due to the USB controller on the Raspberry pi becoming overwhelmed. By telling the SDR to write the data to *dev/null* or essentially dump all data the SDR is able to maintain the consistent write speeds that were seen on the Windows based machines. Using a more capable computer such as a NUC could solve this inconsistent write speed problem. Given the hardware at hand the best solution was to decrease the sample rate. Decreasing the sample rate would delay how long it would take before samples were dropped. This gives longer periods of time that can be used to find a satellite ping. At the same time lowering the sample rate also hurts the accuracy that can archived through TDOA as described in section 4.2.2. Recording data at multiple sample rates, the sample deviation as well as time till sample drops occurred were both recorded and used in a trade study to determine how low the sample rate should be dropped. The final decision was to lower the sample rate to 5M samples/s. At 5M samples per second the samples deviation was  $\pm 2$  samples/second and the average time till dropped samples was 12.5s with a standard deviation of 1.02s. From the trade study it was determined that 5M samples/s gave the best balance between timing accuracy

and consistency while still satisfying **FR 5.2**.

### Verification test for **FR 5.3**

Verification that the sensor units can be placed at least 100 km apart will be done by calling ahead the locations of interest to make sure that we will be able to use the local utilities and place our sensor boxes at the sites. Success is defined here as confirmations from all sites. The proposed setup for **FR 5.3** is shown in Figure 37. The team chose these positions based on either family or friends who live in these locations.

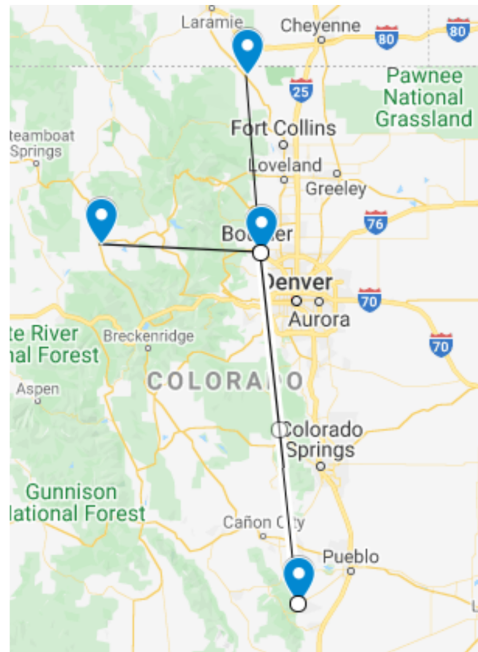


Figure 37: Proposed Test locations for DR 5.3

### Verification test for **FR 5.4**

The onboard SDR should have a total bandwidth of at least 10 MHz. This verification test is done by inspection of the data sheet, and demonstration of the physical SDR unit by powering it on and verifying that it indeed reaches at least 10 MHz in bandwidth.

This requirement was tested as described above. From testing, the HackRF was able to record 20M samples at a bandwidth of 10MHz. However it is worth noting that this seems to depend on the software and hardware used on the host computer. Some software's such as SDR# would have the same inconsistent write speed issues as explained previously.

### Verification test for **FR 5.5**

The verification of **FR 5.5** will be done using a demonstration test. Once the components of a single sensor unit has been integrated, the sensor unit will be turned on and allowed to record sensor data from the SDR at the maximum possible data rate. The sensor unit will be left on for 10 minutes which will bound all expected pass over lengths for each of our two satellite candidates. The resulting data packet size from this test will be multiplied by four to represent the theoretical maximum data size we

would expect from four pass overs of our candidate satellite. This test will be considered a success if the theoretical data limit determined by this demonstration is less than the 64GB of available on-board storage.

Performing the test described above the sensor unit was capable of passing with the recorded maximum data size being 12 GB for a total of 48 GB.

#### 5.4 Position Vector Estimate using TDoA

Once the TDoA values are found, we can use the following method inspired by [5] to find position. Let  $d_1, d_2, \dots, d_M$  be the geometric distances between the target satellite and the sensors  $1, 2, \dots, M$ . Let  $\tau_1, \tau_2, \dots, \tau_M$  be the time of arrival (ToA) of the signal sent from the target, received at sensors  $1, 2, \dots, M$ . Let  $\mathbf{p}_1, \mathbf{p}_2, \dots, \mathbf{p}_M$  be the position vectors of sensors  $1, 2, \dots, M$  in the earth-centered, earth-fixed (ECEF) frame of reference, which is found using GPS measurements through the Google Maps framework. Let  $\mathbf{p}_T$  be the target satellite's ECEF position vector that this algorithm will find. The problem setup diagram is shown in Figure 38.

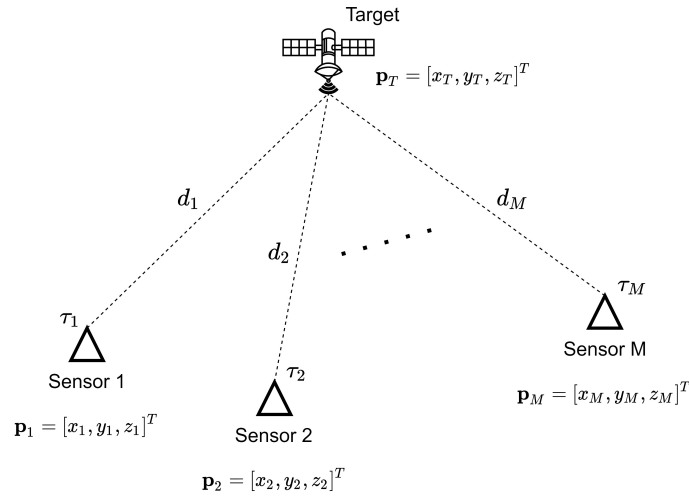


Figure 38: TDoA Positioning Problem Setup

Now using the above method of cross-correlation, taking sensor 1 as the reference, the TDoA value between the first and  $j^{th}$  sensor is found:

$$\tau_{1,j} = \tau_j - \tau_1 \quad (1)$$

where  $j = 2, \dots, M$ . Taking  $c$  as the speed of light in a vacuum, Eq. 1 becomes:

$$\tau_{1,j} = \frac{d_j - d_1}{c} \quad (2)$$

$$\implies d_j = d_1 + c\tau_{1,j} \quad (3)$$

Let  $P_j \equiv d_j - d_1$  such that  $P_j = c\tau_{1,j}$ .

Now due to the fact that  $d_j = |\mathbf{p}_T - \mathbf{p}_j| = \sqrt{(x_T - x_j)^2 + (y_T - y_j)^2 + (z_T - z_j)^2}$  for all  $j = 1, 2, \dots, M$ , the following is true:

$$\begin{aligned}
P_j(x_T, y_T, z_T) &= c\tau_{1,j} = |\mathbf{p}_T - \mathbf{p}_j| - |\mathbf{p}_T - \mathbf{p}_1| \\
&= \sqrt{(x_T - x_j)^2 + (y_T - y_j)^2 + (z_T - z_j)^2} - \sqrt{(x_T - x_1)^2 + (y_T - y_1)^2 + (z_T - z_1)^2}
\end{aligned} \tag{4}$$

where  $j = 2, \dots, M$  since sensor 1 is the reference; this will be implied when a  $j$  subscript is used for the rest of this section. These equations are highly nonlinear, so it is generally very difficult to use them to back-solve for the components of  $\mathbf{p}_T$ . The solution to this is to linearize Eq. 4 and use the linearization to iteratively guess and adjust  $\mathbf{p}_T$  until the adjustment magnitude is sufficiently small. To linearize, first take the Taylor series of the multi-variable, scalar valued function,  $P_j(x_T, y_T, z_T) = P_j(\mathbf{p}_T)$  about some point  $\mathbf{p}_{T_0} = [x_{T_0}, y_{T_0}, z_{T_0}]^T$ :

$$P_j(\mathbf{p}_T) = P_j(\mathbf{p}_{T_0}) + \frac{\partial P_j(\mathbf{p}_{T_0})}{\partial x_T}(x_T - x_{T_0}) + \frac{\partial P_j(\mathbf{p}_{T_0})}{\partial y_T}(y_T - y_{T_0}) + \frac{\partial P_j(\mathbf{p}_{T_0})}{\partial z_T}(z_T - z_{T_0}) + \dots \tag{5}$$

Now, dropping higher order terms, we let  $\Delta x_T = x_T - x_{T_0}$ ,  $\Delta y_T = y_T - y_{T_0}$ ,  $\Delta z_T = z_T - z_{T_0}$ , and  $\Delta P_j = P_j(\mathbf{p}_T) - P_j(\mathbf{p}_{T_0})$ . Equation 5 then becomes:

$$\Delta P_j = \frac{\partial P_j(\mathbf{p}_{T_0})}{\partial x_T} \Delta x_T + \frac{\partial P_j(\mathbf{p}_{T_0})}{\partial y_T} \Delta y_T + \frac{\partial P_j(\mathbf{p}_{T_0})}{\partial z_T} \Delta z_T \tag{6}$$

So, Eq. 4 is linearized. For the specific case of  $M = 4$ , the following system of linear equations used:

$$\begin{bmatrix} \Delta P_2 \\ \Delta P_3 \\ \Delta P_4 \end{bmatrix} = \begin{bmatrix} \frac{\partial P_2(\mathbf{p}_{T_0})}{\partial x_T} & \frac{\partial P_2(\mathbf{p}_{T_0})}{\partial y_T} & \frac{\partial P_2(\mathbf{p}_{T_0})}{\partial z_T} \\ \frac{\partial P_3(\mathbf{p}_{T_0})}{\partial x_T} & \frac{\partial P_3(\mathbf{p}_{T_0})}{\partial y_T} & \frac{\partial P_3(\mathbf{p}_{T_0})}{\partial z_T} \\ \frac{\partial P_4(\mathbf{p}_{T_0})}{\partial x_T} & \frac{\partial P_4(\mathbf{p}_{T_0})}{\partial y_T} & \frac{\partial P_4(\mathbf{p}_{T_0})}{\partial z_T} \end{bmatrix} \begin{bmatrix} \Delta x_T \\ \Delta y_T \\ \Delta z_T \end{bmatrix} \tag{7}$$

This linear system is written as follows:

$$\Delta \mathbf{P} = \mathbf{J} \cdot \Delta \mathbf{x} \tag{8}$$

where  $\mathbf{J}$  is a Jacobian matrix. The least-squares estimate of  $\Delta \mathbf{x}$  (denoted  $\hat{\Delta \mathbf{x}}$ ) can generally be found through the use of the Moore-Penrose inverse [6] of  $\mathbf{J}$  (denoted  $\mathbf{J}^\dagger$ ) as follows:

$$\mathbf{J}^\dagger = \left( \mathbf{J}^H \mathbf{J} \right)^{-1} \mathbf{J}^H \tag{9}$$

$$\hat{\Delta \mathbf{x}} = \mathbf{J}^\dagger \cdot \Delta \mathbf{P} \tag{10}$$

where  $\mathbf{J}^H$  is the Hermitian transpose of  $\mathbf{J}$ .  $\hat{\Delta \mathbf{x}}$  is the least-squares estimate of  $\mathbf{p}_T - \mathbf{p}_{T_0}$ : the error between the true position of the satellite and the initial guess position. Lastly, add  $\hat{\Delta \mathbf{x}}$  to the initial guess and set that as the new guess.

$$\hat{\mathbf{x}} = \hat{\Delta \mathbf{x}} + \mathbf{p}_{T_0} \rightarrow \boxed{\hat{\mathbf{x}} = \mathbf{p}_{T_{0,\text{new}}}} \tag{11}$$

This process then iterates and the guessed position  $\mathbf{p}_{T_0}$  gets progressively closer to the true position. The algorithm is stopped once  $|\hat{\Delta\mathbf{x}}|$  has fallen under some acceptable threshold. Once the algorithm stops, the last position estimate  $\hat{\mathbf{x}}$  will be sufficiently close approximation to the true satellite position.

### Verification Test for FR 5

Given satisfaction of **FR 1** through **FR 4**, all respective design requirement derivatives, and design requirements **FR 5.1** through **FR 5.5**, the next step in the verification of our system is to perform a full suite test. This test incorporates all of our major subsystems and is representative of narrowing in on verification of full system performance.

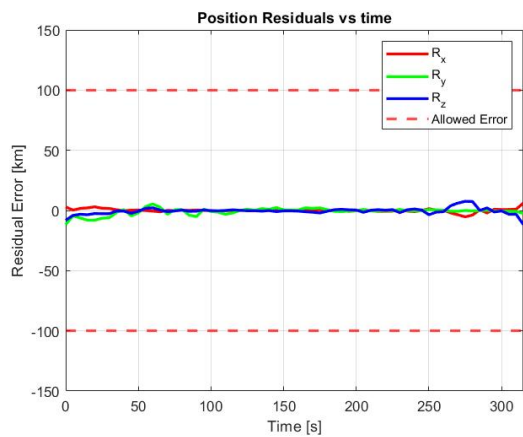
For this test, the team has identified four locations for the sensor units to be deployed at Pueblo, Boulder, Aurora, and Virginia Dale. These locations in Colorado have been identified, by surveying resources available to the team, as places that we have permission to access local utilities for the duration of this test. Next, STK will be referenced to determine the date and time of pass-over opportunities. Those opportunities that work for the team will be used to schedule the test duration. Due to the orbital characteristics of our satellite candidates, we expect three to six pass over opportunities for our given location in the span of a day. Those days that offer three or more pass-overs will be considered prime test conditions. After the sensor units have been installed in their designated locations we plan to leave them in place long enough to collect data for three separate pass-overs. By picking days that offer more than three pass-overs, we can guarantee that we will be able to satisfy the data collection requirement in one day of testing. Once this data has been collected, the sensor units will be brought back to a central location, and the raw data collected by each unit will be compared and post-processed. For the purposes of analysis each set of pass-over data will be reviewed independently. For each pass-over we successfully record, should **FR 4** be satisfied, we will have a unique data set for each of our sensor units. Our matured application of TDoA analysis will be applied to these data sets and an estimate for the satellite candidate's position vector will be generated for the duration of the pass-over. Once this positional data has been generated, an STK simulation will produce the positional vector truth data for our satellite candidate pass-over. If direct comparison of our TDoA generated positional vector data, and the propagated STK positional vector data results in an a relative error that satisfies **FR 5**, then our test will be considered a success. The relative error comparison for **FR 6** is shown in Figure 39. Figure 39a shows how the error in the position estimate varies over a flyby. The error never passes the threshold set by **FR 5**. The estimate was produced by the TDoA algorithm initially, but particle filter produced the majority of the estimates. The particle filter's velocity error or residual is depicted in figure 39b. There is more noise in the velocity error than the position. Filter infers the velocity based on previous measurement and the current measurement. The measurements contain no information about the velocity only information about the position. Hence, the position data is far more consistent.

## 5.5 Orbital Element Determination

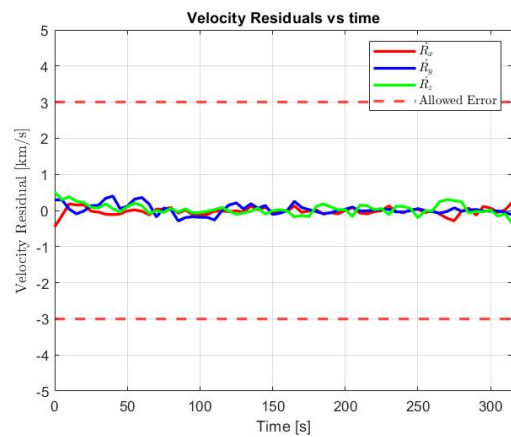
### Verification Test for FR 6

Our verification of **FR 6** was split up into three tests. Tests one and two would serve to increase confidence in our orbital determination process. Test three would prove overall compliance of our final project with **FR 6**.

Our first test utilized analysis to validate our post processing flow by generating a series of state vectors

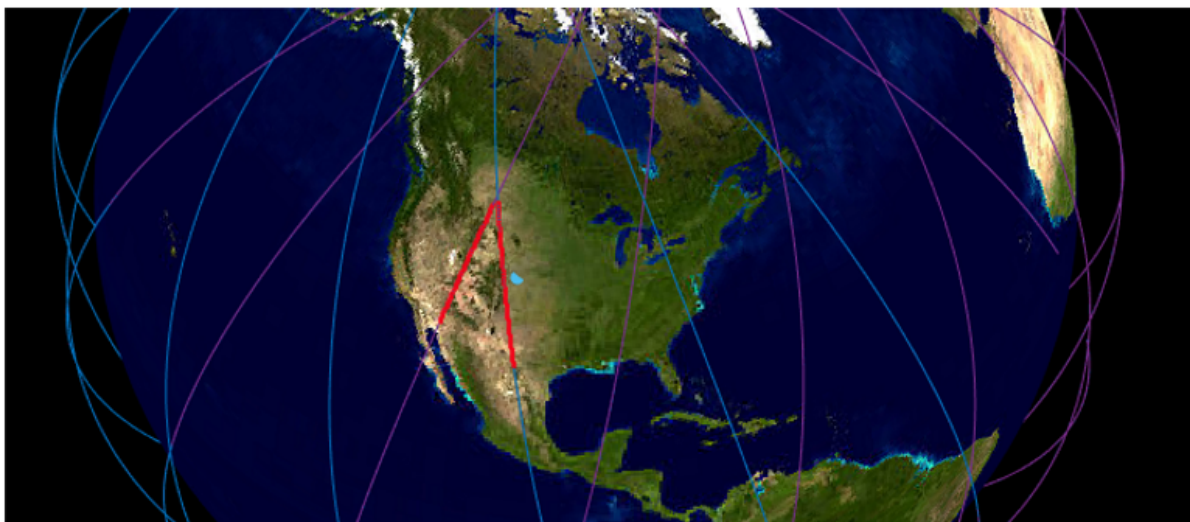


(a) Error in the Position Components



(b) Error in the Velocity Components

Figure 39: Orbital State Error over a Single Flyby



Transit Access Results:			Transit Access Results:			Transit Access Results:		
Comparison	TLE Ref.	TLE Calc.	Comparison	TLE Ref.	TLE Calc.	Comparison	TLE Ref.	TLE Calc.
Prediction Tolerances			Access 1			Access 1		
Start Time +/- [min]	<input type="text" value="45"/>	45	04/27/21 04:52:41 - 04/27/21 04:57:23			04/27/21 04:52:47 - 04/27/21 04:57:24		
Start Az. +/- [deg]	<input type="text" value="30"/>	30	Max Elevation of 82.1023°			Max Elevation of 82.1493°		
Max Elev. +/- [deg]	<input type="text" value="15"/>	15	Start Az. of 171.5058°			Start Az. of 171.7067°		
Access 1			Access 2			Access 2		
04/27/21 04:52:47 - 04/27/21 04:57:24			04/27/21 18:09:41 - 04/27/21 18:13:23			04/27/21 18:09:47 - 04/27/21 18:13:24		
Max Elevation of 82.1493°			Max Elevation of 40.4414°			Max Elevation of 40.4732°		
Start Az. of 171.7067°			Start Az. of 340.2661°			Start Az. of 339.319°		
Access 2								
04/27/21 18:09:47 - 04/27/21 18:13:24								
Max Elevation of 40.4732°								
Start Az. of 339.319°								

Figure 40: Propagated Truth and Calculated TLE's from State Vector

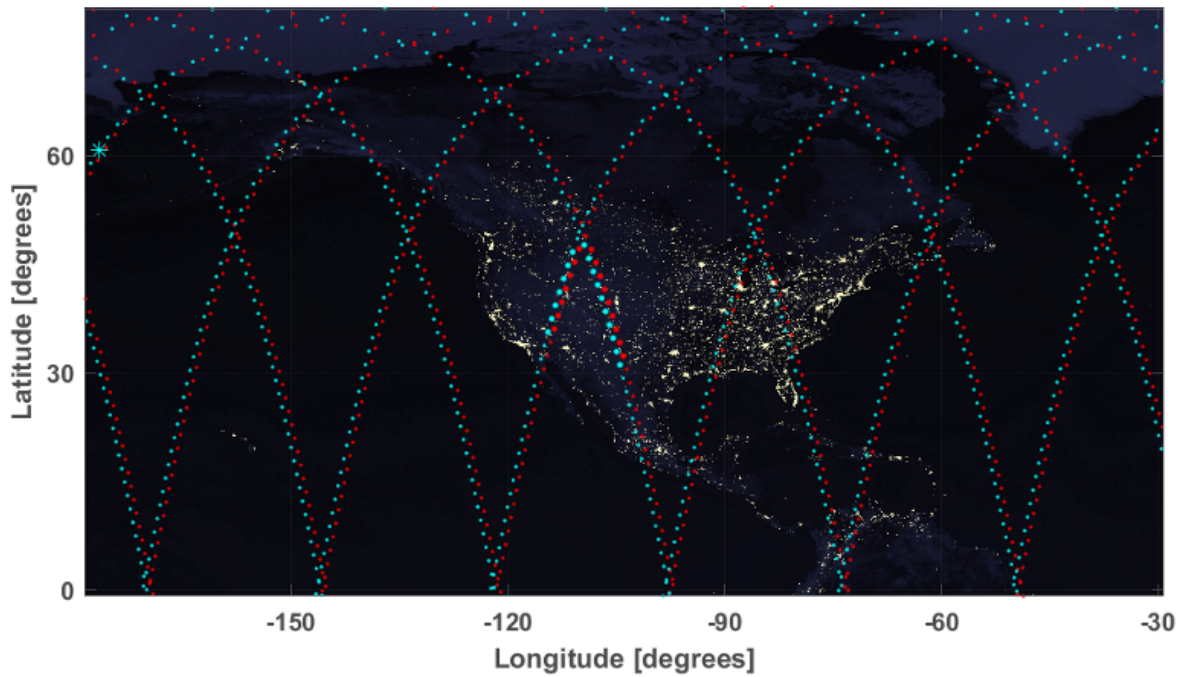
in STK from a known TLE for our CSIM satellite candidate. Taking a state vector and time stamp from that data output file and generating a calculated TLE for comparison, we aimed to characterize inherent bias in our propagation methodology. This calculated TLE was propagated forward alongside a publicly available TLE for the same satellite. The predicted passover opportunities of CSIM from each TLE for Boulder, Colorado were reported by our application and compared to see if this zero-noise case could be handled by our comparison process and metrics. Results from this test can be seen in Figure 40 and satisfy **FR 6** with a healthy margin. Through this test, error inherent in TLE generation process from Truth data only amounts to about a 6 [s] difference in start time, Max Elevation difference of about 0.04 [deg] and Start Azimuth discrepancy of about 0.9 [deg].

Our second test additionally utilized analysis to further validate our intended post-processing procedures and further increase confidence in our orbital prediction model. Instead of using STK simulation data, we streamlined our TDoA modeling and orbital determination processes. Here, position data produced from our TDoA model that sought to incorporate signal noise from timing and GDoP error. A generated state vector incorporating this error was flowed directly into our orbital propagation application as was done in the first test. From here, a TLE was once again calculated, and the predictive abilities were determined. Results from this test can be seen in Figure 41 and again satisfy **FR 6**. This test characterized error inherent in our post processing procedure for both of these steps. The difference in predictive capabilities resulting from each TLE only amounted to about a 3 [min.] variation in start time, Max Elevation difference of about 12 [deg] and Start Azimuth discrepancy of about 3 [deg]. These results show that our predicted margins have decreased a fair amount but are still within specifications of the functional requirements. This increased discrepancy is likely rooted in the use of only a single state-vector from a satellite passover in generating the TLE used for propagation and comparison. Even after passing through the particle filter process, we still expect a certain level of noise to remain on this data. While this test was successful, it shows that further analysis and process development is needed to filter out this noise and systematic error.

Our final test is designed to build off of the previous and validate the foundation of this project as a whole. Rather than flowing simulated STK or data from our TDoA model, all four of our sensor units would be deployed across Colorado and used to record actual data RF ping data from several passovers of our CSIM candidate satellite. Following successful data collection across all four sensor units, we offload each data file to a central computer where our post processing begins. Starting with signal alignment of PPS signal across each data set, we then perform cross correlation and extract out TDoA values for each unit throughout the passover. These TDoA values are then flowed to the particle filter. From here, the process continues just as the previous tests did. First generating a TLE from the recorded data and then comparing the predictive capabilities of the TLE by propagating and comparing to a reference set. Should this final step meet the criteria outlined in **FR 6**, we would complete the intended scope of this senior project. Due to circumstances detailed earlier regarding issues with our sensor units on-board software, we were never able to successfully deploy our sensor units. From a technical standpoint, we maintain confidence in the design of our system. Our failure to achieve this test and consequential de-scoping of this project stems from running out of the necessary debug and deployment time.

## 5.6 Summary of Verification and Validation Tests

When looking at these tests as applied to the scope of this project as a whole, there were many success's and setbacks. From the data and characterization gathered thus far, the team maintains confidence in the overall design of our system. We believe that continued development of this project would see additional



Transit Access Results:			Transit Access Results:			Transit Access Results:			
Comparison	TLE Ref.	TLE Calc.	Comparison	TLE Ref.	TLE Calc.	Comparison	TLE Ref.	TLE Calc.	
Prediction Tolerances			Access 1			Access 1			
Start Time +/- [min]	<input type="text" value="45"/>	45	04/27/21 04:52:59 - 04/27/21 04:56:59			04/27/21 04:56:00 - 04/27/21 05:00:30			
Start Az. +/- [deg]	<input type="text" value="30"/>	30	Max Elevation of 82.1023°			Max Elevation of 74.1658°			
Max Elev. +/- [deg]	<input type="text" value="15"/>	15	Start Az. of 172.1713°			Start Az. of 175.7125°			
			Access 2	Access 2			Access 2		
			04/27/21 18:09:59 - 04/27/21 18:12:59			04/27/21 18:13:30 - 04/27/21 18:16:30			
			Max Elevation of 40.4376°			Max Elevation of 37.2592°			
			Start Az. of 335.3336°			Start Az. of 329.7528°			
Access 1									
04/27/21 04:56:00 - 04/27/21 05:00:30									
Max Elevation of 74.1658°									
Start Az. of 175.7125°									
Access 2									
04/27/21 18:13:30 - 04/27/21 18:16:30									
Max Elevation of 37.2592°									
Start Az. of 329.7528°									

Figure 41: Propagated Truth and Calculated TLE's from Simulated TDoA values

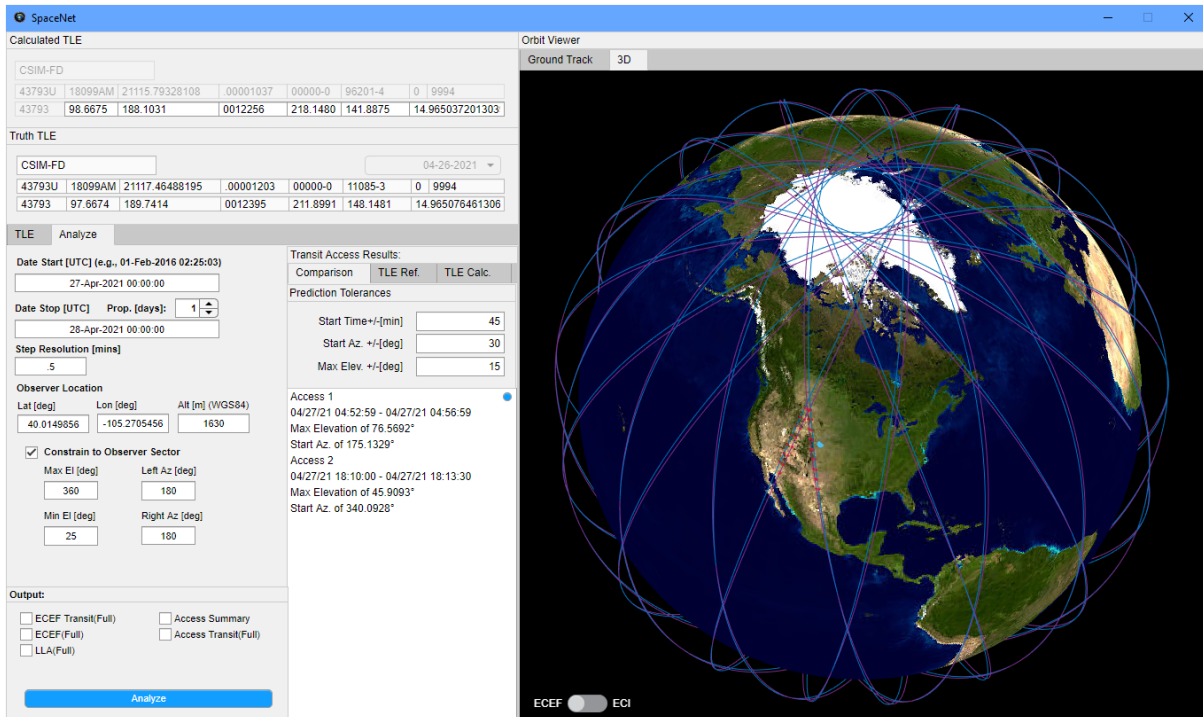


Figure 42: 3D Orbital Propagation

successes in the tests and demonstrations that were sidelined from schedule delays. Looking only at the completed work for this project, we can see how current development stacks up to our initially defined levels of success (Figure 43).

## 6 Risk Assessment and Mitigation

Author: Ryan Prince, Benji Smith

### 6.1 Project Risks

The following section identifies various risks that may prevent the project from achieving its objectives. The section breaks the risk into various categories and justifies their existence as a risk.

#### 6.1.1 Technical Risks

1. The GPS loses lock and its ability to synchronize time with atomic clocks. A small amount of drift in the GPS' PPS signal will have significant error propagated into the orbital estimate.
2. The link budgets fail to close due to weather conditions. The link budgets have been calculated based on the chosen hardware and expected satellite candidates with some margins to account for losses as the signal travels through the atmosphere, but when testing, it is possible the weather conditions exceed the margin assumed in the link budget. If the link cannot be closed the signal may be lost in the noise floor making timing impossible. This a major concern for the L-band link.
3. The SDR or GPS clock is cold. At start up of any Crystal oscillator, there is some kind of warm up time. Some oscillators are temperature compensated which limits this effect; however, there is

Level	Key Objectives & Results	Status
1	<b>TDoA from artificial data</b>	Complete
	<ul style="list-style-type: none"> <li>Signal alignment and cross correlation software successfully developed and verified with artificial data.</li> </ul>	
	<b>Orbital prediction from artificial data</b>	Complete
	<ul style="list-style-type: none"> <li>Successfully flowed simulated TDoA data through the particle filter to generate a state vector. The state vector was then successfully used to generate a TLE and make an orbital prediction within the thresholds defined by <b>FR 6</b>.</li> </ul>	
1	<b>Four units built</b>	Complete
	<ul style="list-style-type: none"> <li>All four planned sensor units were built and able to record and perform necessary data collection.</li> </ul>	
1	<b>Sensor units capable of receiving a single RF band</b>	Complete
	<ul style="list-style-type: none"> <li>Sensor units successfully able to collect data in the UHF RF band.</li> </ul>	
2	<b>TDoA prediction from two sets of data</b>	Incomplete
	<ul style="list-style-type: none"> <li>Sensor units capable of collecting data necessary to perform a TDoA prediction. The size of the raw data files (a single passover can be over 10gb) has crippled the teams ability to collaborate and effectively transfer data in the time left for this project. Solutions to this issue are known but time has run out in the schedule to develop and implement.</li> </ul>	
	<b>Sensor units capable of receiving dual RF bands</b>	Complete
	<ul style="list-style-type: none"> <li>Sensor units equipped and capable of recording RF data in both UHF and L RF bands. Researched and looked into expanding capabilities to receive a third RF band but that proved to be outside of visible range for our antenna choices.</li> </ul>	
	<b>Sensor units shall be able to recover in the result of a power outage</b>	Complete
<ul style="list-style-type: none"> <li>After much debugging, the onboard OS installed on each sensor unit is capable of rebooting itself after a power failure and determining the next passover it needs to record for.</li> </ul>		
2	<b>Sensor units synchronized to UTC through GPS to within 420 [ns]</b>	Complete
	<ul style="list-style-type: none"> <li>Sensor units equipped with GPS modules which injects a PPS into the data stream. Synchronization additionally achieved to within 200[ns].</li> </ul>	
3	<b>All four units deployed and operational</b>	Incomplete
	<ul style="list-style-type: none"> <li>All four units are operational and ready to be deployed. The team was unable to go through full deployment of our sensor suite due to schedule constraints but maintains confidence in the technical foundations of our project and unit design.</li> </ul>	
	<b>Manufacturing analysis, recommendations, and report documentation</b>	Complete
	<ul style="list-style-type: none"> <li>A Cohesive document was delivered to the customer detailing full manufacturing processes, recommendations and advisory on best practices for the continuation of this project.</li> </ul>	
	<b>TDoA prediction from four units of data</b>	Incomplete
<ul style="list-style-type: none"> <li>The units are fully capable of recording the data needed to generate a TDoA prediction. Due to schedule constraints, the team was unable to deploy these units in time to collect the data needed to perform this prediction.</li> </ul>		
3	<b>Orbital prediction from real data</b>	Incomplete
	<ul style="list-style-type: none"> <li>The full post-processing routine has been tested and verified to be within the team's functional requirements. Due to schedule constraints, the team was unable to fully deploy the sensor suite and return the data necessary to generate a real orbital prediction.</li> </ul>	

Figure 43: Levels of Success Breakdown

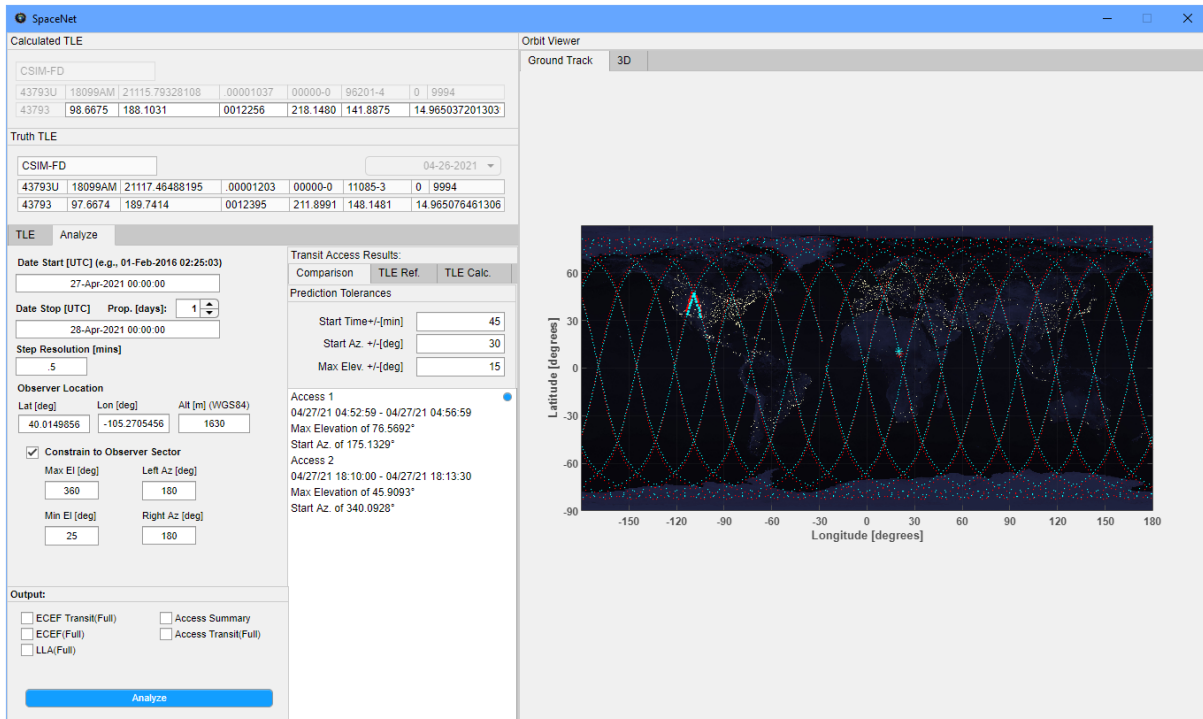


Figure 44: SpaceNet Orbital Propagation Ground Track

still a possibility that the clock will run slower at start up. A slower clock could mean dropped signals which would invalidate some data.

4. The SDR drops samples. This is a concern as explained in the last risk
5. The PPS is lost in the RF signal. There is a possibility that when imposed on the HackRF data stream, the PPS signal can be lost in the RF signal depending on how the demodulator handles the data. If the PPS cannot be picked out of the stream there is no way to align the data.
6. Data rates are too much for the Raspberry pi to handle. There is a possibility that the Raspberry pi cannot handle the sustained data rates of the SDR's outputs. If this is the case two things could happen: 1. the Raspberry pi could drop samples invalidating the data. 2. The Raspberry pi will use its on-board memory as a buffer to ensure it retains all the samples. However, if the Raspberry pi runs out of memory, the units will crash or drop samples.
7. The position vectors are too far out of plane for Gibb's method to produce accurate orbital estimates. The accuracy of Gibb's method is directly tied to how coplanar the position vectors. As they move further out, the error in the orbital estimate increases.

### 6.1.2 Logistical Risks

8. Sensor units cannot be placed in the desired locations. Based on the preliminary TDoA calculations, the sensor units would ideally be placed at least 100 km apart from one another. However, it is possible we do not have access to these locations. This would cause timing error to have even greater effects on the orbital estimation.
9. SDR is out of stock, or there is a long lead time. Due to the current situation with COVID, there has been shortages in materials and extended lead times on a lot of items. If the SDR is unavailable

or will arrive late, it could push the entire project back and reduce the allotted time available for debugging and testing.

- Raspberry pi is out of stock, or there is a long lead time. For the same reasons as above, the Raspberry pi could be out of stock having similar hindrances as the SDR being out of stock.

### 6.1.3 Safety Risks

- Sensor has a short of some kind. In the event of a electrical failure, it is possible that mains power could be exposed. A failure of this kind would essentially render the unit unusable and could be a safety hazard to people nearby.
- The antenna or box mount fails. In the event the antenna or box mount fails depending on its mounted location this could be a safety hazard. Additionally, if the antenna are not pointing upright, the unit is unusable as it posses no pointing control of the antenna.

### 6.1.4 Financial Risks

- We "kill" a SDR while implementing the timing modification. This a big concern as the chosen SDR is 30% of the budget per unit. Having to replace these units could quickly deplete our remaining funds.

## 6.2 Risk Matrix

The severity of risks listed in the previous section are plotted against their likelihood of occurring in the risk matrix shown in Figure 45.

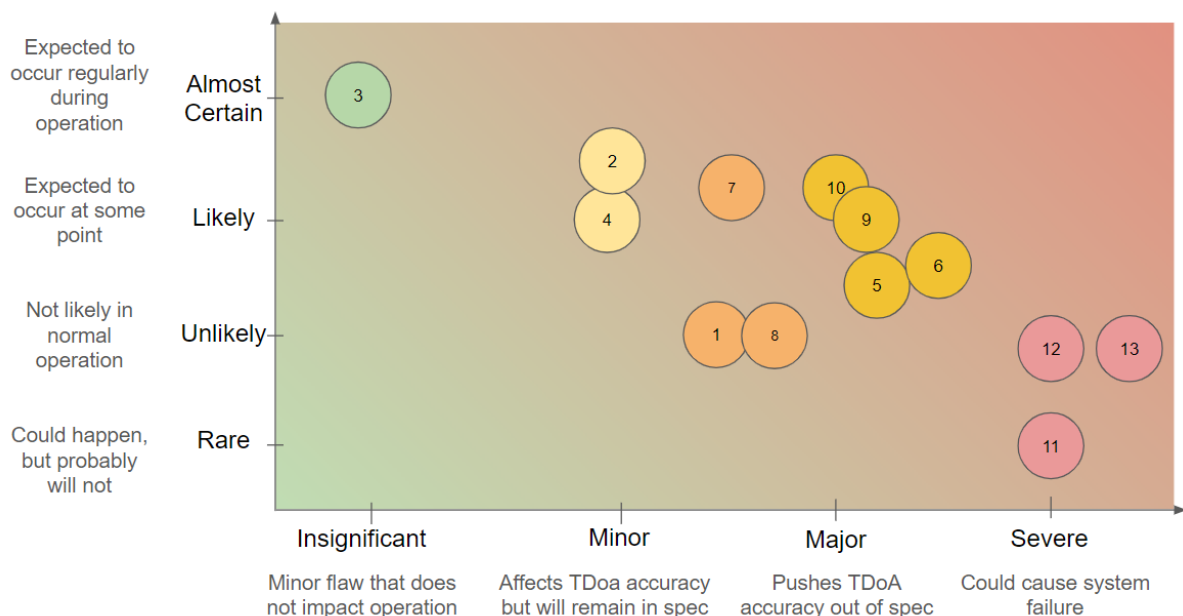


Figure 45: Risk Matrix

The plot shows the likelihood of each risk occurring, and the relative severity each risk has on the TDoA measurement and the orbital determination method as a result. The most severe consequences come from hardware failures where the system will be rendered inoperable if these occur. The worst of the

hardware failures is if we manage to disable a SDR while trying to set up timing sync abilities. Without that ability to sync data with the other SDRs, the SDR as a part of the system becomes useless.

Other major concerns which are likely to occur are logistical. In the current state of things, long lead times could cause problems and limit our selection of hardware forcing us to make compromises or go over budget. Other concerns are the holidays. Some items, such as the Raspberry pi, are popular presents and often go out of stock for months.

Likely failures include internal error with the SDR and GPS. Both have internal oscillators that will have unavoidable warm ups from a cold start reducing their accuracy.

### 6.3 Risk Mitigation

Table 2 shows the relative risk mitigation strategies employed to reduce the overall high risk items. Figure 46 shows the updated matrix and where the mitigated values lie.

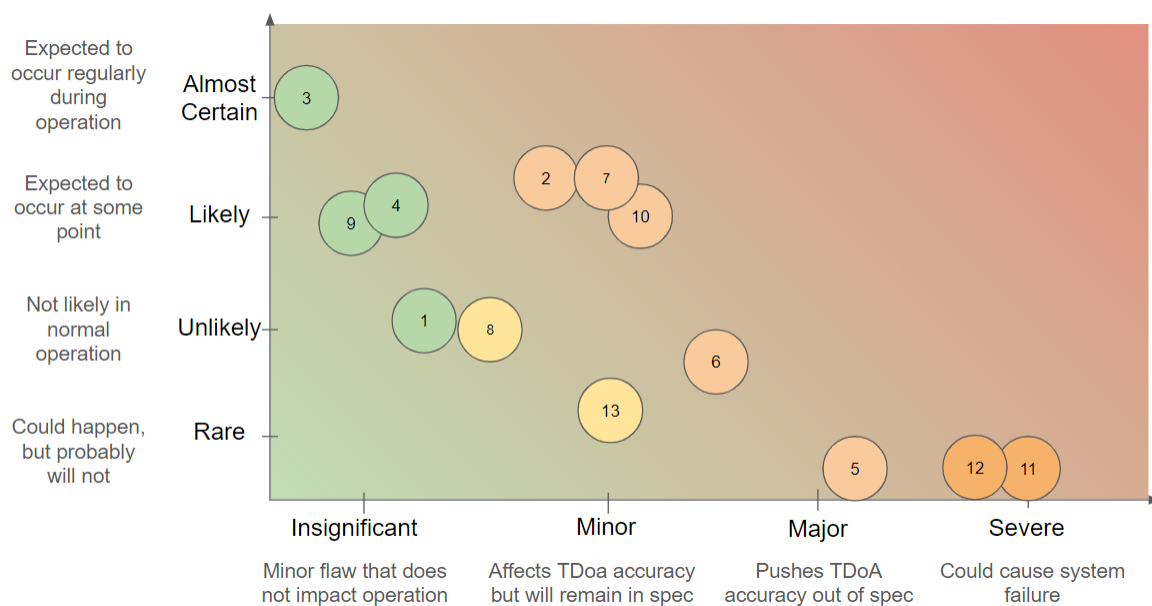


Figure 46: Risk matrix after considering the mitigation's shown above in table 2

### 6.4 Risk Realization

The main issues we did not account for in our initial risk analysis was the factor of human error and inexperience when it came to the complexity of this project. Errors in the file formatting on the onboard operating system, along with insufficient file storage led to bugs and operating problems during unit testing, and made the full scale deployment of the units incompatible during this spring semester. The other risks on this risk matrix were understood and analyzed throughout the course of subsystem level testing, or were unable to be analyzed due to the onboard operating system issues. Major risk #1 and #2 were not verifiable as multiple units needed to be tested to test the risk protocol, Risk #3 was mitigated by ordering components early, Risks #4 and #5 were mitigated through testing the software defined radio in base level testing, PPS was able to be verified by the single-unit deployment, Electrical short, water damage, and antenna mount failure was tested in several modes, and the risk was mitigated, System noise was characterized as low through connection testing with subsystem level testing, particle filter

Table 2: Risks and their associated mitigation's

Risk	Mitigation
1 The GPS loses lock.	The GPS has minimal drift over the course of few minutes. Taking longer passes to achieve a lock at the start and end of data set is enough to correct this.
2 The link budgets fail to close due to weather conditions.	The chosen hardware can only provide so much gain one strategy is to use software to try and artificially increase the gain of the signal. Another approach is to take enough data points that loose a few due to cloud coverage is not a problem.
3 The SDR or GPS clock is cold.	When starting the sensor the SDR and gps will be started before the expected pass time to account for the warm up time ensure the oscillators are operation correctly
4 The SDR drops samples.	Testing will be done before hand to quantify the error and try an establish the expected dropped samples per second. This can be used to artificially recover some data in the event samples are lost.
5 The PPS is lost in the RF signal.	The PPS can be fitted with a "less sensitive" high pass filter to allow more of the DC component through.
6 Data rates are too high.	If run times are kept short as planned this should give the pi time to buffer and offload the data. If this is still not possible a Raspberry pi with more ram can be used.
7 The position vectors are too far out of plane.	Smoothing can be applied to reduce this error to within acceptable margins
8 Sensor units cannot be placed in the desired locations	Backup locations can be used. The currently chosen SDR should also provide some leeway as it can achieve better timing precision than the minimum required at the 100km spacing.
9 SDR is out of stock, or there is a long lead time	The team has alternative suppliers and SDRS that they can go with.
10 Raspberry pi is out of stock, or there is a long lead time.	There are alternative computers but for a greater cost.
11 Sensor has a short of some kind	mains wiring will be placed inside the box to use the Nema rating to prevent live wires from being exposed. Cables will also be fitted with strain relief's to ensure the connectors are not stressed.
12 The antenna or box mount fails.	The mitigation here would be to make sure the antenna and box are mounted securely and preferable in an area sheltered from wind and foot traffic.
13 Dead SDR	Lower cost SDRs with out the quality guarantee will be used for testing before modifying the quality controlled models.

was completed for the project, and the Gibb's method risk was not categorized due to the lack of a multi-unit deployment.

## 7 Project Planning

Authors: Jordan Gage, Ryan Prince

The following section outlines the plan leading out of the design phase into Spring semester.

### 7.1 Organizational Chart

The team organization throughout the Fall semester and that we plan to carry into Spring is shown in Figure 47. The team operated in sub teams that were responsible for various aspects of the project. While this summarizes the teams operation structure there was a large amount of cross talk between teams. As such individuals work was not limited to the team they are claimed by.

<b>SpaceNet</b>			
<b>Software</b>	<b>Structures</b>	<b>Electronics and Data</b>	<b>RF Communications</b>
<p>The software team is responsible for the TDoA algorithm for positional estimates and both orbital determination methods: Gibbs, Particle filter.</p> <p>The team is also responsible for determining how error will propagate into orbital estimates based on system characteristics.</p>	<p>The structures team is responsible for designing, sourcing, and ultimately building the packaging for the sensor units.</p> <p>They maintain and up-to-date CAD model of the system</p>	<p>The Electronics and data team handles everything related to electrical hardware and power distribution as well as the onboard OS and the data rates the onboard computer must handle.</p>	<p>The communications team manages the RF front end. This includes performing the link budget analysis as well as selecting and sourcing the hardware to build the front end.</p>
<p><b>Sam Firth</b> Safety Lead</p> <p><b>Noah Francis</b> Software Lead</p> <p><b>Jordan Gauge</b> Financial Lead</p> <p><b>Keith Poletti</b> Lead Analyst</p> <p><b>Colin Ruark</b> Asst. Project Manager</p>	<p><b>Ryan Burdick</b> Manufacturing Lead</p>	<p><b>E Forest Owen</b> Data/Power Lead</p> <p><b>Ryan Prince</b> Project Manager</p> <p><b>Israel Quezada-Cordova</b> Electrical Lead</p>	<p><b>Tyler Pirner</b> Network Lead</p> <p><b>Benji Smith</b> Systems Engineer</p>

Figure 47: Organizational chart showing the team members their sub-teams and roles.

### 7.2 Work Breakdown Structure

Figure 48 shows the deliverable-based work breakdown structure for the Spring semester. The deliverables are broken up by the main sections of project as displayed in the CBD in Figure 4.

The deliverables are milestone events or events that block other major deliverables that ultimately block the CBD work flow. The goal for spring will be to try and prepare the timing modifications, RF front

end, Software, Power System and packaging in such a way that all subsystems are completed simultaneously. By ensuring all systems are ready to be integrated, full scale testing can begin with a minimal time lag between subsystem testing and full scale testing. In order to make sure the subsystems are operational and meet system requirements, subsystem verification testing has to be complete ideally before system integration; this will make debugging process smoother. As such, critical tests that may block a subsystem are listed as design deliverables in addition to the hardware and software products.

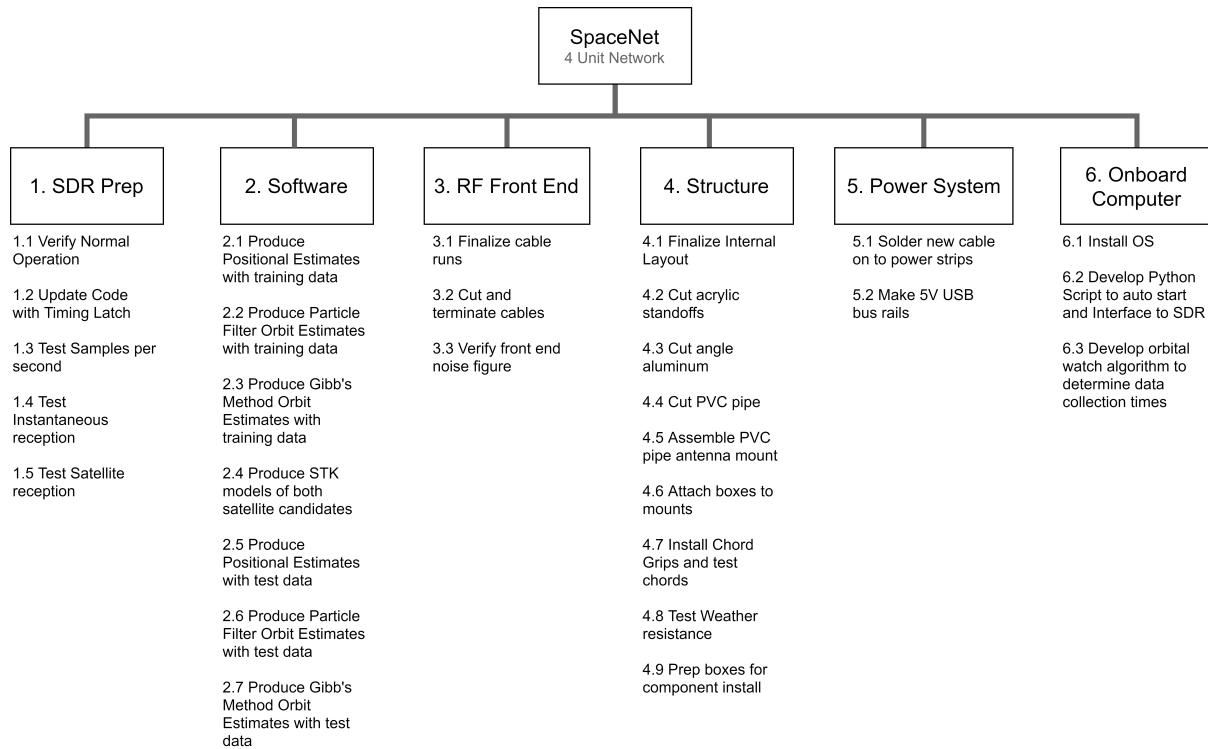


Figure 48: Deliverable based work break down structure for the fall semester. The deliverables are based on the CBD in Figure 4

### 7.3 Work Plan

The work plan for the Spring semester can be found in Figure 49. The work plan reflects the conceptual logic that was used when selecting what design deliverables to include in the work breakdown structure. Critical paths consists of major tests and hardware/ software deliverables that block system integration and full scale system testing.

Schedule margins were based on the progress the team has made leading into the spring semester. The post processing software had already been developed to a working state before entering CDR due to the research and development aspect of the project. The software needed to be developed to fully understand how error would propagate and what kind of performance the hardware has to achieve. The schedule then tries to leverage agile management by building up and testing one unit before ordering and building the other 3. While this plan was good in theory due to covid the limited hardware made it difficult for teams to perform tests as needed and small delays from one team would cascade pushing all teams behind during final integration. The biggest hold up was the On-Board os and making sure that it was robust enough to both meets system requirements and cope with other errors that may exist during normal operation.

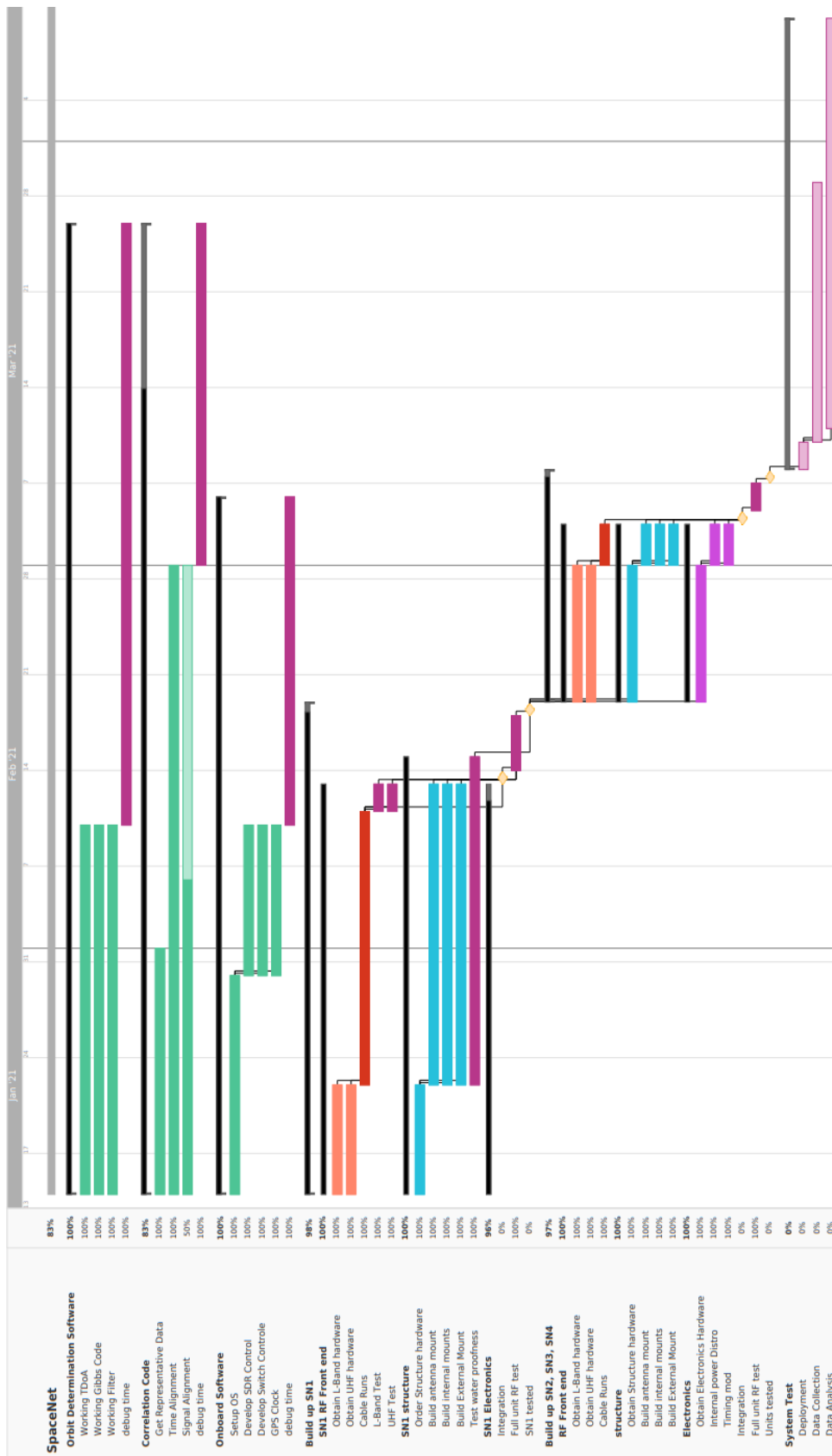


Figure 49: Gantt chart that outlines the workflow for the Spring semester. The gantt chart shows the conceptual critical pathing that was used when selecting the design deliverables shown in Figure 48. The sections relating to school deadlines were omitted in this screen capture.

The delays caused by the extended development time of the On-Board os and lack of hardware were amplified by a general struggle to communicate well. Ultimately this pushed the schedule so far behind that only zero TDOA testing could be started. Currently the team has four built and operational units that are capable of recording UHF data. However due to large data sizes its time consuming to both upload and parse the data sets to find a set of four files that contain satellite flybys.

## 7.4 Cost Plan

A complete itemized Bill of Materials(BOM) can be found in appendix C. The BOM shown in the appendix is an over estimate of cost of the system as it assuming that each box needs its own set of hardware when in reality the hardware cost will be split four ways reducing the cost shown. Figure 50 shows the major elements and this cost correction.

### Cost Plan

Item	Description	Price	Single Unit Cost
Raspberry Pi 4 Model B (4 GB)	on-board computer	\$55.00	\$ 848.23
HackRf One	software defined radio	\$299.95	
SD Card	32Gb SD card for OS and data storage	\$10.29	Four Unit Cost
L-Band Low Noise Amp	ZX60-242GLN-S+	\$74.82	\$3392.92
UHF Low Noise Amp	SPF5189Z RF amplifier	\$15.00	
L-Band Antenna	1.2 GHz 8 dBi flat patch antenna	\$50.00	Remaining Development Budget
UHF Antenna	HYS YAGI antenna high gain 9dBi UHF	\$50.00	\$800
Electronic RF Logic Switch	F2932EVBI evaluation board	\$83.13	
Housing	WH-16 hinged nema enclosure	\$50.75	
GPS Module	GPS module GPS NEO-6M	\$39.95	
Miscellaneous Electronics Hardware	power supply, cords, ProtoBoards, etc.	~\$69.34	
Miscellaneous Hardware	mounting hardware, screws, etc.	~\$50	

Figure 50: Cost budget. This budget includes major elements or the projects and accounts for the hardware per unit cost.

Figure 50 shows the cost plan as presented at CDR. The cost of the major elements remained correct throughout the spring semester. Leaving the team with around \$800 to work with in case anything unforeseen occurred. Figure 51, shown below, outlines the total cost of the project if this was to be done in industry.

The total labor cost was calculated assuming an entry level salary of \$65,000 for 2,080 hours, and a 200% assumed overhead. This including the final material cost, including the miscellaneous developmental costs, left the total cost of the project, if it was to be done in industry, at around \$126,000.

## 7.5 Test Plan

Table 3 outlines the major tests described in section 5 above. Tests were scheduled based on the gantt chart shown in Figure 49. Most tests were unrestricted by other tests and could be completed as soon as development/bring up was complete. The only tests that were in theory restricted by the completion

# Industry Cost of Project

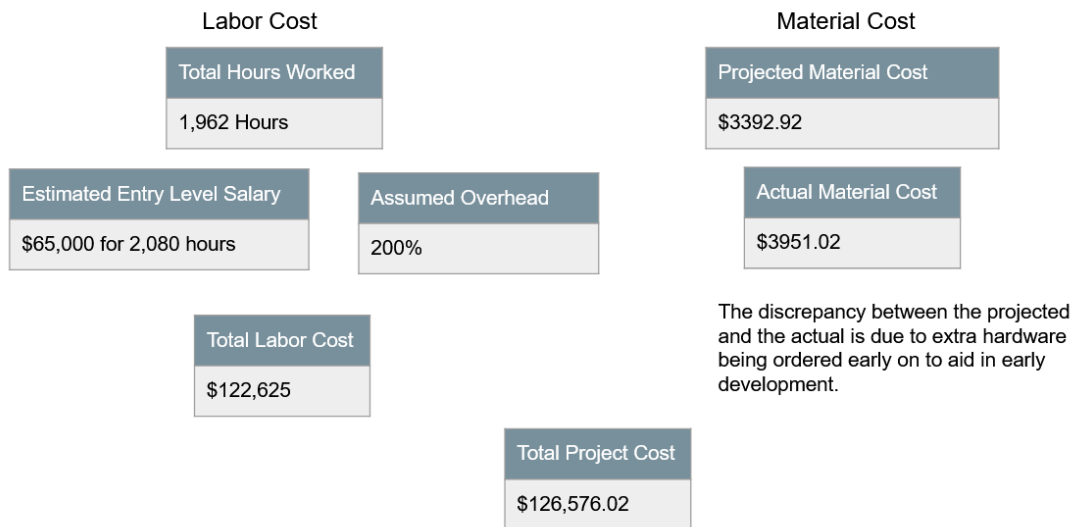


Figure 51: Total Project Cost

of others were the final integration tests: zero TDOA and full suite testing. As explained in section 7.3 some tests were inadvertently restricted by others due to the lack of hardware and covid. Currently four units are tested and operational but the full suite performance is yet to be quantified.

Table 3: Test Plan summarizing Rough Time line for critical Test Paths

Completion Date	Test	Status	Description
3/25/21	RF Front End(DR 3.1/2/3/4 )	Pass	Proves that single unit hardware can see RF signals in the desired bands.
2/28/21	Component level Time Synchronization testing(DR 5.1)	Pass	Proves that the timing mechanism is operating as expected on the SDR
<del>2/4/21</del> 4/2/21	Component level On board OS and script testing(DR 5.2)	Pass	Proves the auto start and SDR interfacing scripts are operational
<del>2/8/21</del> 4/2/21	Fully Integrated Single Unit RF Test (DR 5.2)	Pass	Proves that single fully integrated unit can receive RF signals, handle the data rates, and sample at the expected frequency.
2/9/21	Environment Survival Test (DRs 1.1-1.2)	Pass	Proves that a single fully integrated unit can survive the environment.
<del>3/22/21</del> 4/2/21	Fully Integrated Remaining Units RF Test (DR 5.2)	Pass	Proves all fully integrated units can see RF signals, handle the data rates and sample at the expected frequency.
3/23/21	Remaining Units Environment Survival Test (DRs 1.1-1.2)	Pass	Proves all fully integrated units can survive environment.
<del>4/5/21</del> 4/2/21	Full Suite Time Synchronization Test (DR5.1)	In Progress	Proves timing between units is sufficiently synchronized before moving them to final testing locations
<del>4/12/21</del>	TDoA Accuracy Test (DR 5.3 & FR5)	Incomplete	Proves data measured by 4 units can be turned into an orbital position of sufficient accuracy when compared to a truth data set.
<del>4/19/21</del>	TLE Accuracy Test	Incomplete	Further processes the data to prove the data collected and algorithms used produce a TLE of sufficient accuracy when compared to a truth TLE.

## 8 Lessons Learned

Authors: Ryan Prince

From a lessons learned perspective there are some general ones that can be applied to any large project.

Some of these are: The first 99% of integration takes 99% of the time and the last 1% also takes 99% of the time. Give more time than expected for trouble shooting. Divide work and make sure no individuals are falling behind. Try and separate critical paths as much as possible to reduce cascading delays. All of these are general systems engineering notes that can and should be taken into consideration when planning a project.

More specifically somethings that would have helped the team and projects success would be more group education sessions. Some of the challenges the team faced was our overall lack of knowledge in areas related to RF and predictive methods. While the team members were capable of self educating some information was conflicting and some times multiple members would spend time looking for answers another team member had already found. Talking to both our sponsor and CU professors who are well versed in areas related to our project was a huge help and provided us with invaluable information. Having more information or tech exchanges would have help tremendously by keeping everyone on the same page.

## 9 Individual Report Contributions

---

Ryan Burdick

Section 3, 4, and 5 in regards to structures and environmental readiness

---

Samuel Firth

Contributions to Section 2.3, Section 2.5

---

Noah Francis

Contributions to Section 5 on orbital determination.

---

Jordan Gage

Section 7

---

E Forest Owen

Contributions to Section 2, Section 3, Section 4, and 5 in regards to electronics, data handling, timing, and sections of on-board operating system.

---

Tyler Priner

Contributions to Sections 2, 5, as well as anything else pertaining to the RF front end. Primarily focused on SDR/timing research, in conjunction with link budget analysis

---

Keith Poletti

Contributions to Section 2.3, 4.3.3, Verification test for FR 2.5, Verification test for FR 5.3 Verification Test for FR 5,

---

Ryan Prince

Section 1, Sections 2.1, 2.2, 2.4, Contributions to 2.3, 2.5, Section 4.2.3, 4.2.4, 4.4, Section 5.3, Section 6, Section 7.1, 7.2, 7.3, 7.5, Section 8 set up document formatting,

---

Israel Quezada-Cordova

Contributions to Section 3, Section 4, and Section 5 in regards to electronics, data handling, timing, and sections of on-board operating system.

---

Colin Ruark

Section 5 relating to orbital determination methods

---

Benji Smith

Section 5 in regards to RF Front end , Baseline Trade Studies, and Risk Realization

---

## References

- [1] Defense Intelligence Agency. Challenge to security in space. <https://www.dia.mil/Military-Power-Publications/>, 2019.
- [2] N et al Tchorowski. Modeling and simulation of phased array antennas to support next-generation satellite design. <https://ntrs.nasa.gov/citations/20170001538>, 2016.
- [3] Jakub Kaderka and Tomas Urbanec. Time and sample rate synchronization of rtl-sdr using a gps receiver. *IEEE*, 2020.
- [4] Johnny L. Worthy III; Marcus J. Holzinger. Uncued satellite initial orbit determination using signals of opportunity, 2015.
- [5] Ufuk Tamer. Localization using tdoa and fdoa. *Middle East Technical University*, September 2015.
- [6] Roger Penrose. A generalized inverse for matrices. *Proceedings of the Cambridge Philosophical Society*, 1955.
- [7] Michael A Dornheim. Planetary flight surge faces budget realities. *Aviation Week & Space Technology*, 145(24):44–46, 1996.
- [8] Richard Volpe. Techniques for collision prevention, impact stability, and force control by space manipulators. In S. B. Skaar and C. F. Ruoff, editors, *Teleoperation and Robotics in Space*, Progress in Astronautics and Aeronautics, pages 175–212. AIAA, Washington, DC, 1994.
- [9] Dan Simon. *Optimal State Estimation Kalman, H-inf, and Nonlinear Approaches*, chapter 5, 15. John Wiley & Sons, Inc., 1 edition, 2006.
- [10] Howard D. Curtis. *Orbital Mechanics for Engineering Students*, chapter 5. Elsevier Ltd., 1 edition, 2014.
- [11] CertifyGroup. Introducing: Nema enclosure rating chart.
- [12] European Space Agency. Space environment statistics. <https://sdup.esoc.esa.int/discosweb/statistics/>, 2019.

- [13] Space News. Starlink constellation. <https://spacenews.com/spacex-submits-paperwork-for-30000-more-starlink-satellites/>, 2019.
- [14] Space.com. Kuiper constellation. <https://www.space.com/amazon-kuiper-satellite-constellation-fcc-approval.html>, 2020.
- [15] Oneweb. Oneweb constellation. <https://www.oneweb.world/media-center/oneweb-streamlines-constellation>, 2021.
- [16] European space agency. Space environment statistics. <https://sdup.esoc.esa.int/discosweb/statistics/>, 2020.
- [17] Genshiro KITAGAWA. Monte carlo filter and smoother for non-gaussian nonlinear state space models. *Journal of Computational and Graphical Statistics*, 1996.
- [18] Dan Simon. *Optimal state estimation: Kalman, h,, and nonlinear approaches*. John Wiley & Sons, Inc., 2006.
- [19] George H. Born Byron D. Tapley, Bob E. Schutz. *Statistical orbit determination*. Elsevier Inc., 2004.
- [20] Branko Ristic. *Beyond the kalman filter*. DSTO, 2004.
- [21] Simon Shuster. *Initial relative-orbit determination using heterogeneous tdoa*. IEEE, 2017.
- [22] Brita longlast filter, 2015.
- [23] Javier Díez-González Rubén Álvarez Lidia Sánchez-González Laura Fernández-Robles Hilde Pérez and Manuel Castejón-Limas. *3d tdoa problem solution with four receiving nodes*, 2019.
- [24] Hyeondeog Seo. *3d moving target tracking with measurement fusion of tdoa/fdoa/aoa*. The Korean Institute of Communications and Information Sciences (KICS), 2019.
- [25] Jacek Stefanski. *Hyperbolic position location estimation in the multipath propagation environment*. IFIP International Federation for Information Processing, 2009.

## **A Baseline Design and Trade Studies**

To select the baseline design from each of the critical elements each of the trade study results were quantitatively assessed but also qualitatively considered with respect to the project goal approached as a proof of concept to see if small low cost ground stations can be used to monitor the orbit of satellites and their positions. The satellite target trade study was designed to choose satellites that would be used for the proof of concept experiment, due to our location here at CU Boulder and a team members connection we decided to use the LASP-operated satellite CSIM, as the data could be used to quantitatively compare our data and validate our systems performance. For our L-Band satellite, we chose the iridium constellation as the documentation on orbital paths was well documented, and the L-band downlinks were consistent. The On Board Computer trade study suggested Raspberry Pi 4 due to the computer's community services, providing a large amount of forum support and hardware compatibility. The HackRF was chosen due to factors including availability, along with low cost. The GPS trade study

selected the ACROBOTIC NEO-6M breakout board based on equal weightings between cost, update rate and positional accuracy. The sensor unit housing selected via trade study was a NEMA-4 rated electrical enclosure, as it offered excellent off-the-shelf weatherproofing, along with a community of cheap environmentally rated connectors for cable passthrough and connection covers.

## B Electronics System Schematics

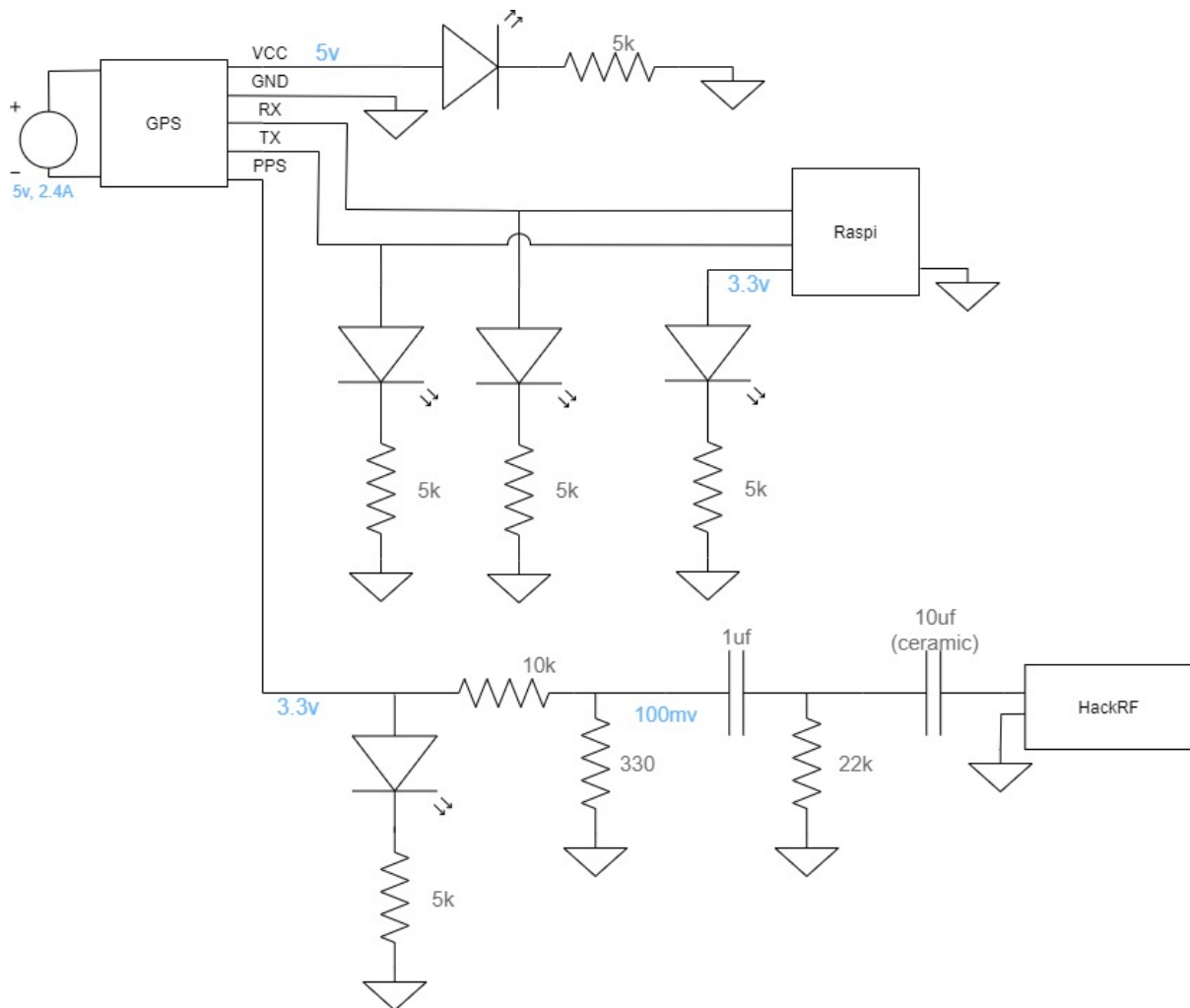


Figure 52: Full Schematic of the circuit board

## C Bill of Materials



94639A536	Off-White Nylon Unthreaded Spacer, 1/2" OD, 1" Long, for Number 8 Screw Size	Used for offesting electronics from the hardware rack	<a href="https://www.mcmaster.com/panel-standoffs/nylon-unthreaded/">https://www.mcmaster.com/panel-standoffs/nylon-unthreaded/</a>	1	pack of 100		\$ 13.04	\$ 13.04	
92470A204	Phillips Rounded Head Screws for Sheet Metal, 18-8 Stainless Steel, Number 8 Size, 1-3/4" Long	Used for offesting electronics from the hardware rack	<a href="https://www.mcmaster.com/stainless-steel-screws/18-8-stainless-steel/">https://www.mcmaster.com/stainless-steel-screws/18-8-stainless-steel/</a>	1	pack of 50		\$ 7.25	\$ 7.25	
94613A086	Nylon Bolt	threaded nylon bolt	<a href="https://www.mcmaster.com/bolts/length-1-2/length-1/plastic/">https://www.mcmaster.com/bolts/length-1-2/length-1/plastic/</a>	1	pack of 100		\$ 6.69	\$ 6.69	
94812A100	Nyoln Nut	threaded nylon nit	<a href="https://www.mcmaster.com/nuts/material-plastic/nut-type-hex/height-1/">https://www.mcmaster.com/nuts/material-plastic/nut-type-hex/height-1/</a>	1	pack of 100		\$ 7.14	\$ 7.14	
8982K124	4 ft long, 2 1/2 ", Angled Aluminum	For anetenna Mounting	<a href="https://www.mcmaster.com/angles/multi-purpose-6061-aluminum-90/">https://www.mcmaster.com/angles/multi-purpose-6061-aluminum-90/</a>	1	ea		\$ 26.92	\$ 26.92	
89015K232	4ft long, Aluminum flat stock	For anetenna Mounting	<a href="https://www.mcmaster.com/aluminum-stock/multipurpose-6061-aluminum/">https://www.mcmaster.com/aluminum-stock/multipurpose-6061-aluminum/</a>	1	ea		\$ 19.68	\$ 19.68	
	Rivets	For anetenna Mounting	<a href="https://www.homedepot.com/p/Arrow-1-8-in-Aluminum-Short-Rivets-100-Pack/">https://www.homedepot.com/p/Arrow-1-8-in-Aluminum-Short-Rivets-100-Pack/</a>	1	pack of 50		\$ 5.98	\$ 5.98	
69915K54	Nema Cord Grips	For power and coax cable pass through	<a href="https://www.mcmaster.com/cord-grips/compact-plastic/">https://www.mcmaster.com/cord-grips/compact-plastic/</a>	3	ea		\$ 3.34	\$ 10.02	
	Coaxial cable	Outdoor Rated Coaxial Cable to antennas	<a href="https://www.amazon.com/CIMPLE-CO-Connectors-Internet/">https://www.amazon.com/CIMPLE-CO-Connectors-Internet/</a>	2	ea		\$ 8.97	\$ 17.94	
	Coaxial cable	LNA to Switch/Switch to SDR Coaxial Cable:	<a href="https://www.amazon.com/Monoprice-Shield-Coaxial-Cable/">https://www.amazon.com/Monoprice-Shield-Coaxial-Cable/</a>	3	ea		\$ 4.99	\$ 14.97	
8505K737	Acrylic	Plastic Sheet for Mounting Plate:	<a href="https://www.mcmaster.com/sheets/clear-scratch-and-uv-resistant/">https://www.mcmaster.com/sheets/clear-scratch-and-uv-resistant/</a>	1	ea		\$ 39.86	\$ 39.86	
7177K67	Zip ties	For mounting box to something	<a href="https://www.mcmaster.com/zip-ties/high-strength-cable-ties-7/">https://www.mcmaster.com/zip-ties/high-strength-cable-ties-7/</a>	1	pack of 100		\$ 13.50	\$ 13.50	
	T-post	to mount box to	<a href="https://www.homedepot.com/p/Everbilt-1-3-4-in-x-3-1-2-in-x-6-ft-Green-Steel/">https://www.homedepot.com/p/Everbilt-1-3-4-in-x-3-1-2-in-x-6-ft-Green-Steel/</a>	1	ea		\$ 4.70	\$ 4.70	
	PVC pipe	Antenna mount, 10ft, 2inch, Schedule 40	<a href="https://www.homedepot.com/p/2-in-x-10-ft-280-PSI-Schedule-40-PVC-DWV/">https://www.homedepot.com/p/2-in-x-10-ft-280-PSI-Schedule-40-PVC-DWV/</a>	2	ea		\$ 8.84	\$ 17.68	
	PVC cap	Antenna mount	<a href="https://www.homedepot.com/p/Charlotte-Pipe-2-in-PVC-Schedule-40/">https://www.homedepot.com/p/Charlotte-Pipe-2-in-PVC-Schedule-40/</a>	2	ea		\$ 1.86	\$ 3.72	

